VON KARMAN INSTITUTE FOR FLUID DYNAMICS
TURBOMACHINERY DEPARTMENT
CHAUSSEE DE WATERLOO, 72
B - 1640 RHODE SAINT GENESE, BELGIUM

CR 1981-6 DECEMBER 1980

THE EFFECT OF SUPPORT STRUT GEOMETRY ON FLOW UNIFORMITY IN THE TF-10 LP COMPRESSOR SCALE MODEL

P.M. LIGRANI, C. CAMCI, F.A.E. BREUGELMANS

TUR 7916/PML-CC-FAEB/LK

TABLE OF CONTENTS

1. INTRODUCTION

The flow uniformity at the inlet plane traversed by the eye of impeller blades in a compressor is greatly influenced by upstream inlet geometry. In particular, the way in which the flow interacts with the support struts affects uniformity. The separated flow behind struts may be convected throughout the entire inlet plenum to produce a flowfield with significant spatial non-uniformity. Such non-uniformities lead to large total pressure losses, low velocities and varying flow inlet angles. The purpose of this report is to present the results of several support strut geometry changes on total pressure loss and flow uniformity at the impeller inlet of the Thomassen LP compressor.

2. EXPERIMENTAL TEST FACILITY AND INSTRUMENTATION, MODEL DESCRIPTION

The general experimental procedure and test rig for the present tests have been described earlier (Refs. 1, 2). Because of the large spatial non-uniformities present in the inlet for the present configurations, some difficulty was encountered in measuring a suitable average velocity to normaliz results. To solve this problem, the volumetric flow rate through the inlet was determined for many of the tests by mean of the static pressure drop across a sharp edged orifice plate in the piping leading to the test rig. The average velocity at the inlet determined from this flow rate agrees very closel with values determined using the earlier method described in references 1 and 2, as shown in table 1. The earlier method consists of the average of six velocity measurements determine from shielded pressure probe traverses, and from wall static pressure tappings at three inner circumference locations and at three outer circumference locations. The values of $\rho\overline{V^2}/2$ used for normalization are also presented in table 1.

TABLE 1

VALUES OF $\overline{V}$ AND $\rho\overline{V^2}/2$ FOR CONFIGURATIONS TESTED

Configuration	G	H	I	J	K
$\overline{V}$ (m/sec)(orifice plate)	45.5	45.5	45.1		
$\overline{V}$ (M/sec)(static tappings)	45.6	46.5	46.1	54.1	46.
$\rho\overline{V^2}/2$ (mm water)(for normalization)	127.0	127.0	124.7	179.3	132.

The configurations tested in the present study are labelled G, H, I, J and K. For configurations G, H, J and K, circular support struts having a diameter of 42 mm were used in the inlet.

The locations of the struts are shown in figure 1, which indicates that five struts were used for G and J, and nine struts for H and K. Figure 2 shows the strut locations and orientations for configurations I. Streamlined struts were used, placed at the same angles as for design F described in reference 2. All strut cross-section gemetries are shown in detail in figure 3. The inlet area of the compressor inlet was reduced for configurations J and K. Details of the inlet for these configurations are shown in figures 4 and 5.

The repeatability of total pressure loss traces is documented in figures 19-G1*, 19-G1**, and 19-G1. As can be seen by comparison of these three figures, the general trend and magnitude of $\Delta P_0/\rho\overline{V}^2/2$ versus clockwise angular position does not change from one trace to another. However small differences occur due to localized losses resulting from vortex shedding or possibly from some other highly unsteady flow behaviour. The traces shown in the three figures were made at the same radial position with the same inlet geometry, but at different times.

Other test traces are also shown in figure 19 labelled according to configuration and radius. For radial position, 1 corresponds to the innermost radius and 5 corresponds to the outermost radius. See references 1 and 2. An asterisk (*) indicates a repeated test.

3. EXPERIMENTAL RESULTS

Total pressure loss contours are shown plotted in figures 6-10 for configurations G-K, respectively. Consider the first three of these (without a reduced inlet area), the largest losses occur with configuration H, where nine circula support struts are used in the inlet. Streamlining the strut configuration I, reduces losses slightly from those of config ration G, however additional orientation angle adjustment of the streamlined struts is necessary to further reduce configu ration I losses. For the reduced inlet configurations J and losses are greater than corresponding non-reduced inlet cases with the same strut geometries. Results for all configuratio are summarized in figures 11 and 12. Figure 13 shows the sta pressure drop averaged over the inside circumference for all configurations tested.

Flow angle contours are shown plotted in figures 14-18. The most uniform flows in terms of flow angle occur when nine circular support struts are used in the inlet. Configuration K produces a flow which is more uniform than configuration J, and configuration H produces a flow which is mor uniform than configuration G. Configuration I with streamline struts produces an in inlet flow which is about the same uniformity of slightly more uniform than that produced by G.

4. CONCLUSIONS

1. Normalized total pressure losses increase as the number of circular support struts increases from five (G, J) to nine (H, K).

2. Streamlined support struts (I) result in slightly decreased normalized total pressure losses compared to losses which exist when circular support struts (G) are used.

3. Reducing the inlet flow area (J, K) results in increased normalized losses when configurations with the same strut geometries (G, H) are compared.

4. A reduced inlet flow area (J, K) results in higher mean velocities at the plane nominally traversed by the eyes of impeller blades, than are present without a reduced inlet (G, H).

5. Increasing the number of circular support struts from five (G, J) to nine (H, K) results in reduced angle variations of the flow.

6. Strut streamlining (I) does not significantly decrease flow angle variations at the compressor impeller inlet, compared to non-streamlined circular results (G).

REFERENCES

1. LIGRANI, P.M. & BREUGELMANS, F.A.E.: The influence of inlet geometry characteristics on flow uniformity in a Thomassen compressor.
VKI CR 1980-1, November 1979.

2. LIGRANI, P.M. & BREUGELMANS, F.A.E.: Further studies on the influence of inlet geometry characteristics on flow uniformity in a Thomassen compressor.
VKI CR 1980-17, April 1980.

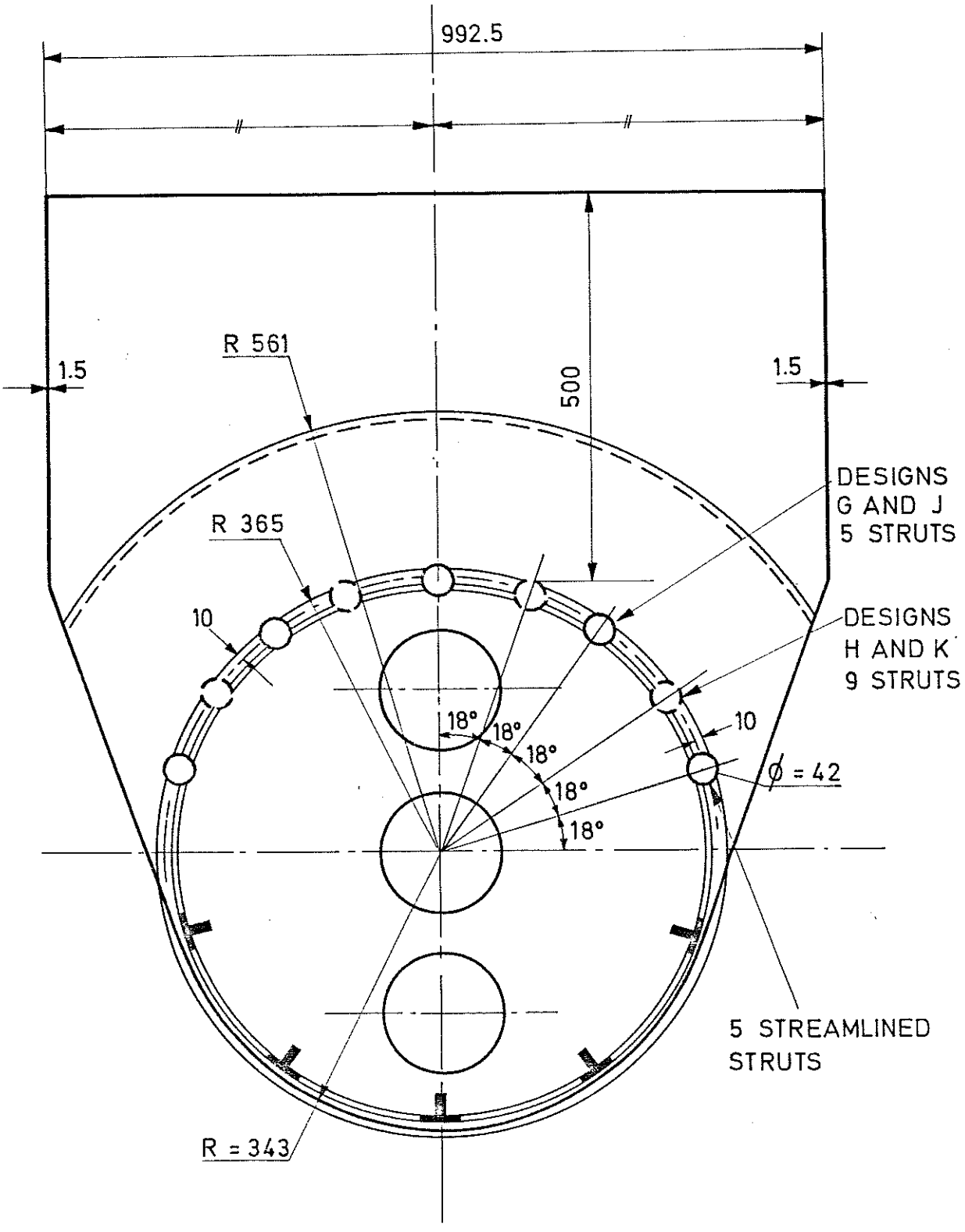

FIG. 1 - INSIDE OF CASING FOR COMPRESSOR INLET TEST FACILITY. SHOWING STRUT LOCATIONS FOR DESIGNS G, H, J AND K.

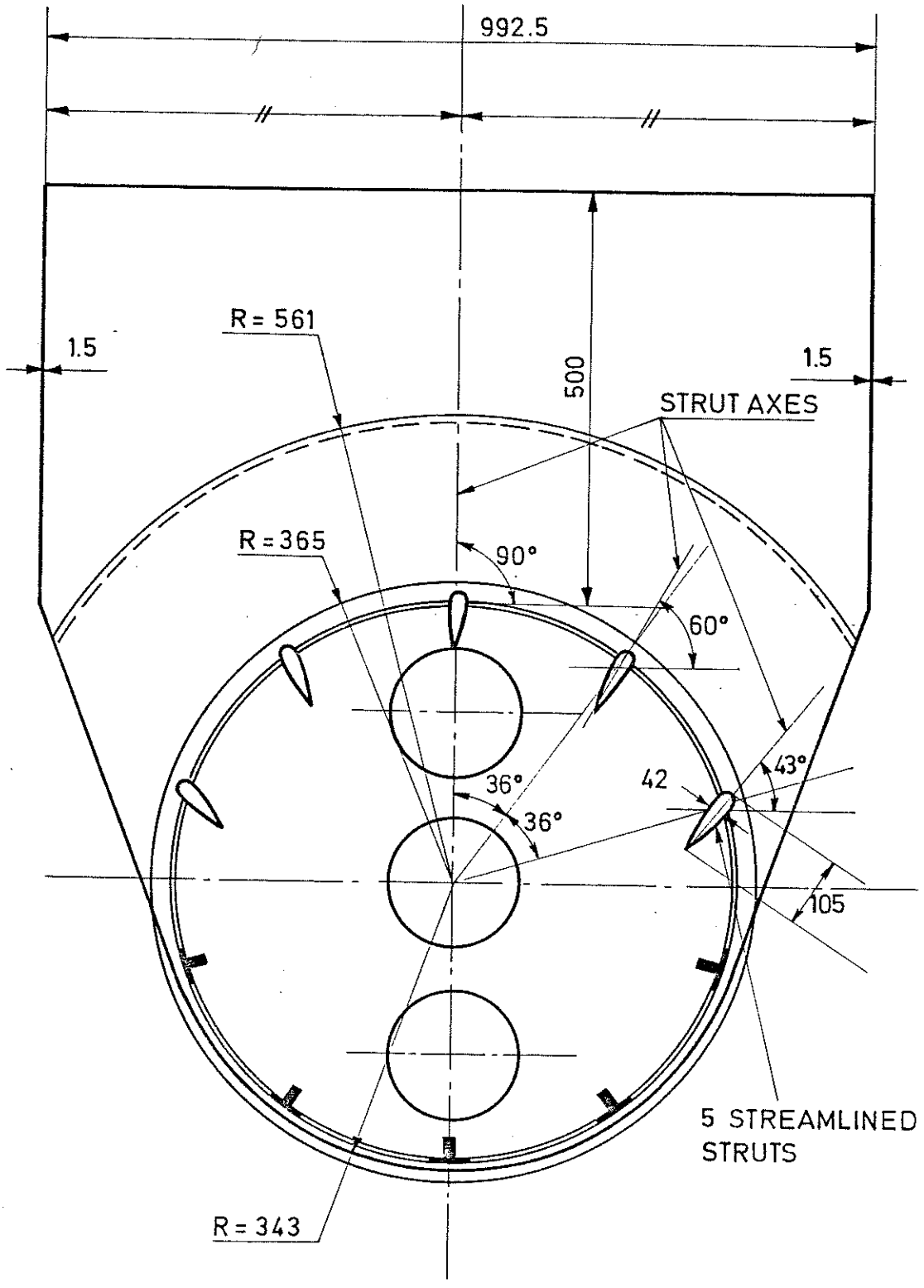

FIG. 2 - INSIDE OF CASING FOR COMPRESSOR INLET TEST FACILITY. SHOWING STRUT ORIENTATIONS FOR DESIGN I

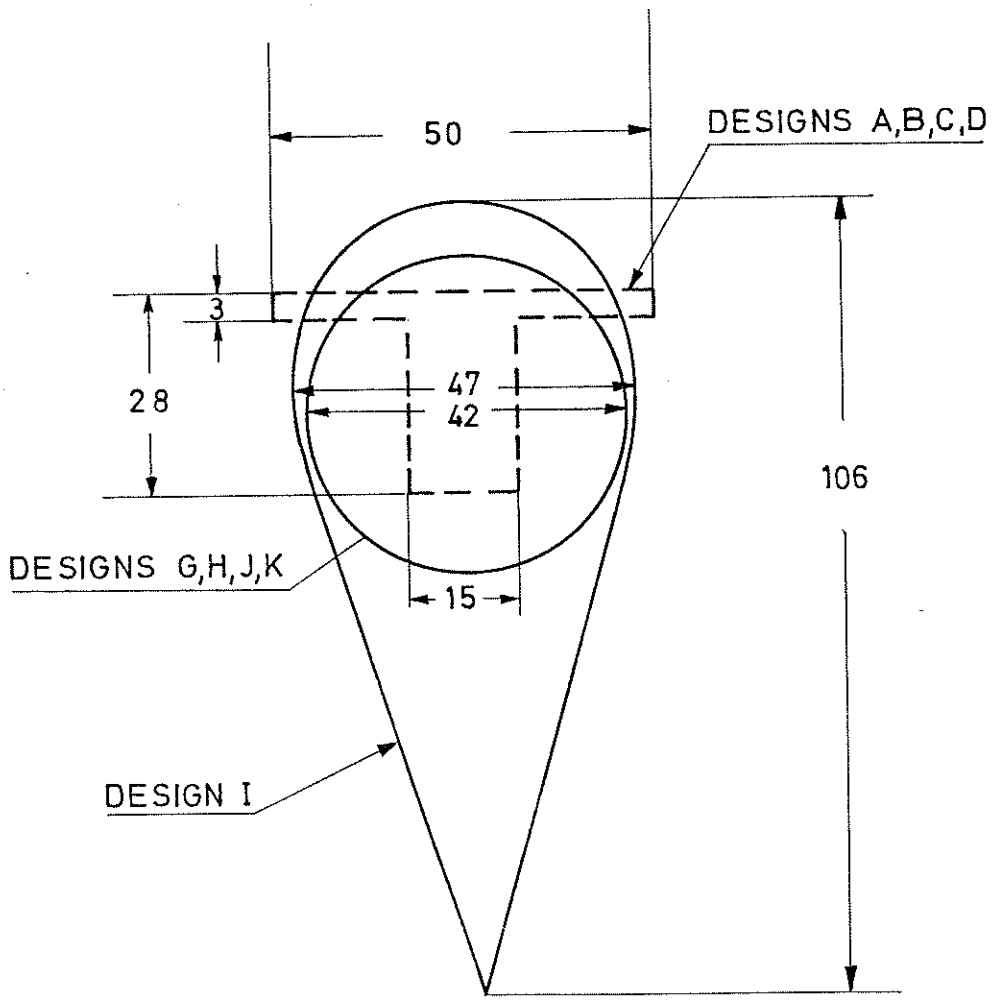

FIG. 3 - STRUT CROSS SECTIONS

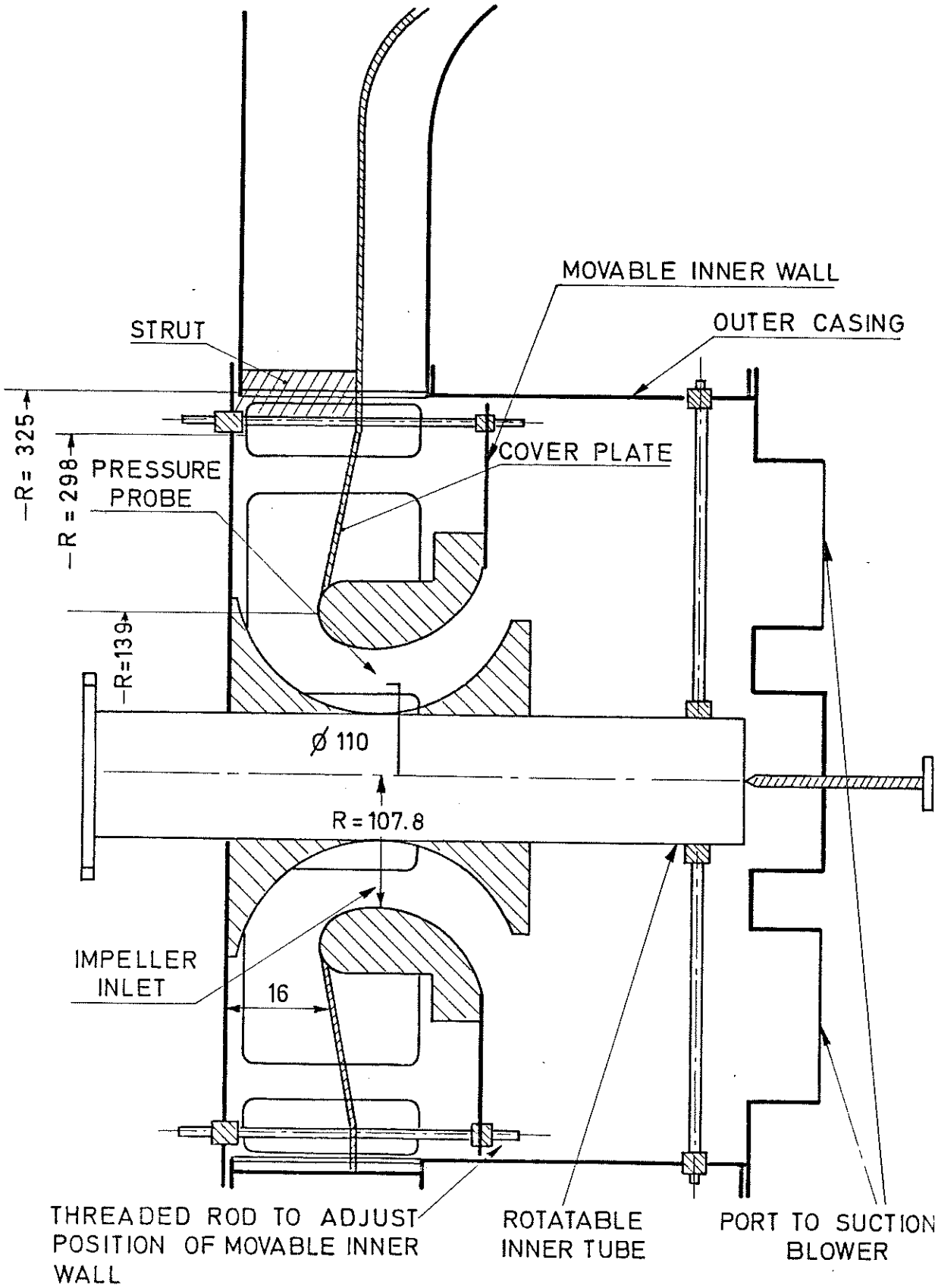

FIG. 4 - COMPRESSOR INLET SECTION MODIFICATION FOR DESIGNS J AND K.

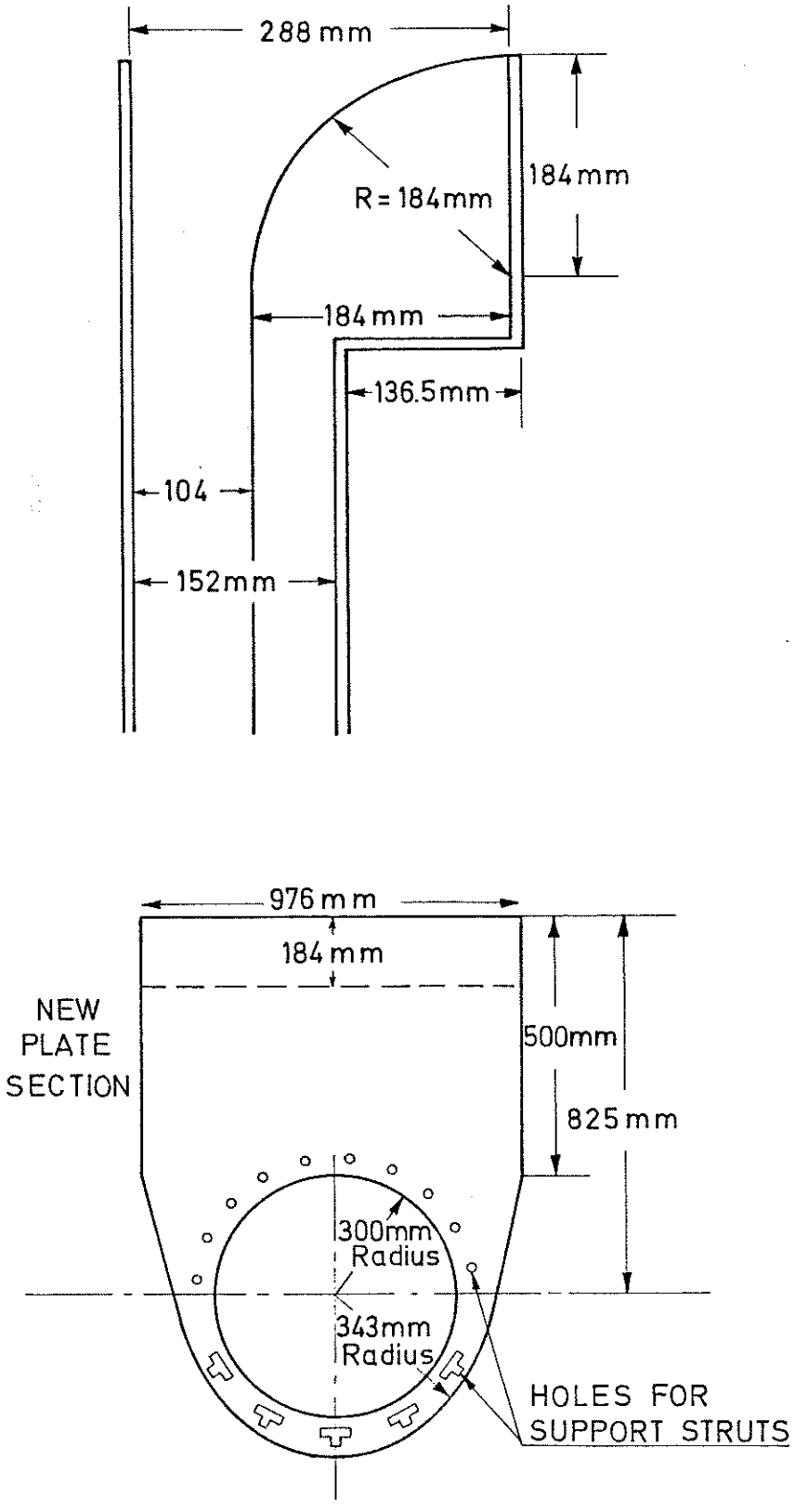

FIG. 5 a - INLET COVER PLATE FOR DESIGNS J AND K.

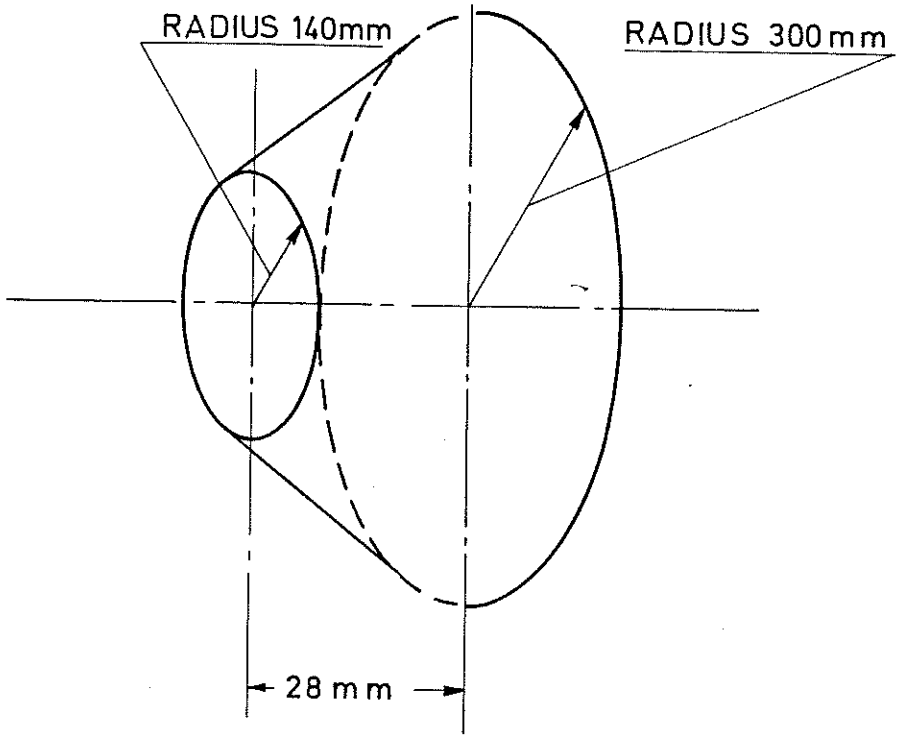

3 DIMENSIONAL VIEW

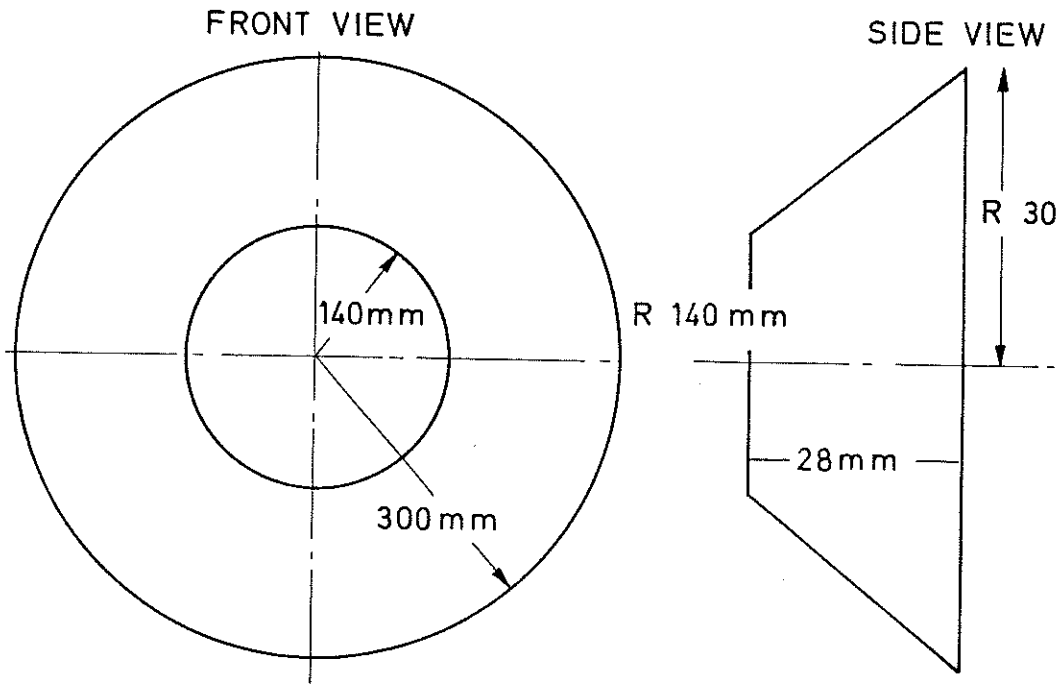

FIG. 5 b - INLET COVER PLATE FOR DESIGNS J AND K.

TOTAL PRESSURE LOSS CONTOURS

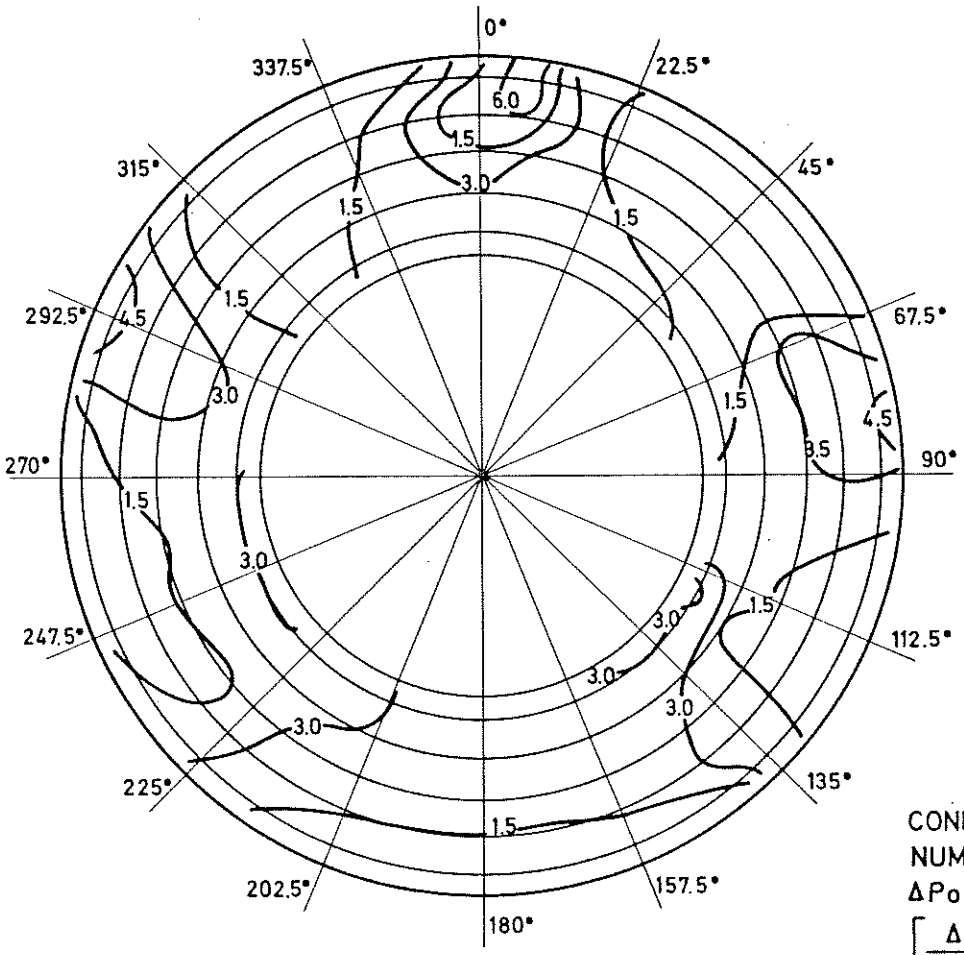

CONFIGURATION G
NUMBERS REPRESENT
ΔP_o (mm H_2O) OR

$$\left[\frac{\Delta P_o}{\rho \bar{V}^2/2}\right] \times 127.0$$

FIG. 6

TOTAL PRESSURE LOSS CONTOURS

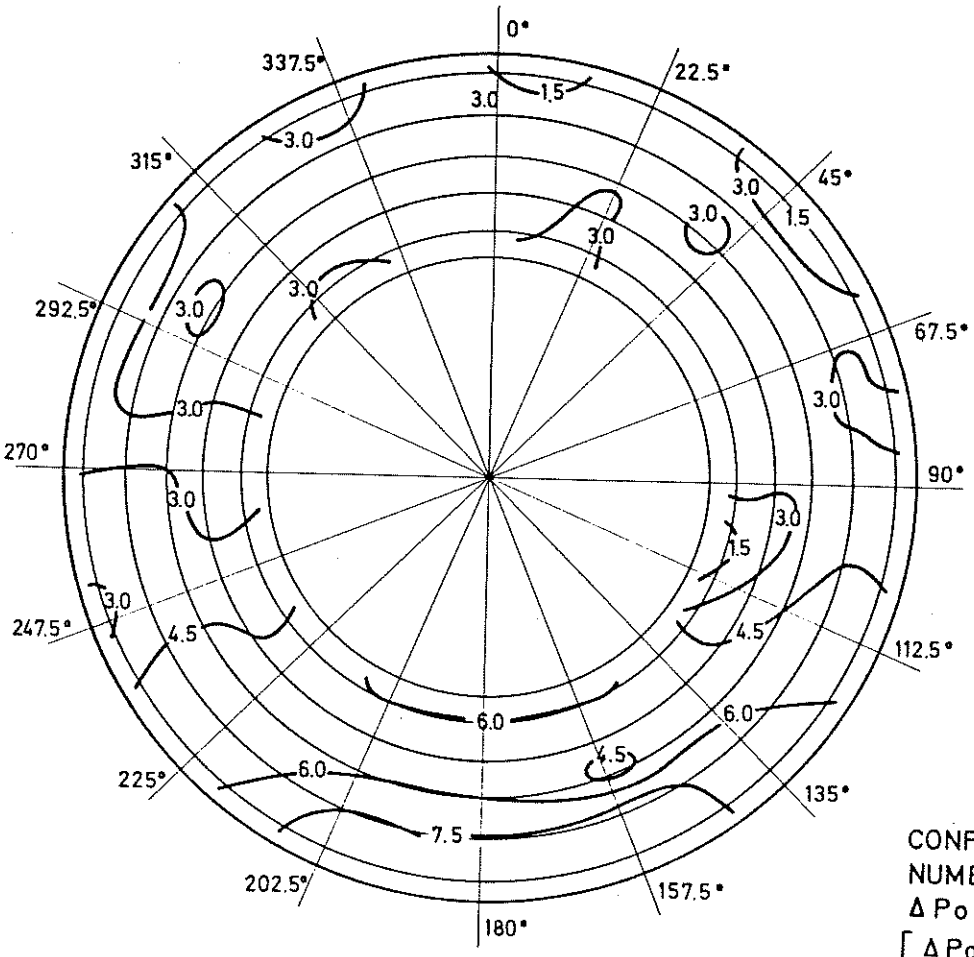

CONFIGURATION H
NUMBERS REPRESEN
ΔP_o (mm H_2O) OR
$\left[\frac{\Delta P_o}{\rho \bar{V}^2/2}\right] \times 127.0$

FIG. 7

TOTAL PRESSURE LOSS CONTOURS

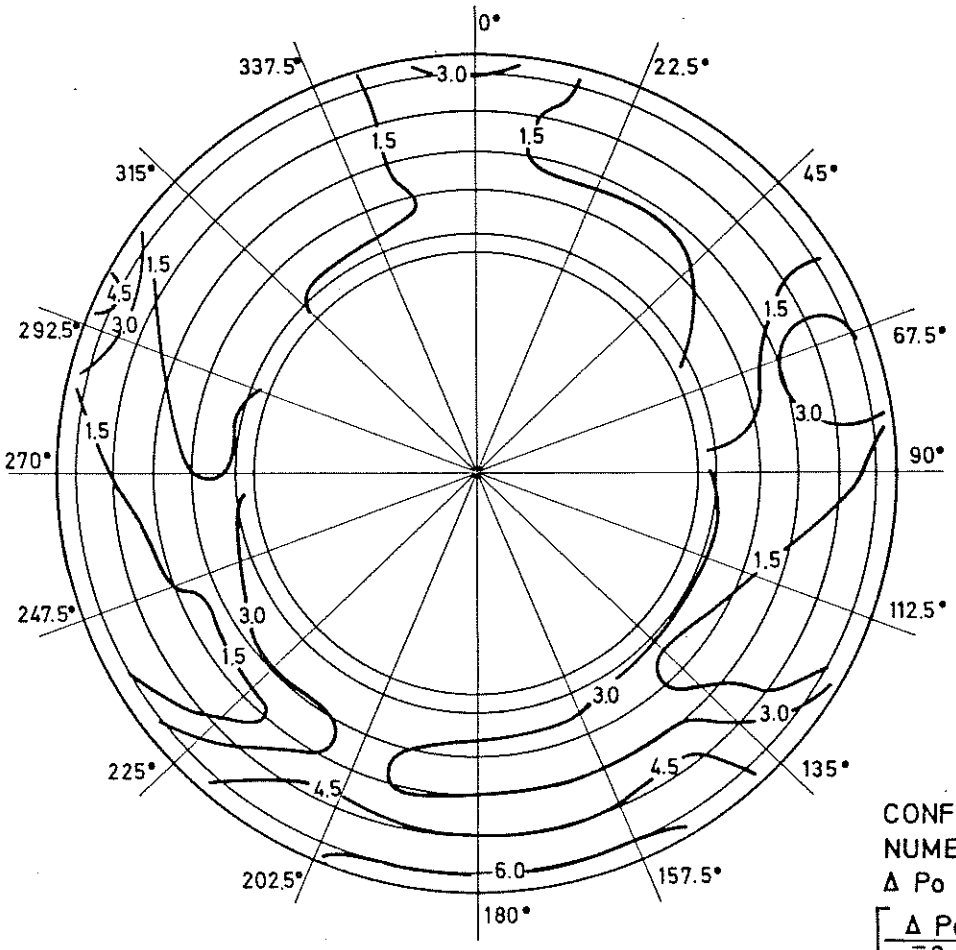

CONFIGURATION I
NUMBERS REPRESENT
ΔP_o ($mm H_2O$) OR

$$\left[\frac{\Delta P_o}{e\bar{V}^2/2}\right] \times 124.7$$

FIG. 8

TOTAL PRESSURE LOSS CONTOURS

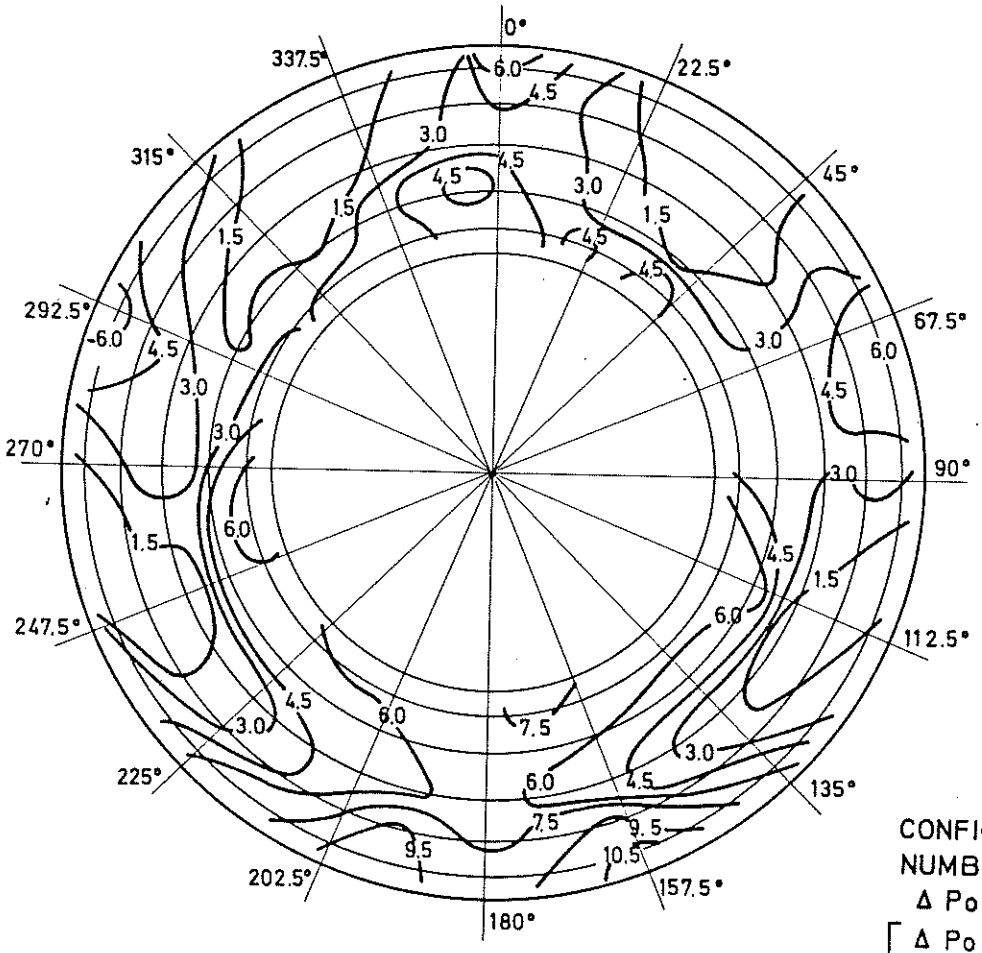

CONFIGURATION J
NUMBERS REPRESE
ΔP_o (mm H_2O) OR

$$\left[\frac{\Delta P_o}{\rho \bar{V}^2/2}\right] \times 179.3$$

FIG. 9

TOTAL PRESSURE LOSS CONTOURS

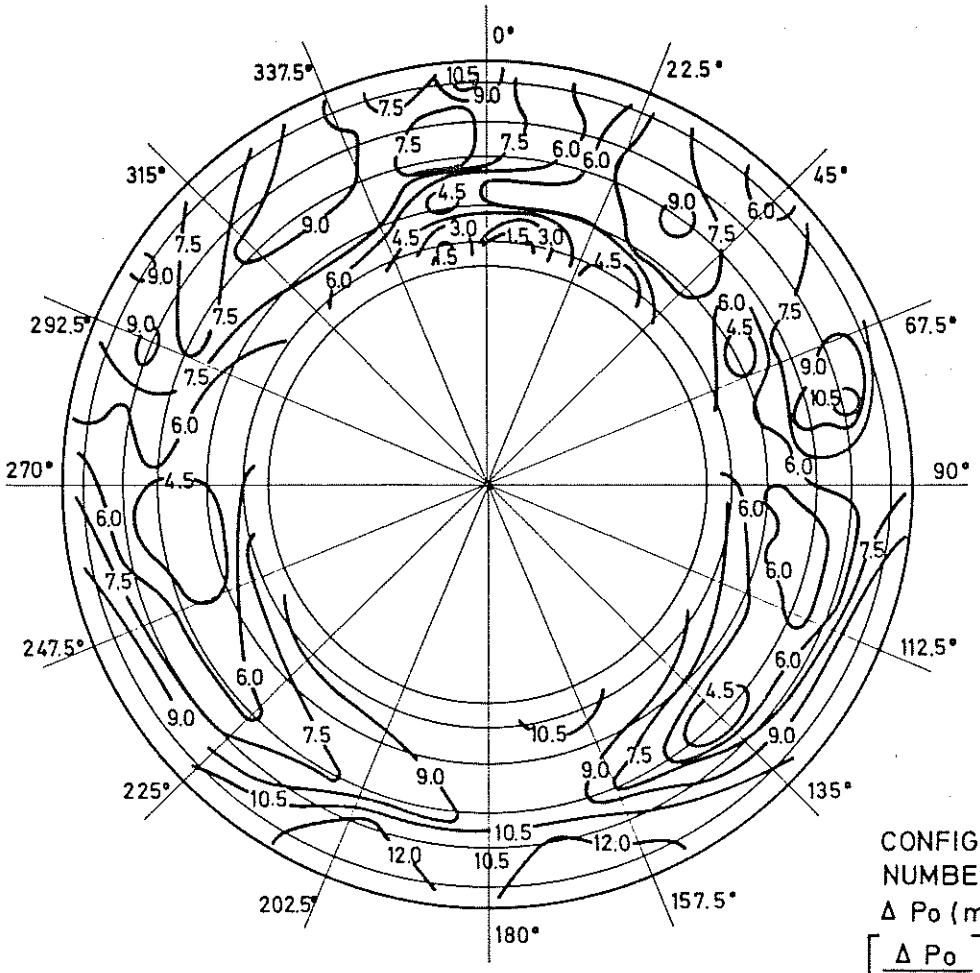

CONFIGURATION K
NUMBERS REPRESENT
ΔP_o (mm H_2O) OR

$$\left[\frac{\Delta P_o}{\rho \bar{V}^2/2}\right] \times 132.5$$

FIG. 10

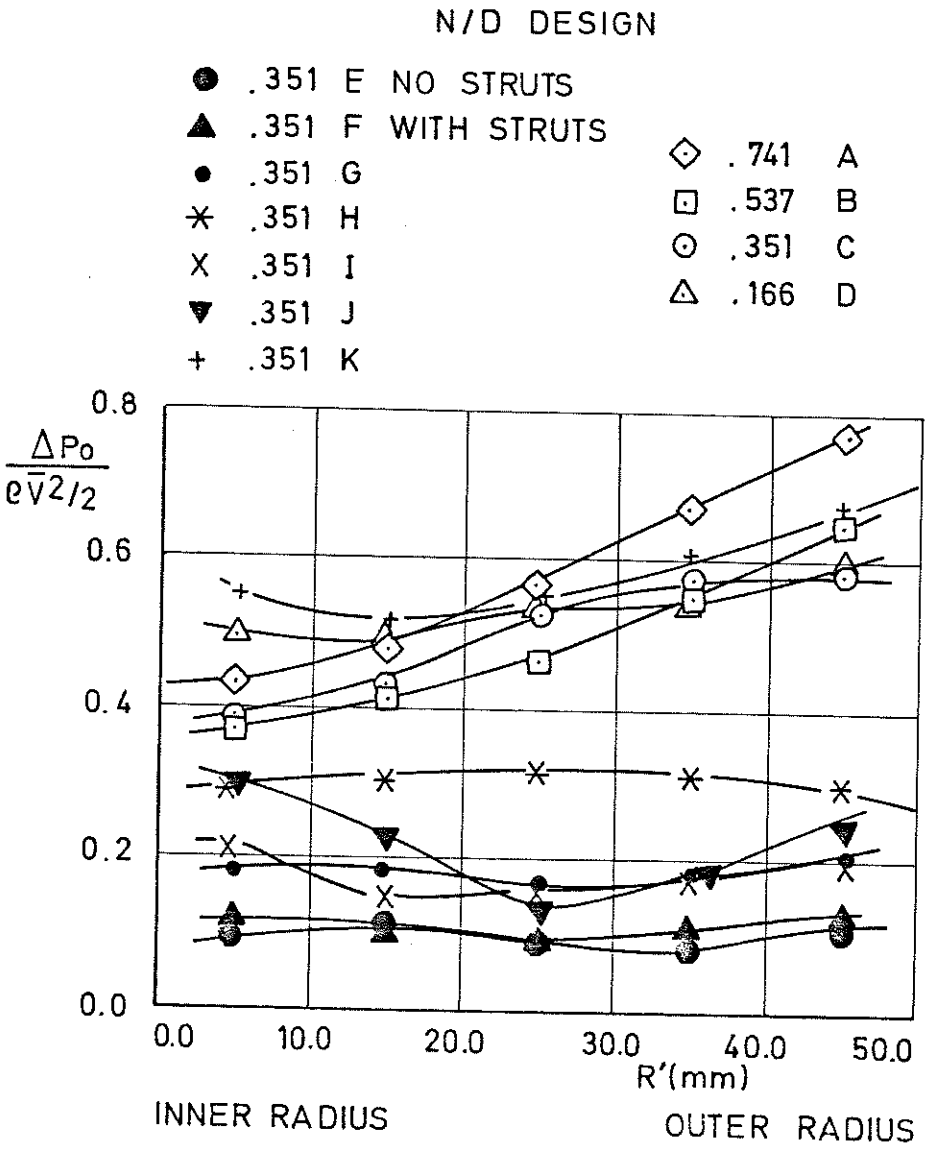

FIG. 11 - TOTAL PRESSURE LOSS AVERAGED OVER EACH CIRCUMFERENCE.

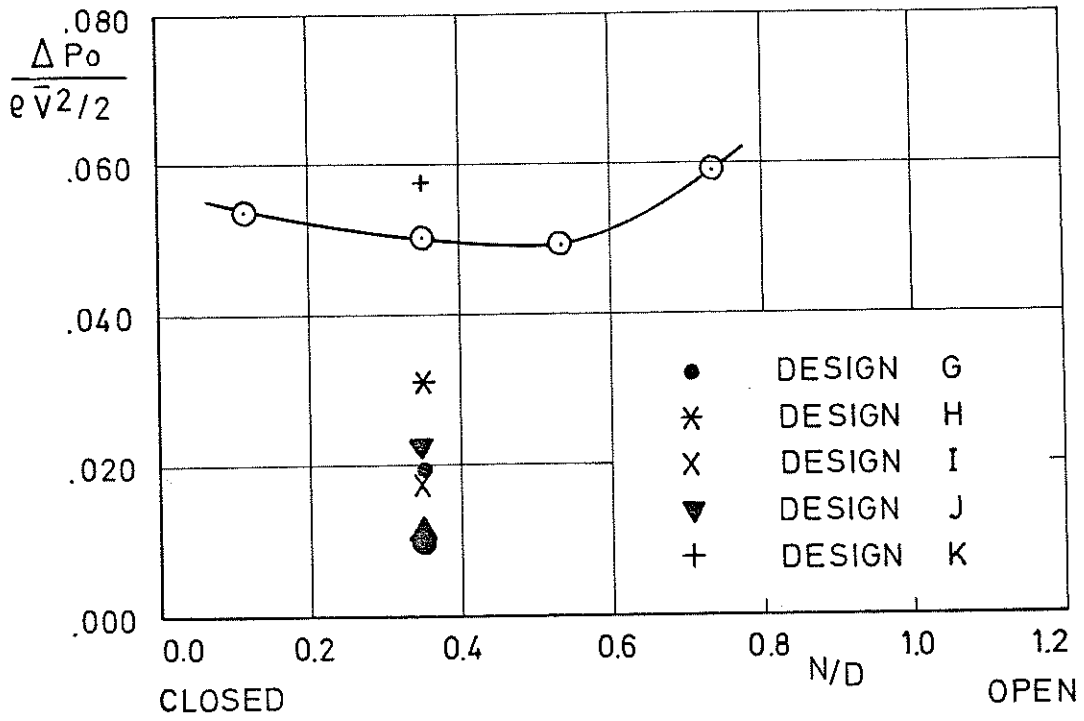

FIG. 12 - TOTAL PRESSURE LOSS AVERAGED OVER ALL CIRCUMFERENCES AS A FUNCTION OF N/D.

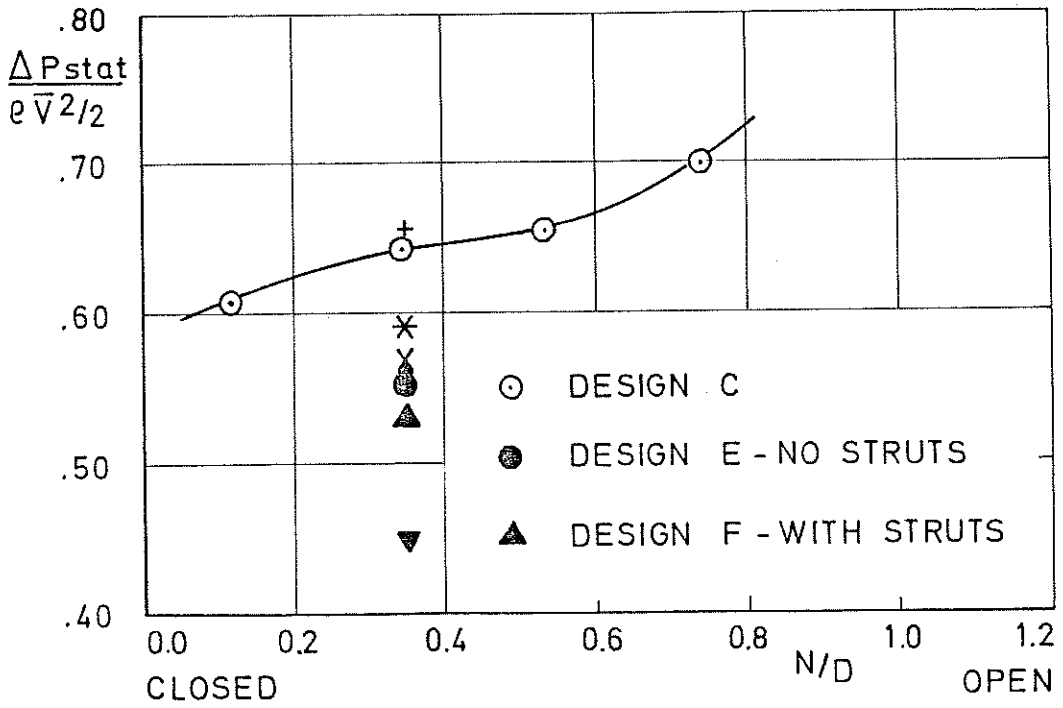

FIG. 13 - STATIC PRESSURE DROP AVERAGED OVER INSIDE CIRCUMFERENCE AS A FUNCTION OF N/D

FLOW ANGLE CONTOURS

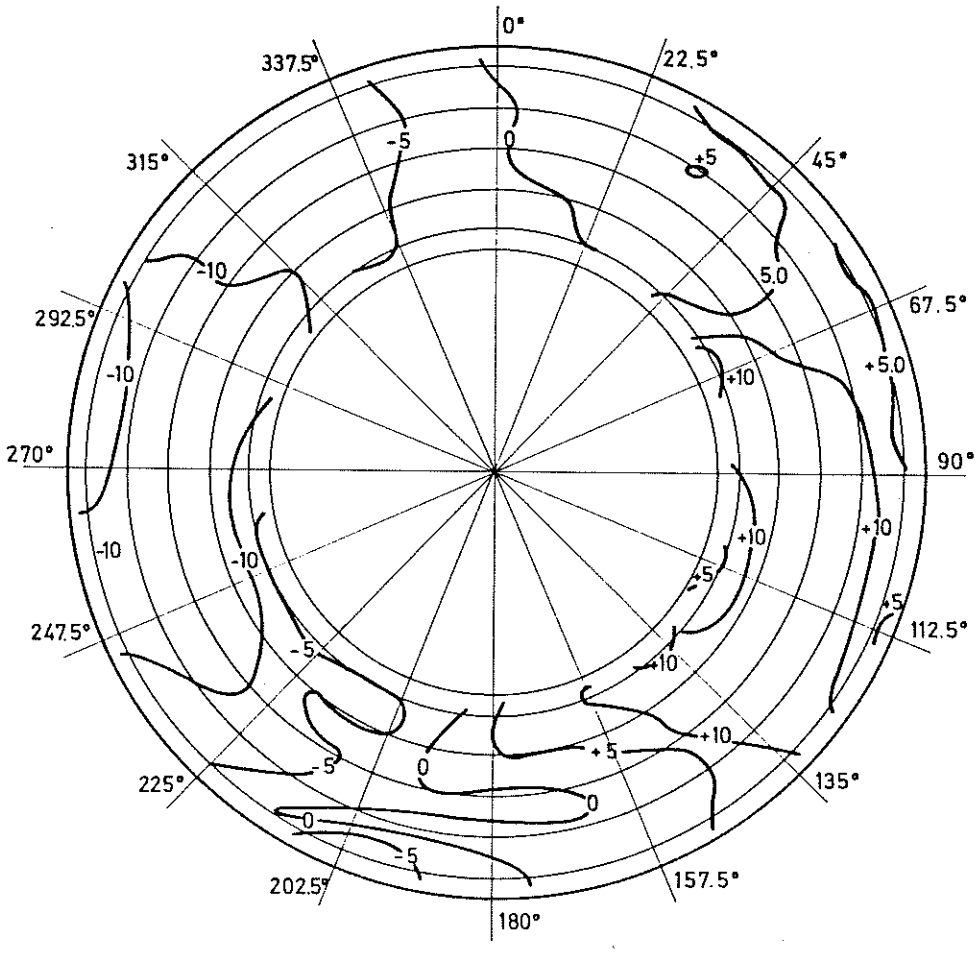

CONFIGURATION G
NUMBERS REPRESENT
OF THE FLOW AS IT M
TOWARDS THE PROBE

POSITIVE - TO THE RIGHT
NEGATIVE - TO THE LEFT
} WITH
TO TH

FIG. 14

FLOW ANGLE CONTOURS

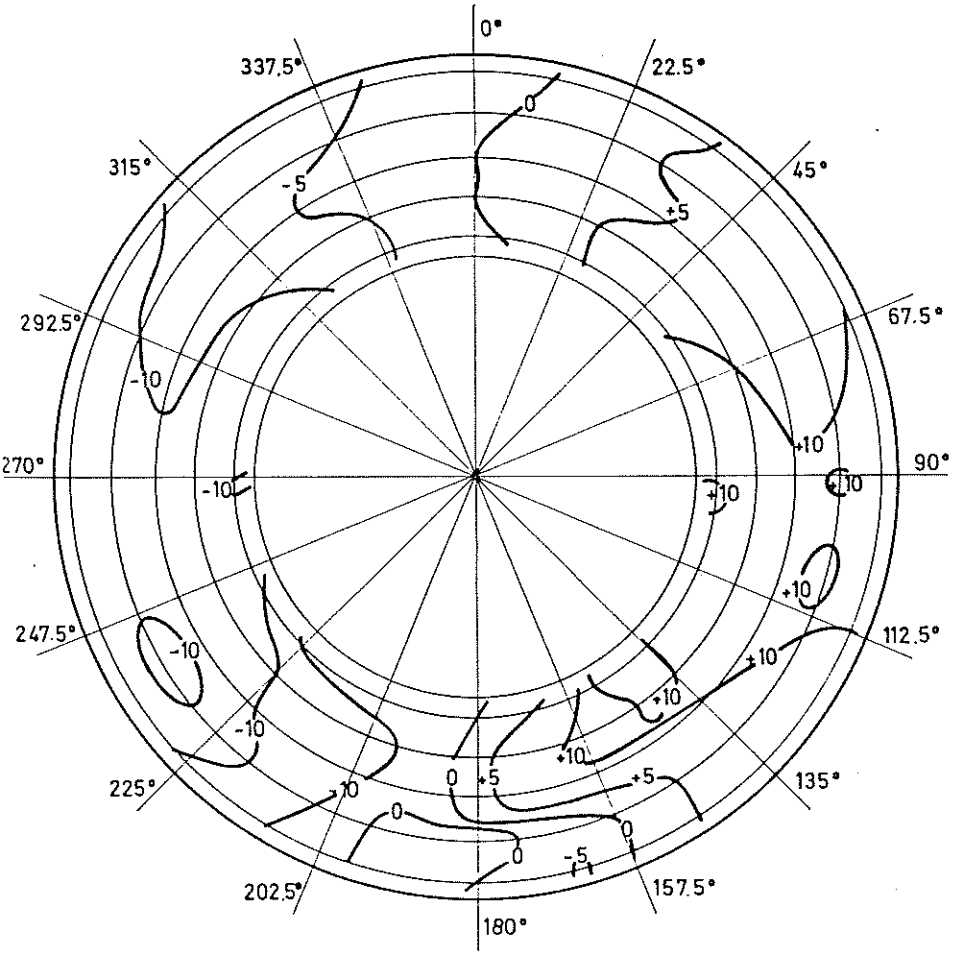

CONFIGURATION H
NUMBERS REPRESENT ANGLE OF THE FLOW AS IT MOVES TOWARDS THE PROBE.

POSITIVE - TO THE RIGHT
NEGATIVE - TO THE LEFT
} WITH RESPECT TO THE PROB

FIG. 15

FLOW ANGLE CONTOURS

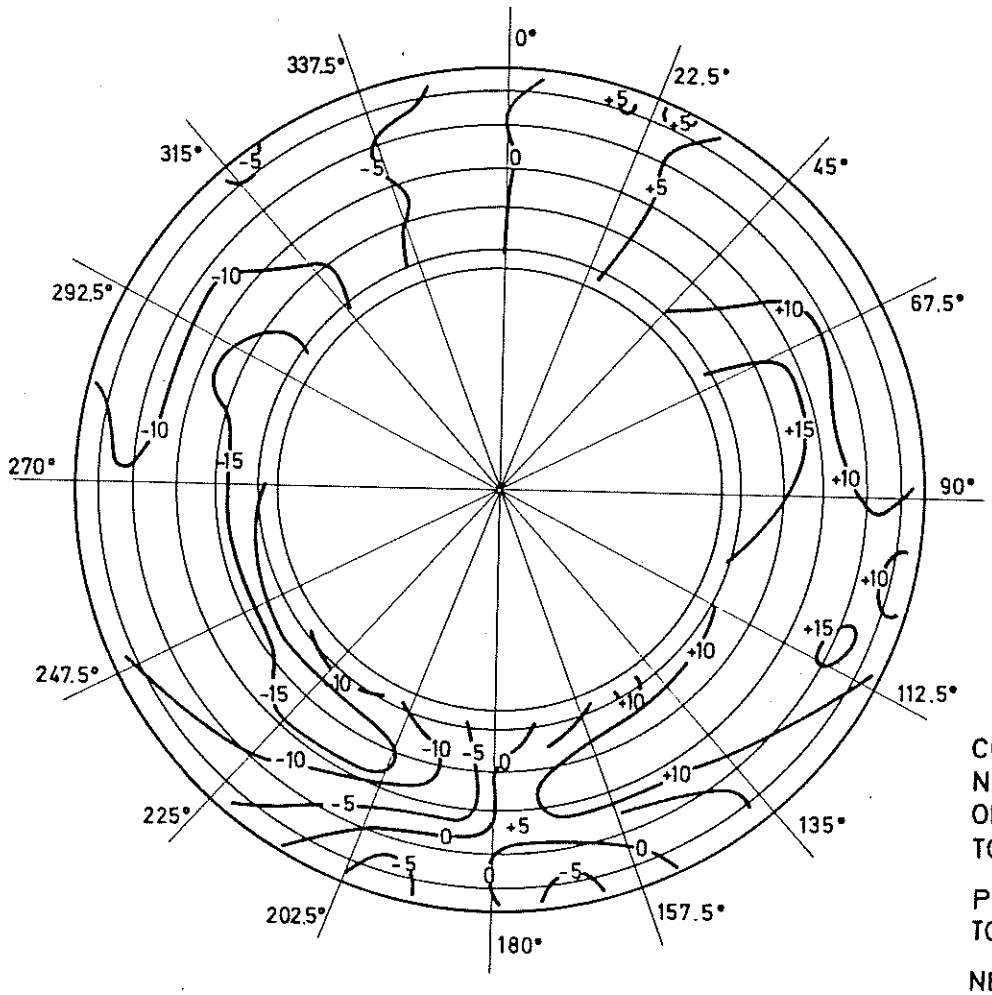

CONFIGURATION I
NUMBERS REPRESENT
OF THE FLOW AS IT M
TOWARDS THE PROBE

POSITIVE-
TO THE RIGHT

NEGATIVE-
TO THE LEFT

WITH
TO T

FIG. 16

FLOW ANGLE CONTOURS

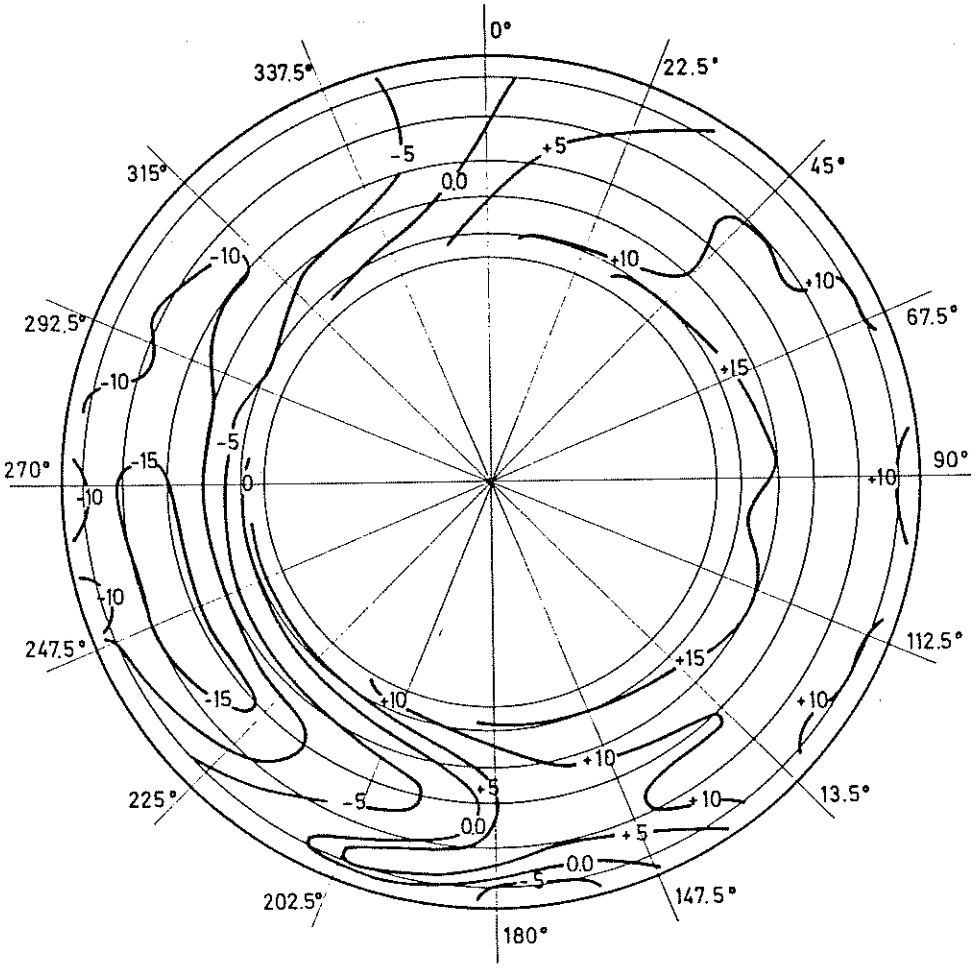

FIG. 17

FLOW ANGLE CONTOURS

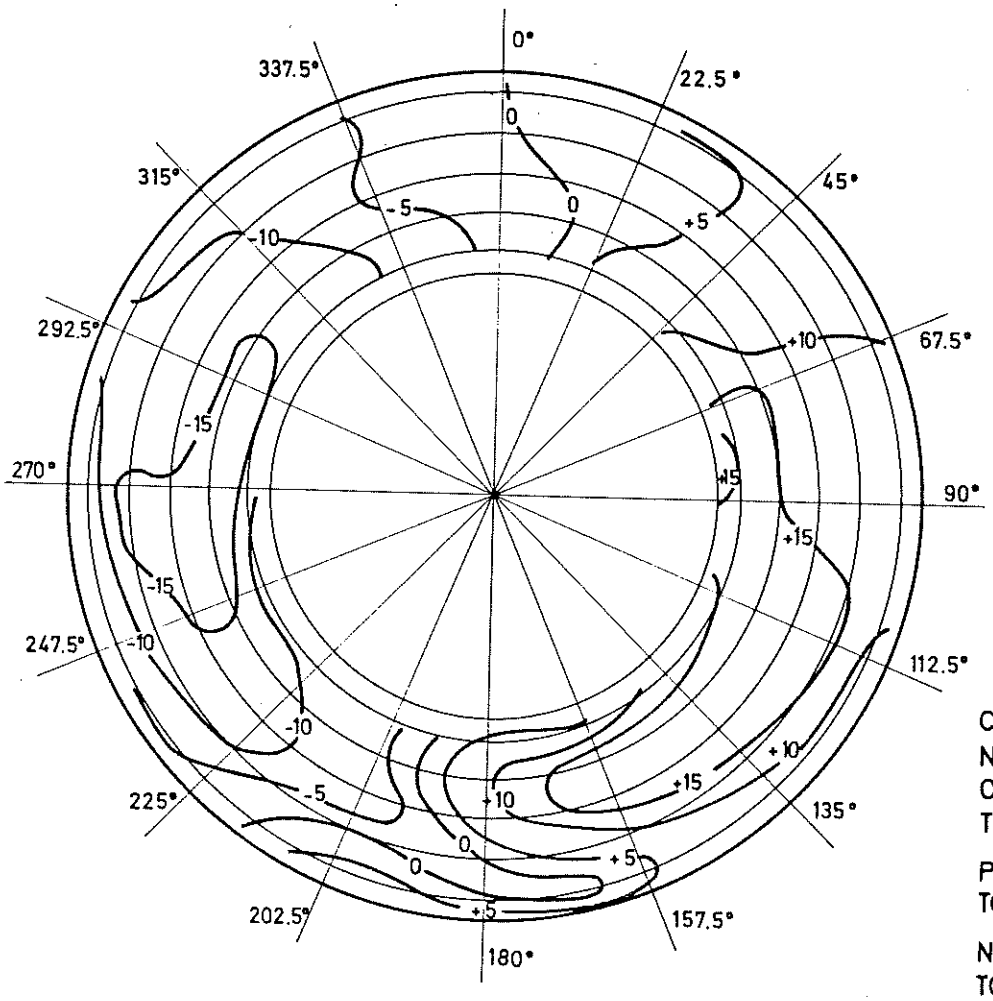

CONFIGURATION K
NUMBERS REPRESENT
OF THE FLOW AS IT MO
TOWARDS THE PROBE

POSITIVE -
TO THE RIGHT

NEGATIVE -
TO THE LEFT

WITH
TO THE

FIG. 18

FIG. 19-G1*

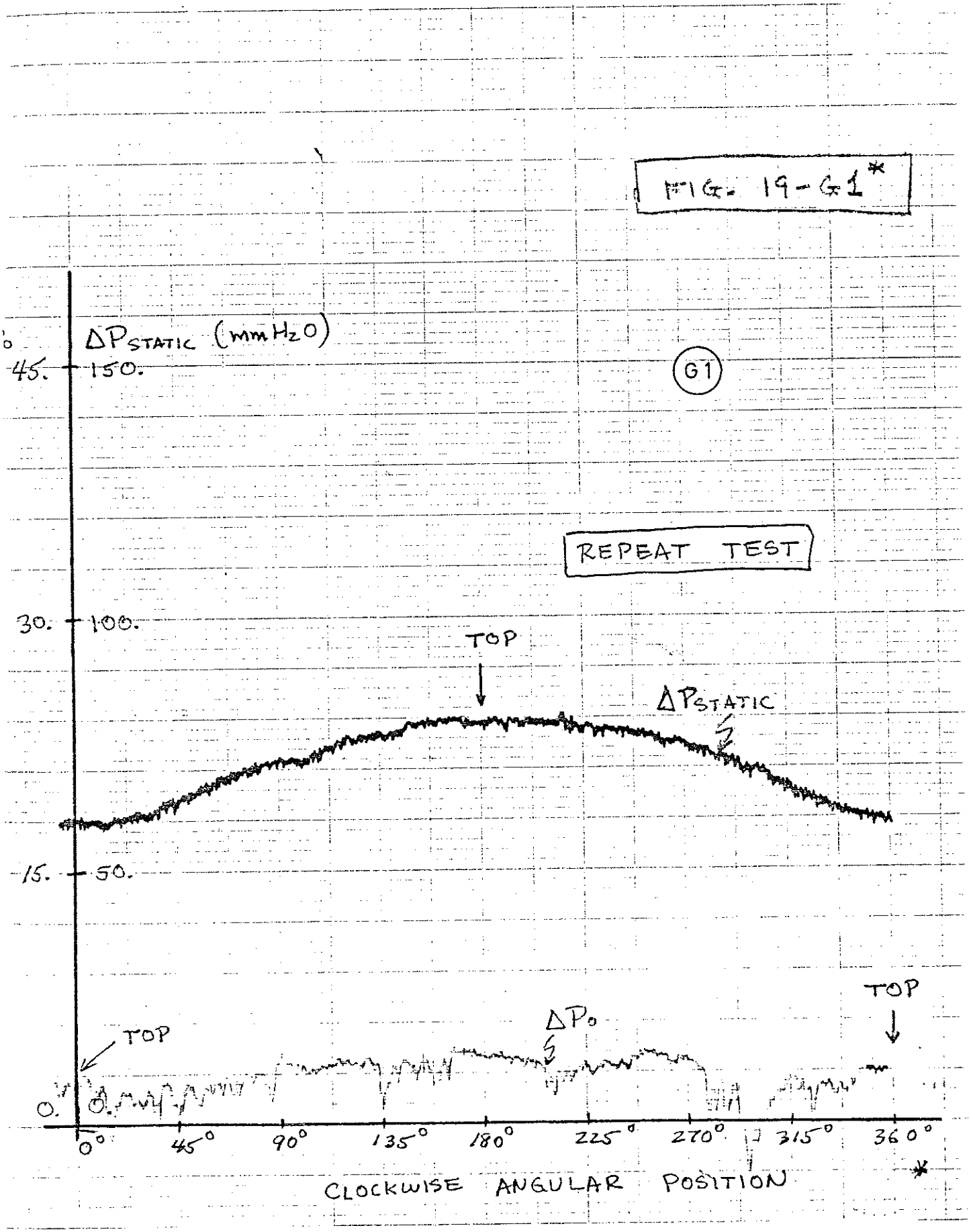
ΔP STATIC (mm H2O)
45.
150.
G1
REPEAT TEST
30.
100.
TOP
ΔP STATIC
15.
50.
TOP
ΔP0
TOP
0.
0°
45°
90°
135°
180°
225°
270°
315°
360°
CLOCKWISE ANGULAR POSITION
*

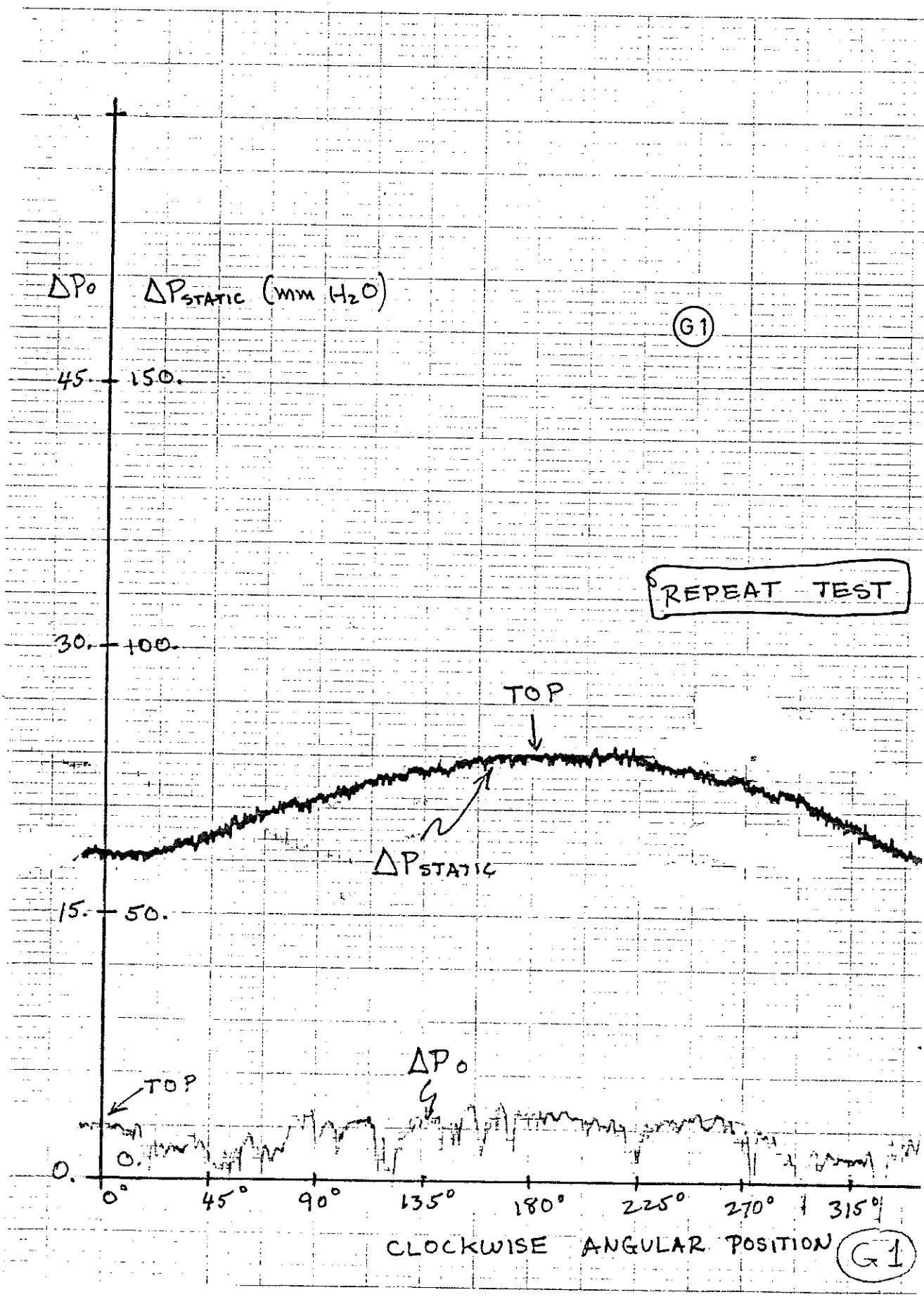
ΔPo
ΔPSTATIC (mm H2O)
G1
45.
150.
REPEAT TEST
30.
100.
TOP
ΔPSTATIC
15.
50.
ΔPo
TOP
0.
0.
0°
45°
90°
135°
180°
225°
270°
315°
CLOCKWISE ANGULAR POSITION
G1

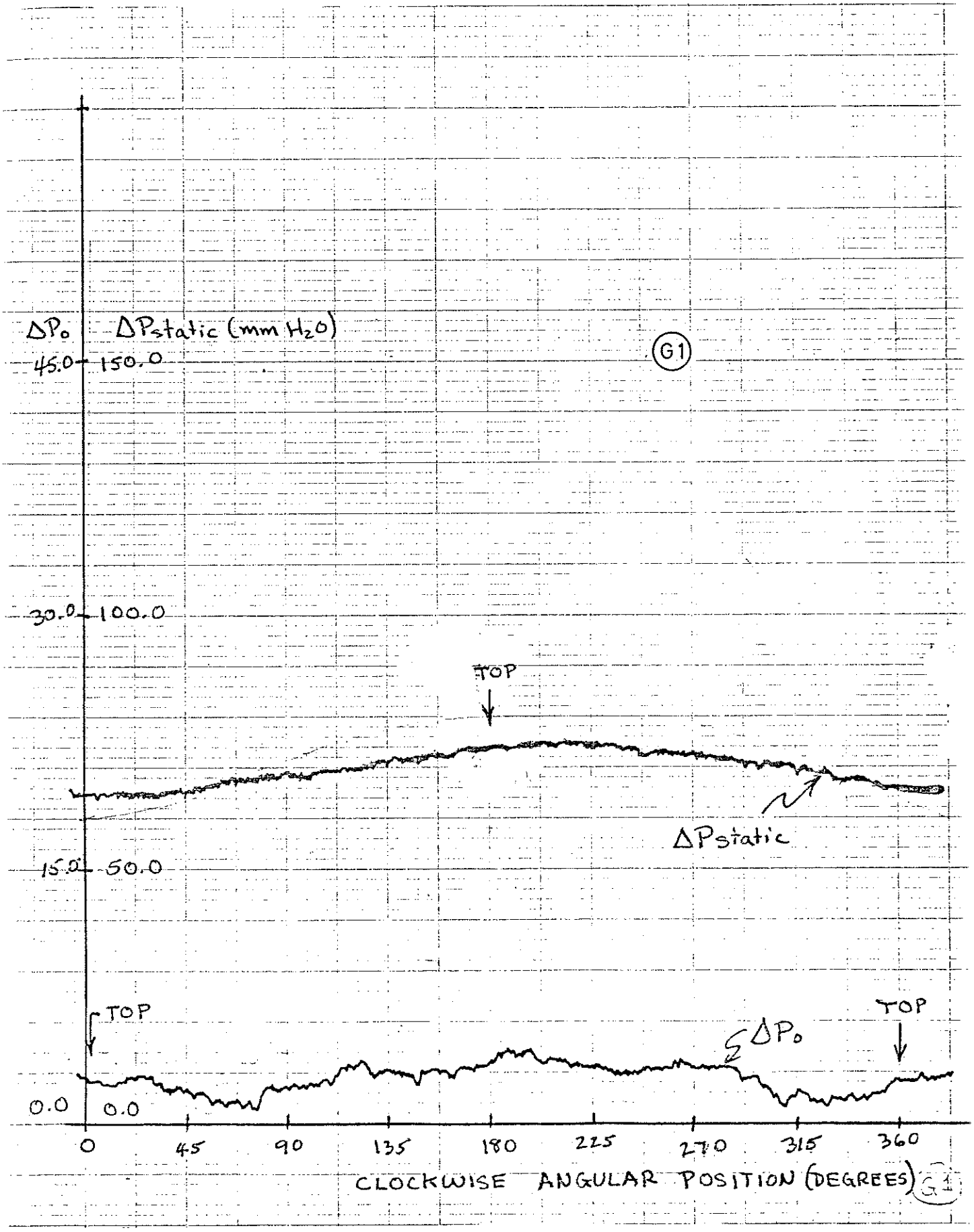
ΔPo
ΔPstatic (mm H2O)
G1
45.0
150.0
30.0
100.0
TOP
ΔPstatic
15.0
50.0
TOP
ΔPo
TOP
0.0
0.0
0
45
90
135
180
225
270
315
360
CLOCKWISE ANGULAR POSITION (DEGREES)
G1

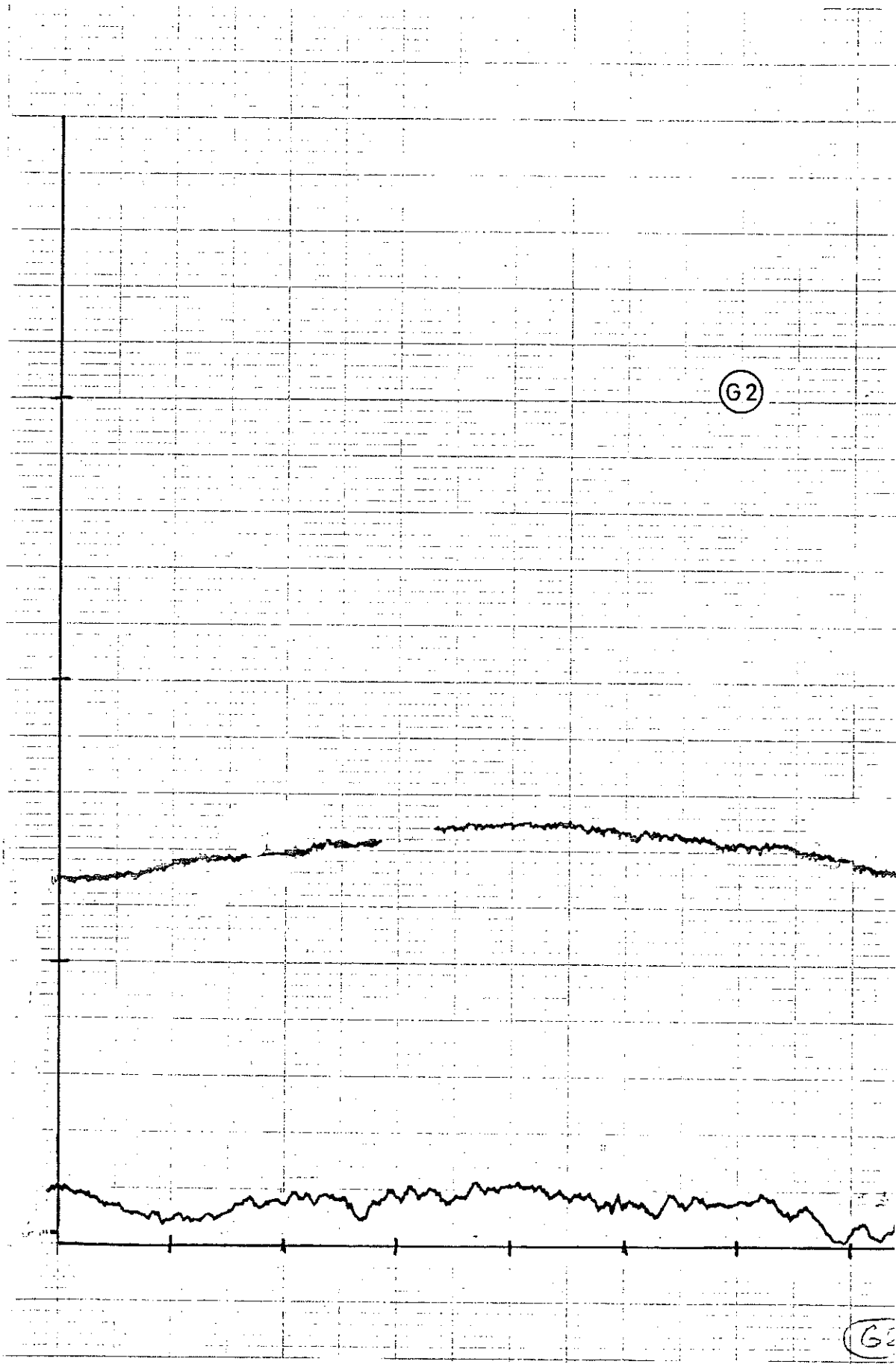
G2
G2

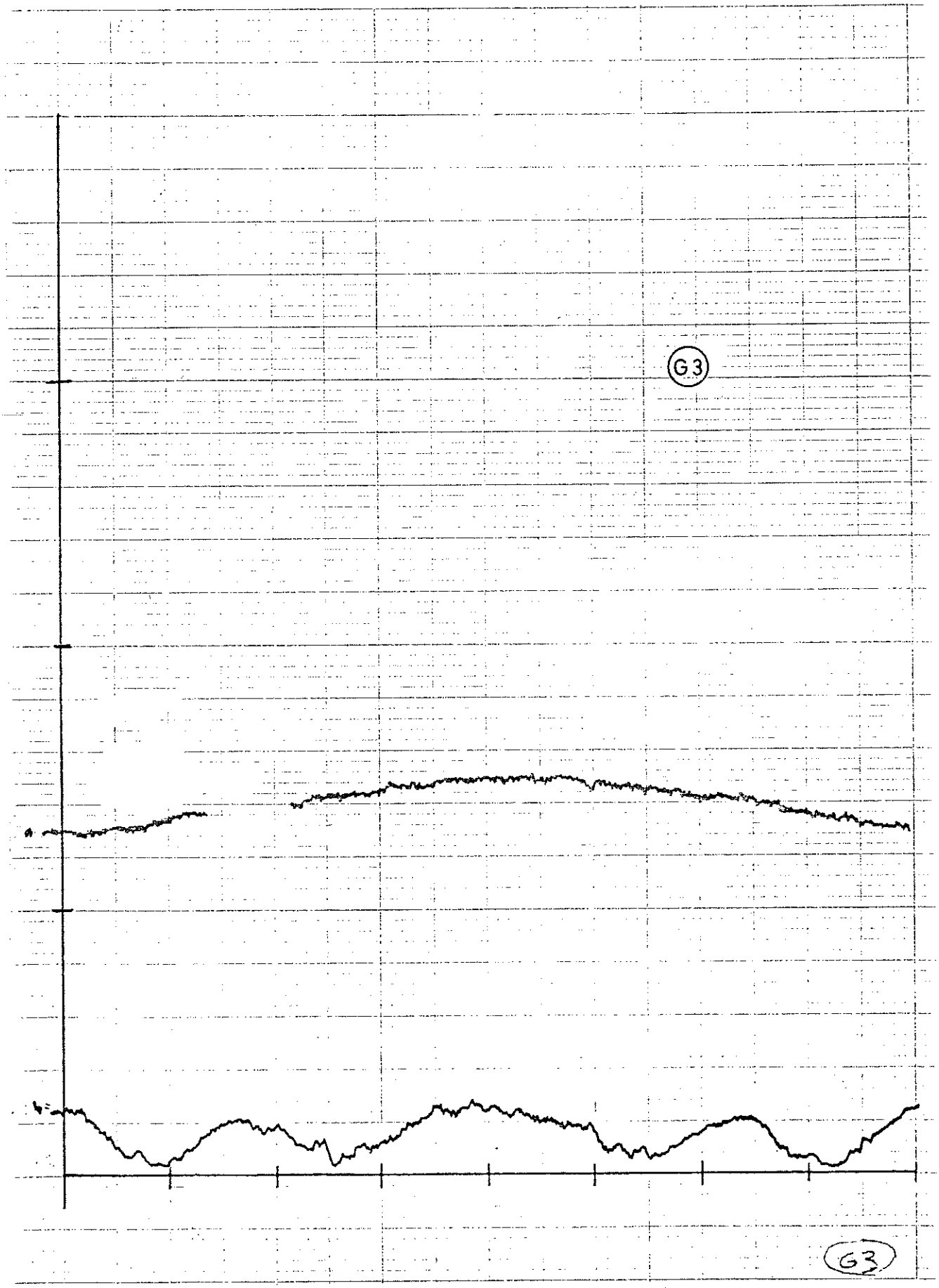
G3
G3

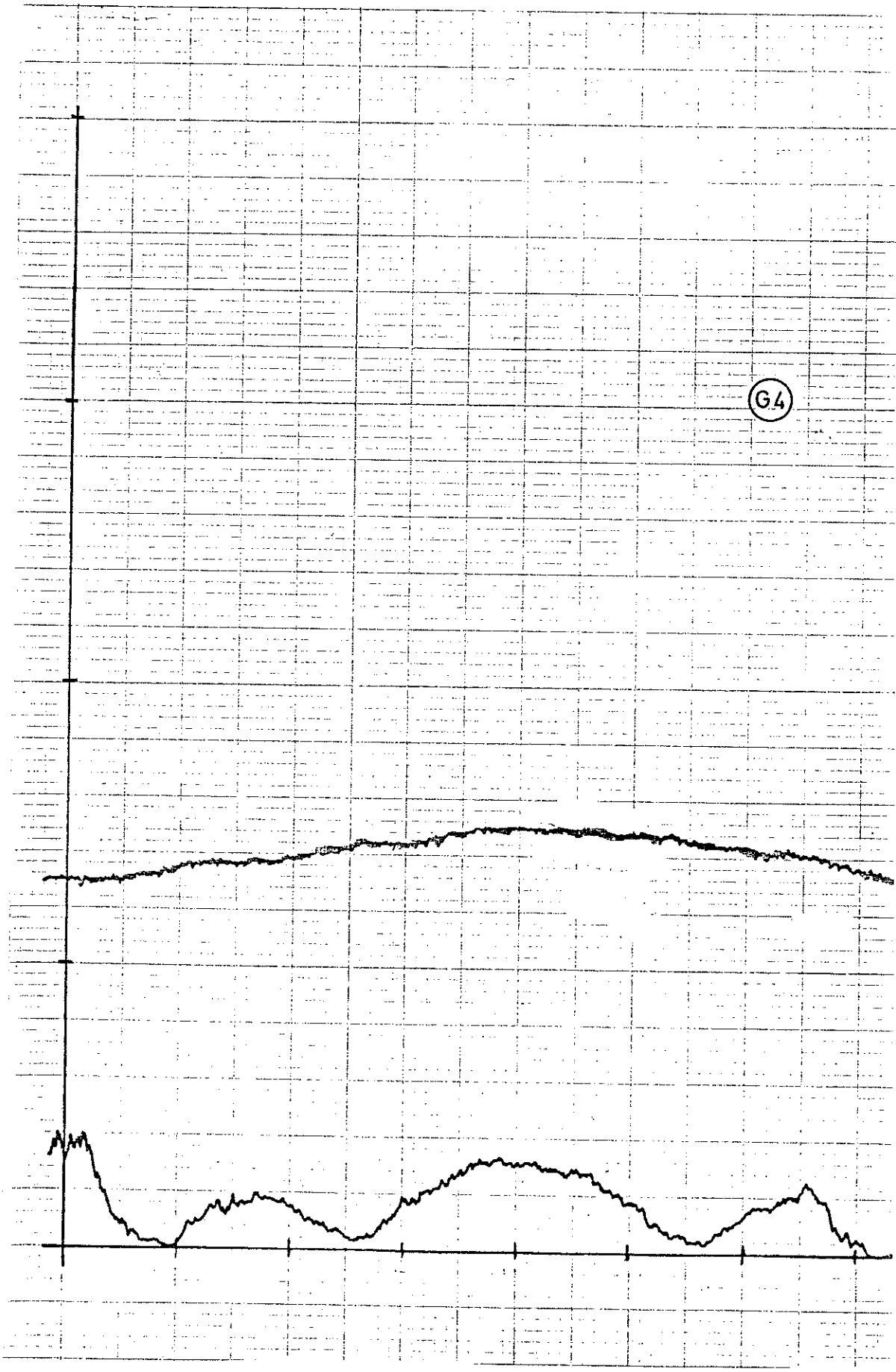
G4

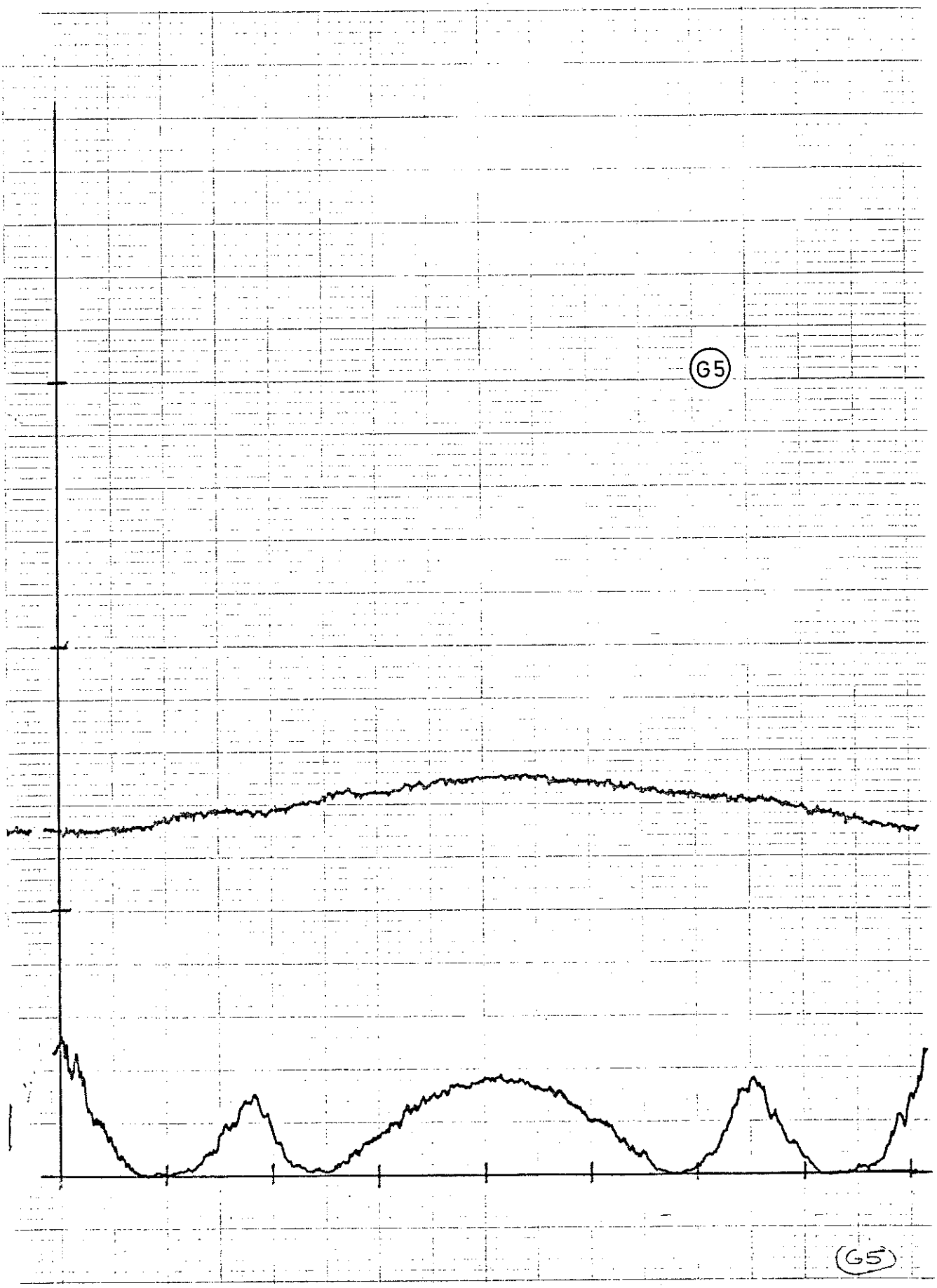
G5
G5

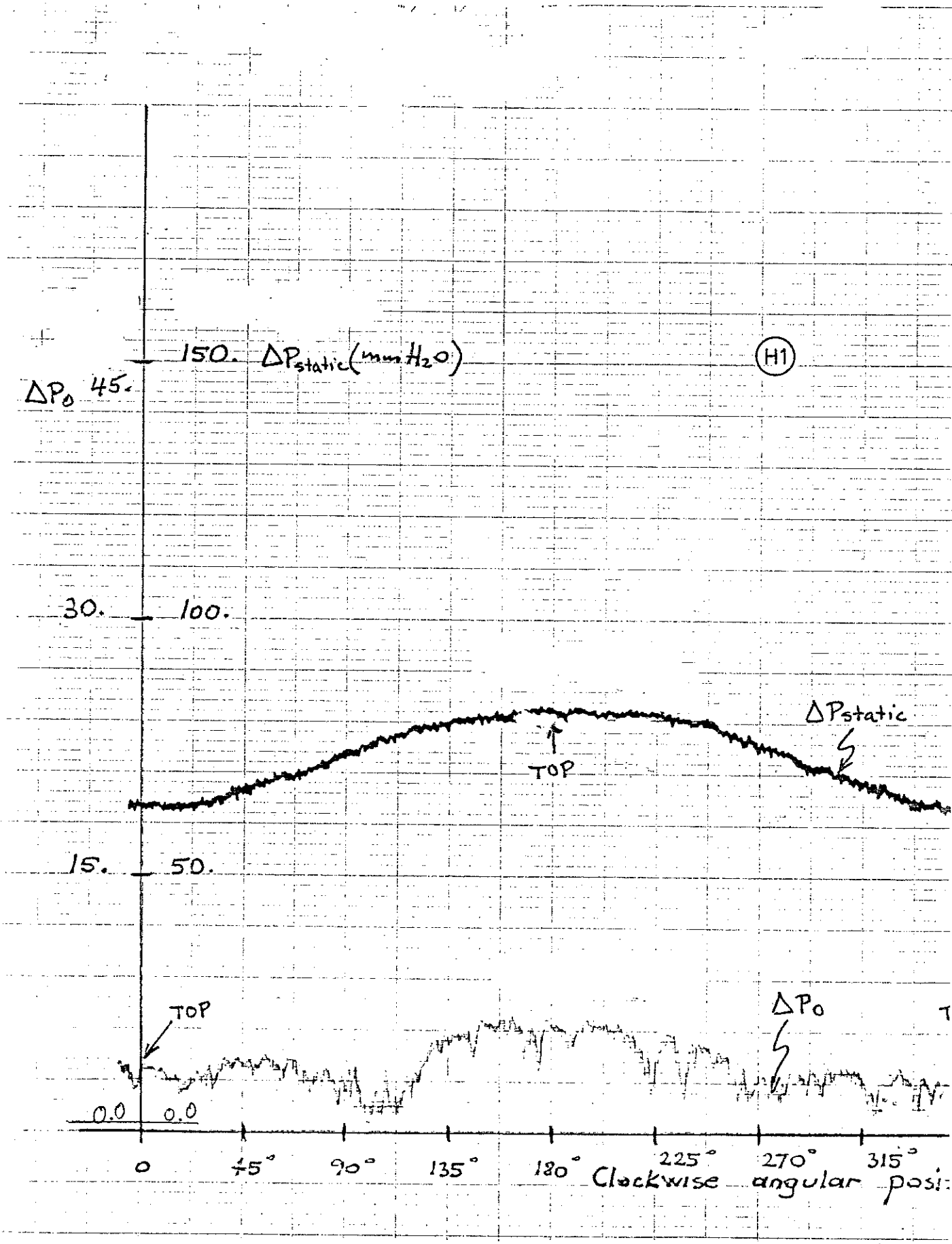
150. ΔPstatic (mm H2O)
H1
ΔP0 45.
30.
100.
ΔPstatic
TOP
15.
50.
TOP
ΔP0
0.0
0.0
0
45°
90°
135°
180°
225°
270°
315°
Clockwise angular posi

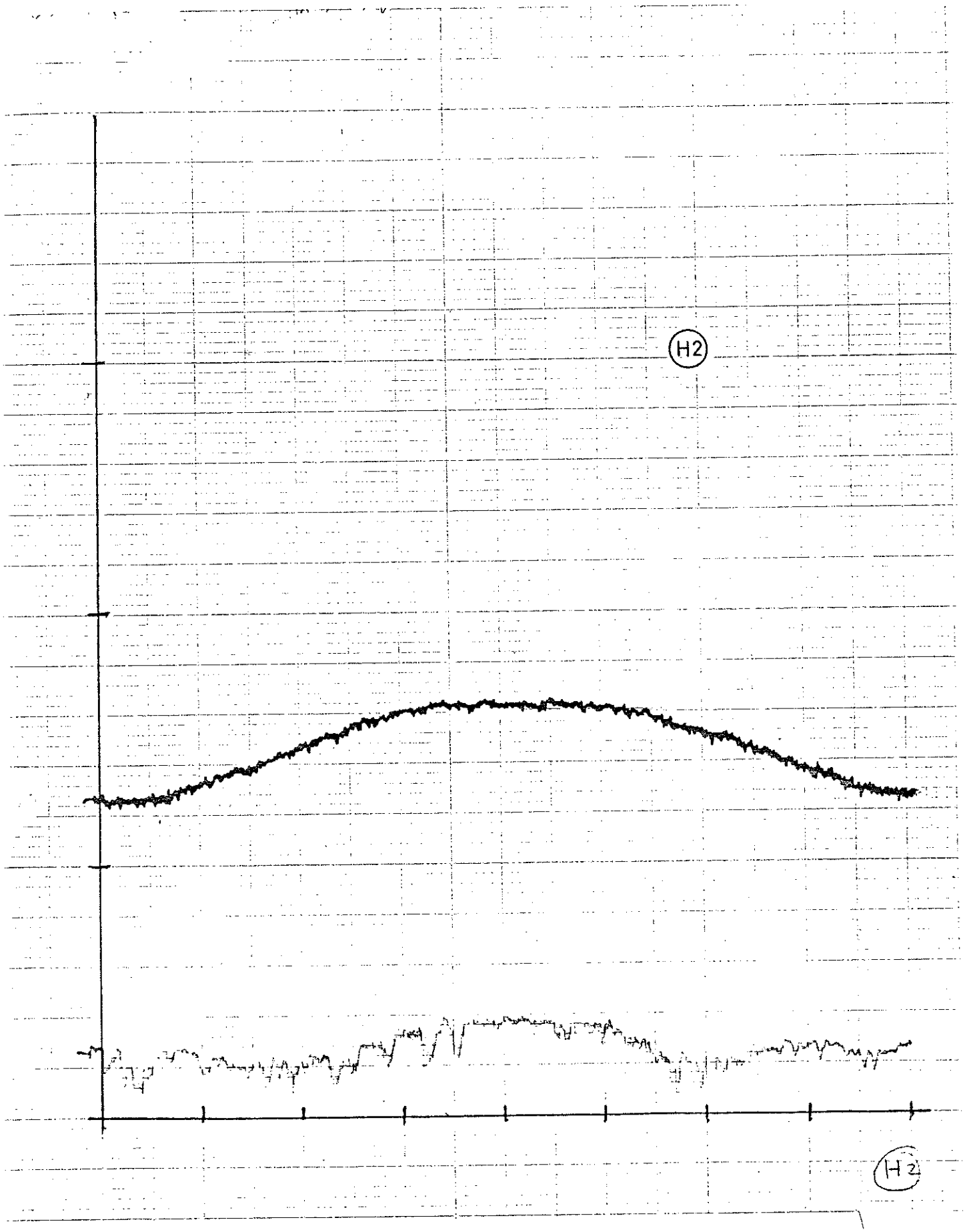
H2
H2

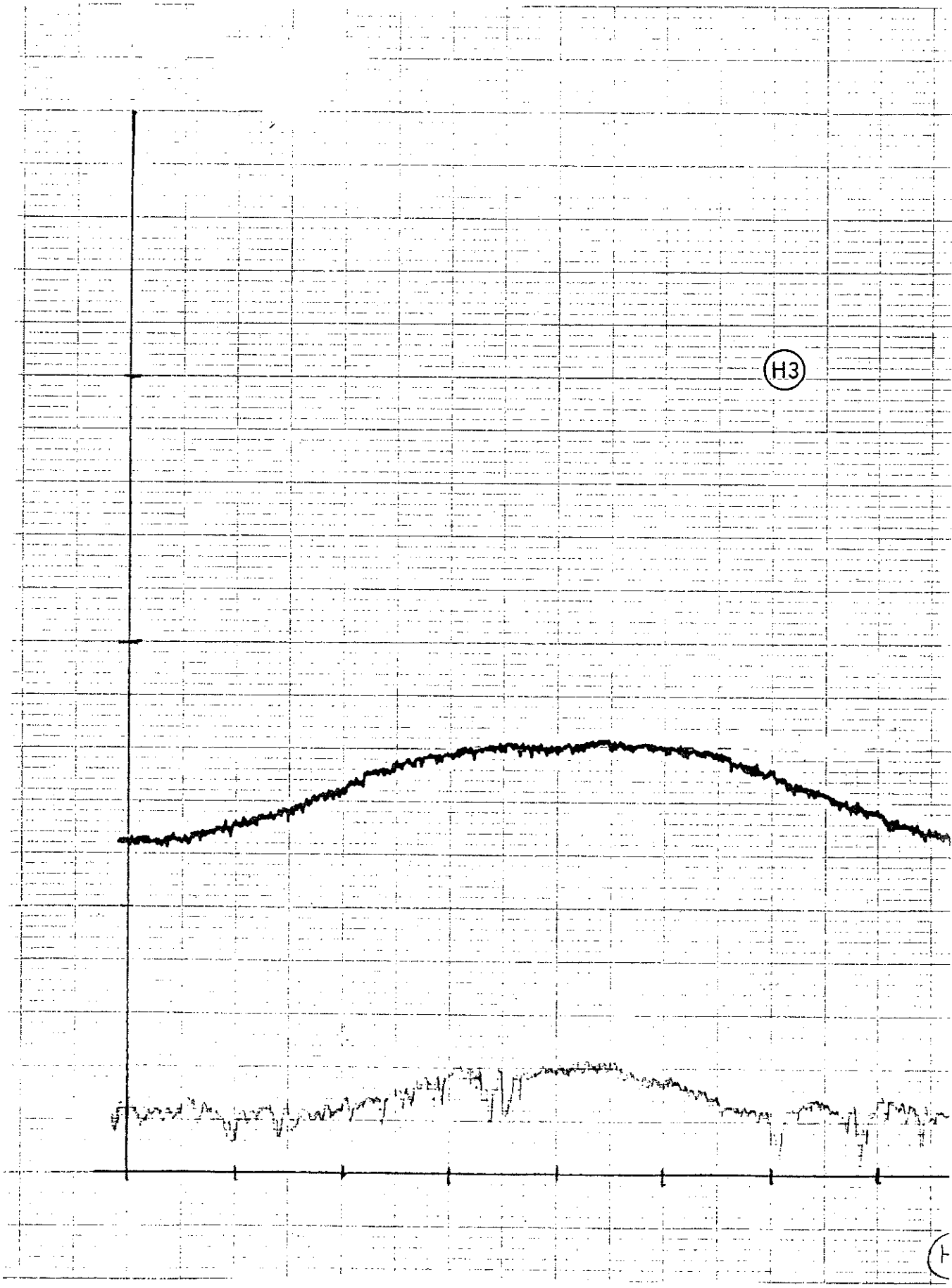
H3

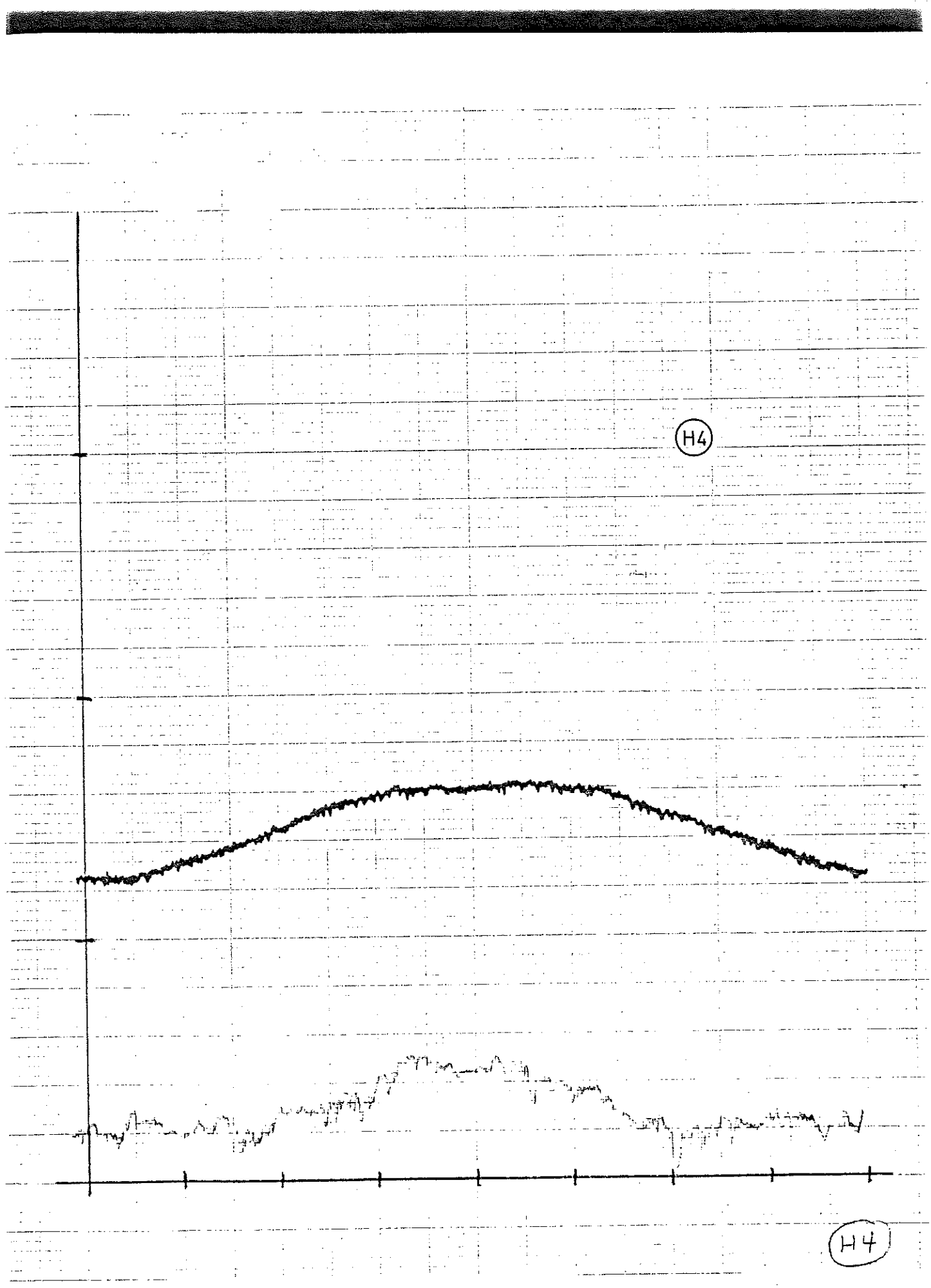
H4
H4

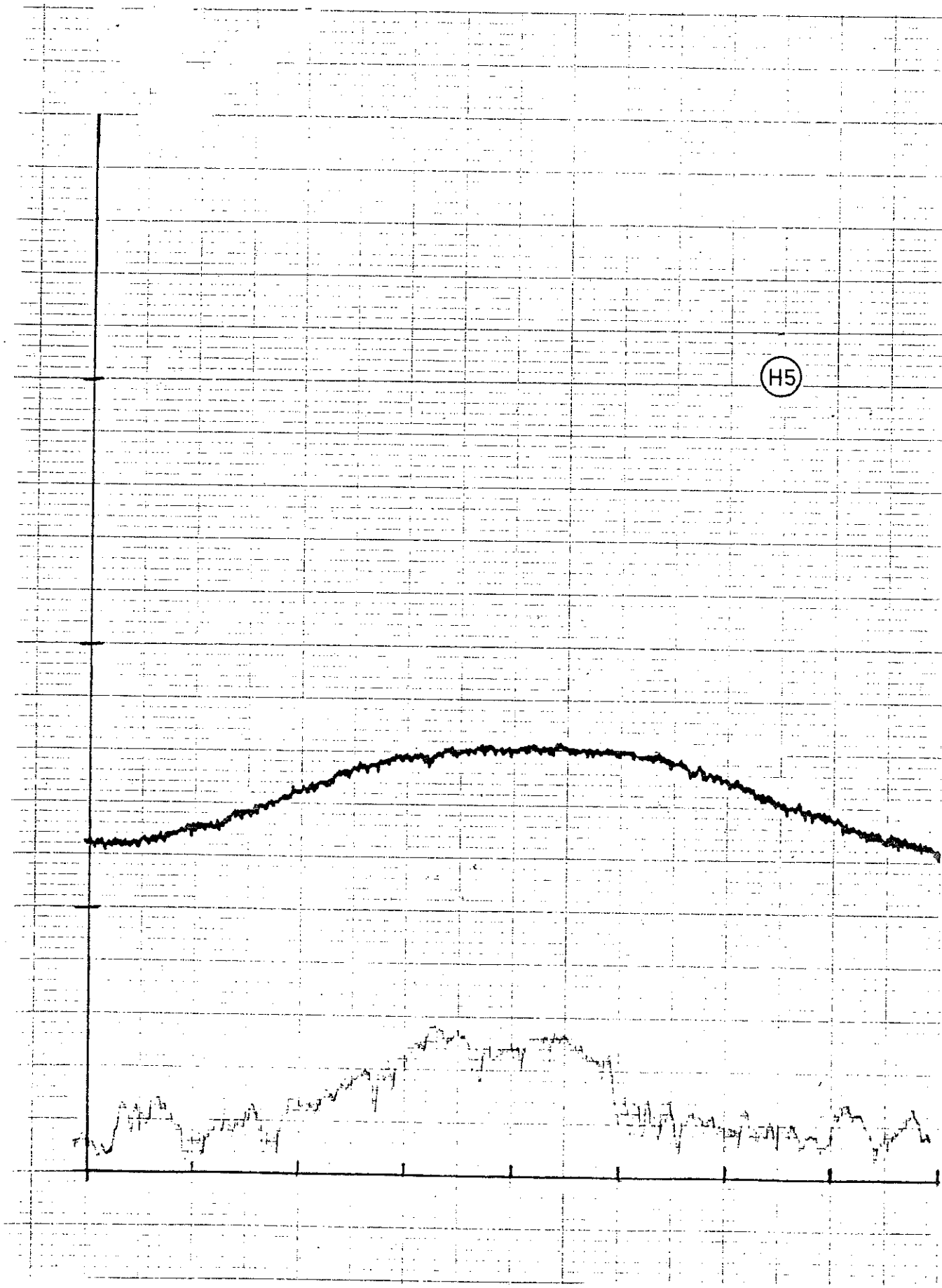
H5

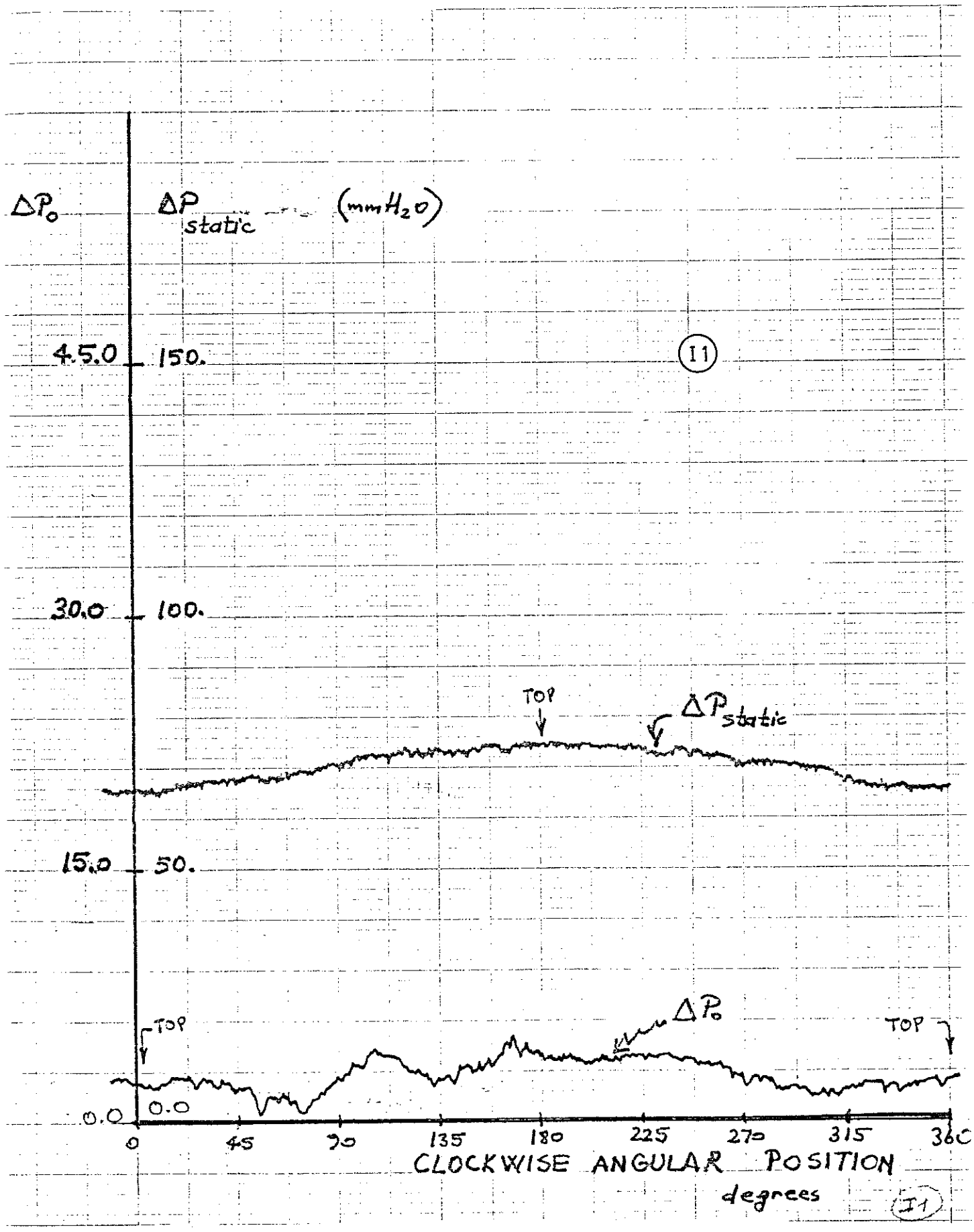
ΔP_o
ΔP_static (mmH2O)
45.0
150.
I1
30.0
100.
TOP
ΔP_static
15.0
50.
TOP
ΔP_o
TOP
0.0
0.0
0
45
90
135
180
225
270
315
360
CLOCKWISE ANGULAR POSITION
degrees
I1

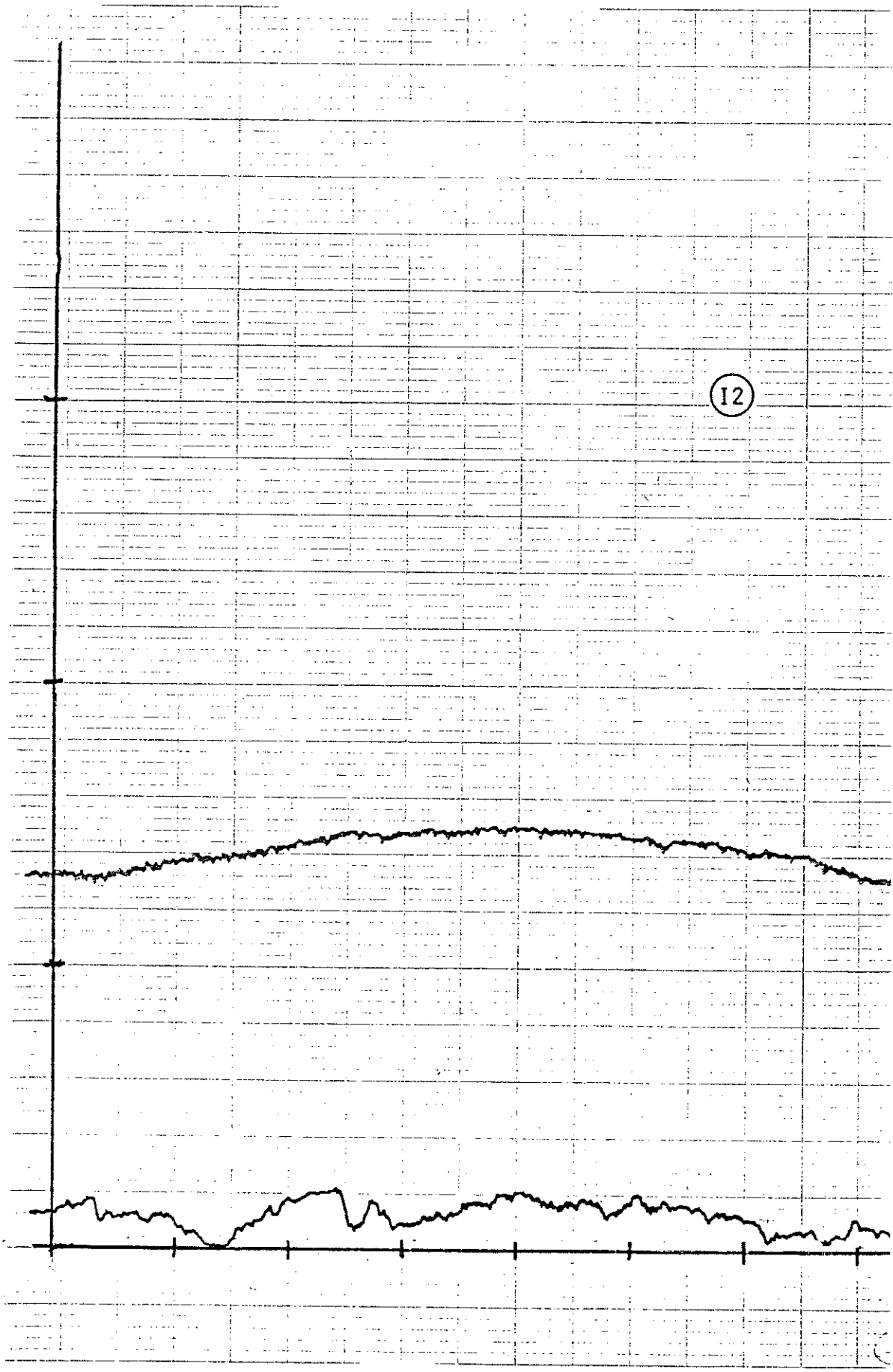
I2

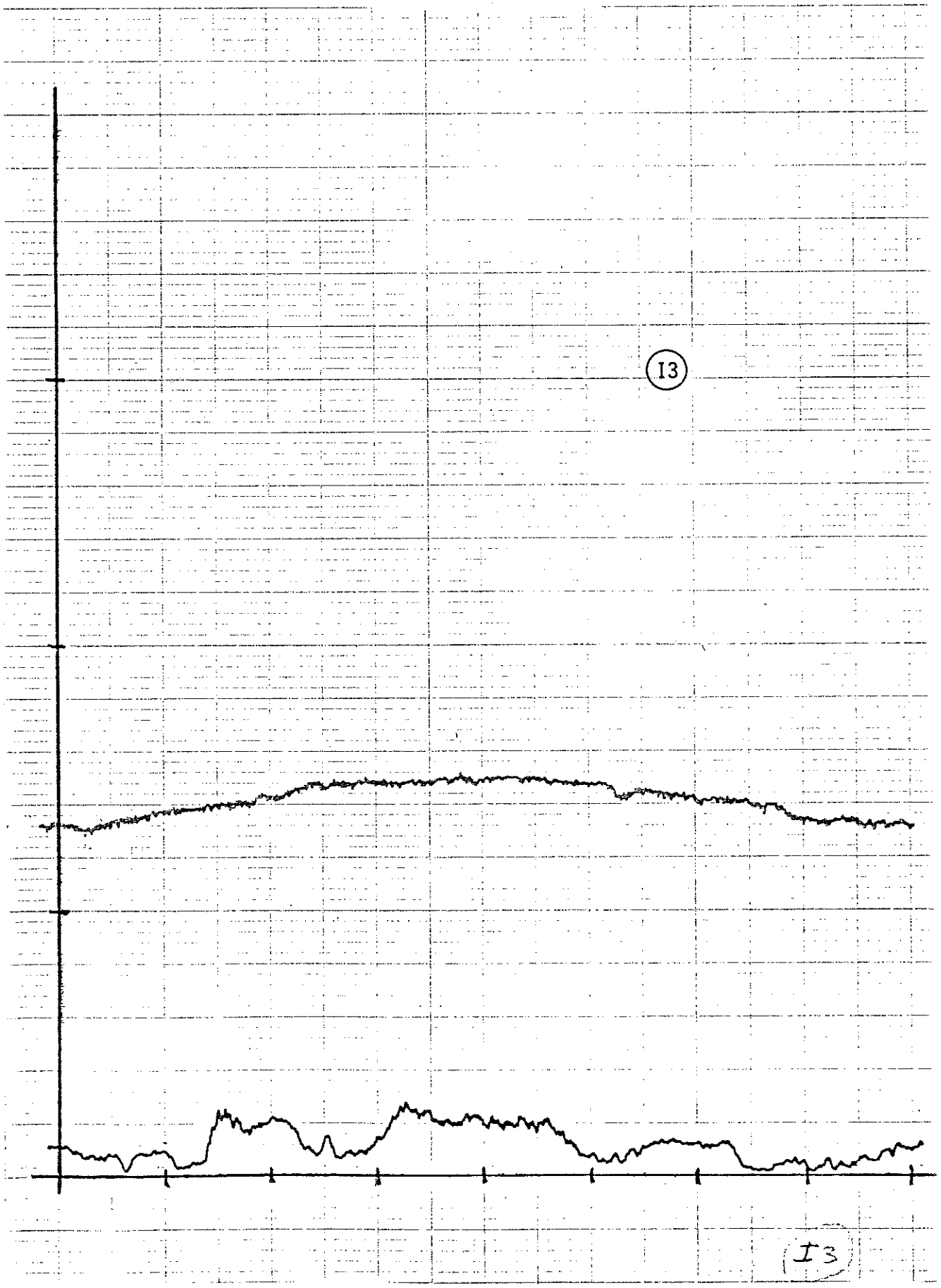
I3
I3

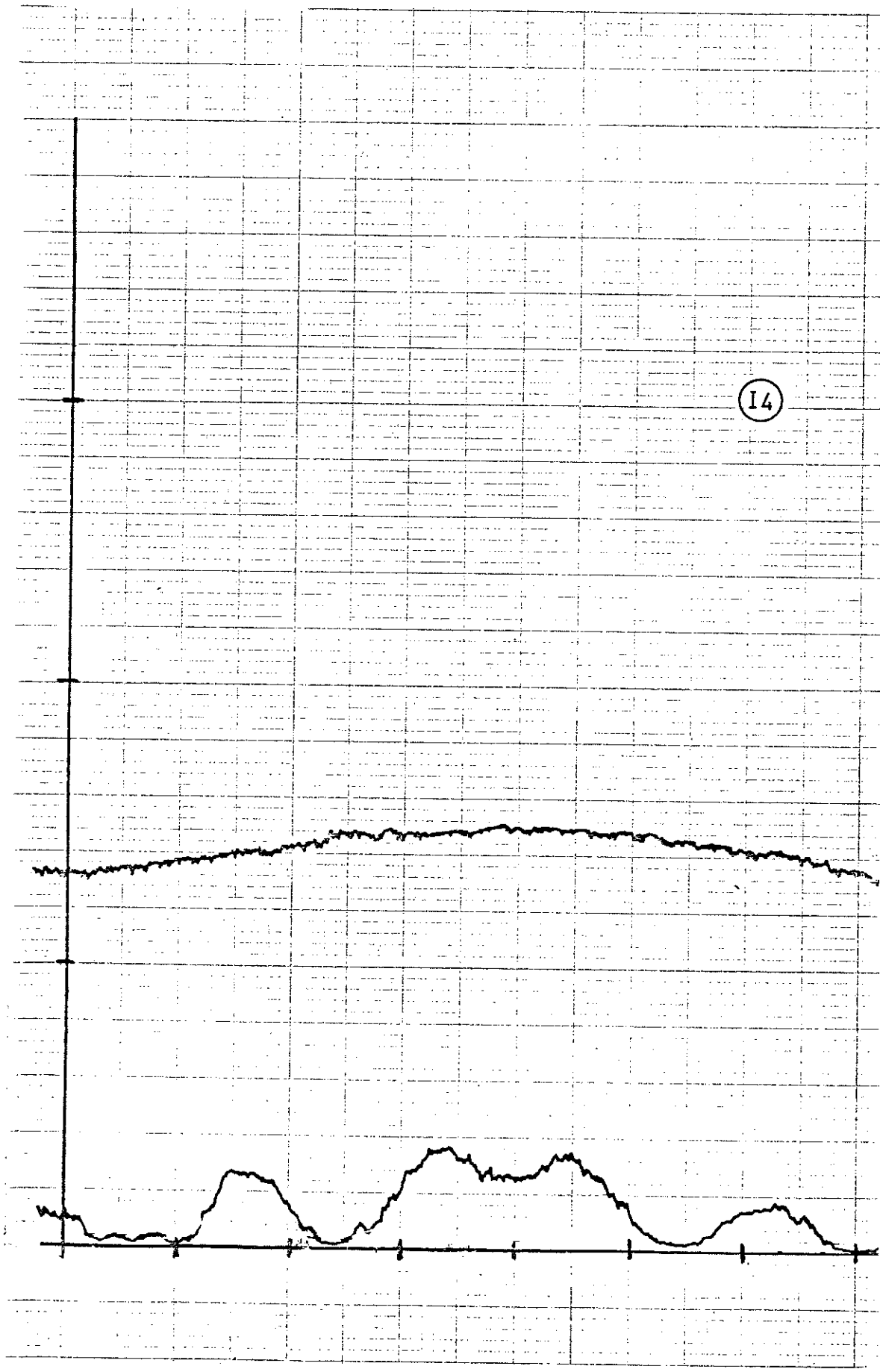
I4

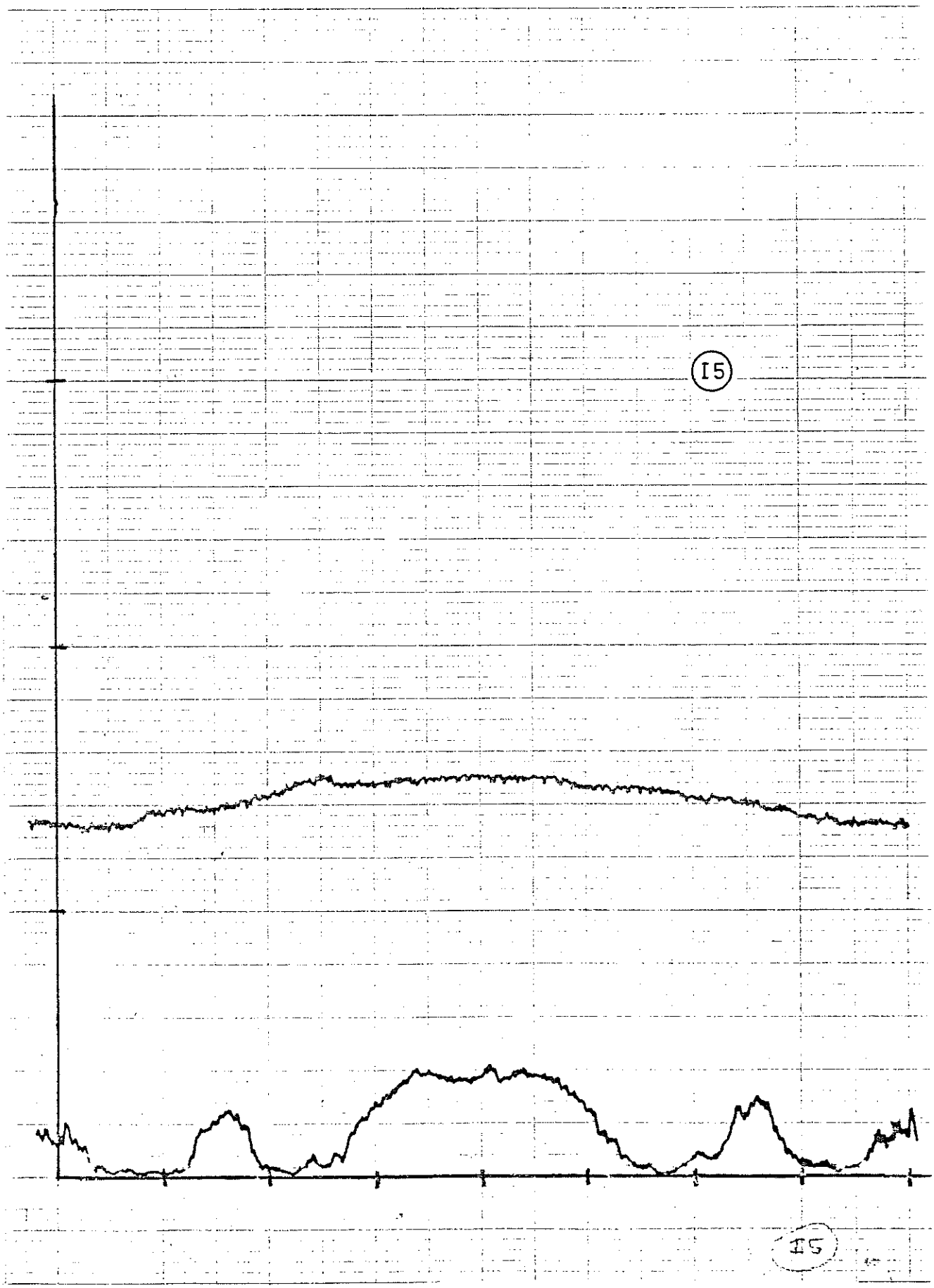
I5
I5

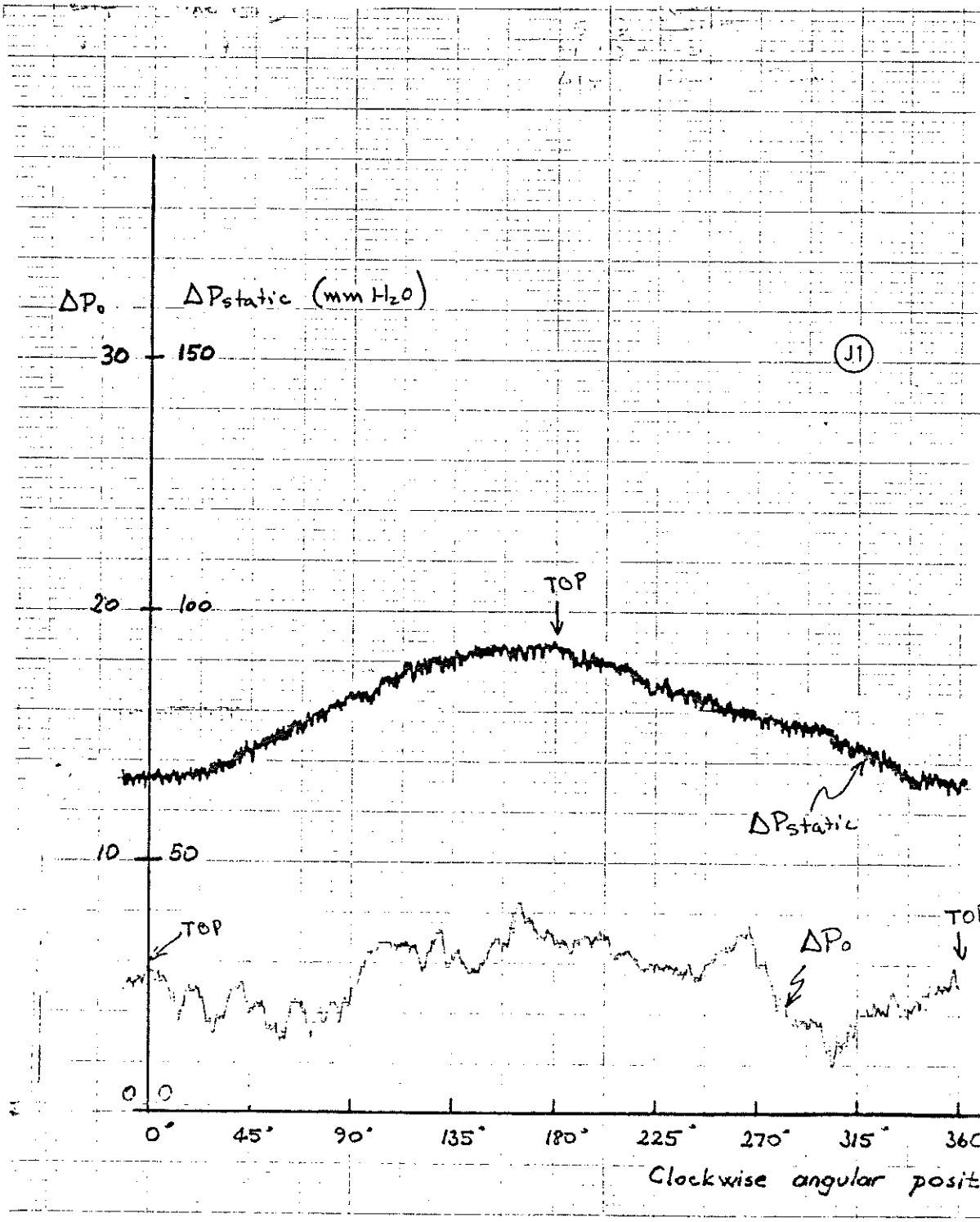
ΔP₀
ΔPstatic (mm H₂O)
30
150
J1
20
100
TOP
ΔPstatic
10
50
TOP
ΔP₀
0
0
0°
45°
90°
135°
180°
225°
270°
315°
Clockwise angular posit

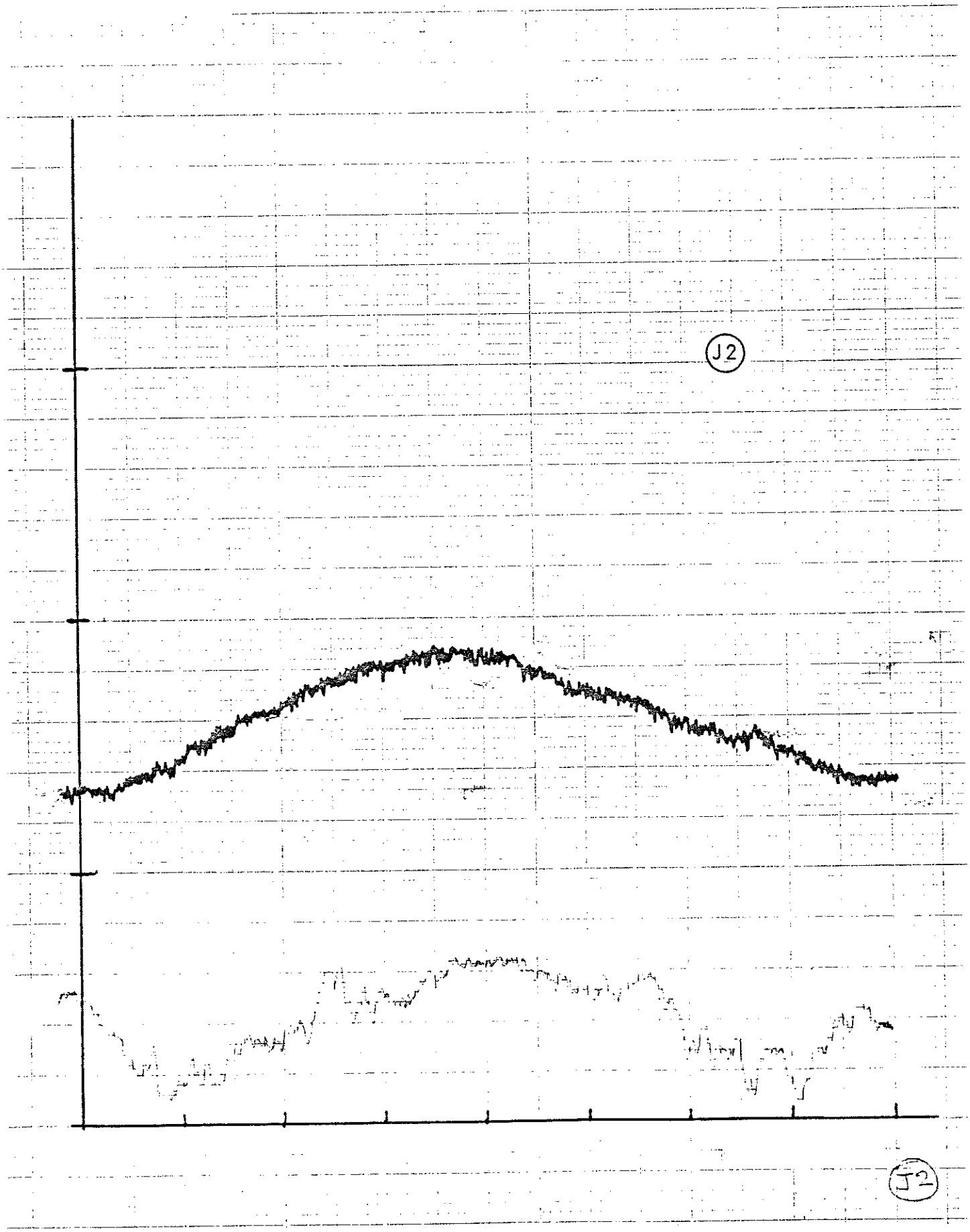
J2
J2

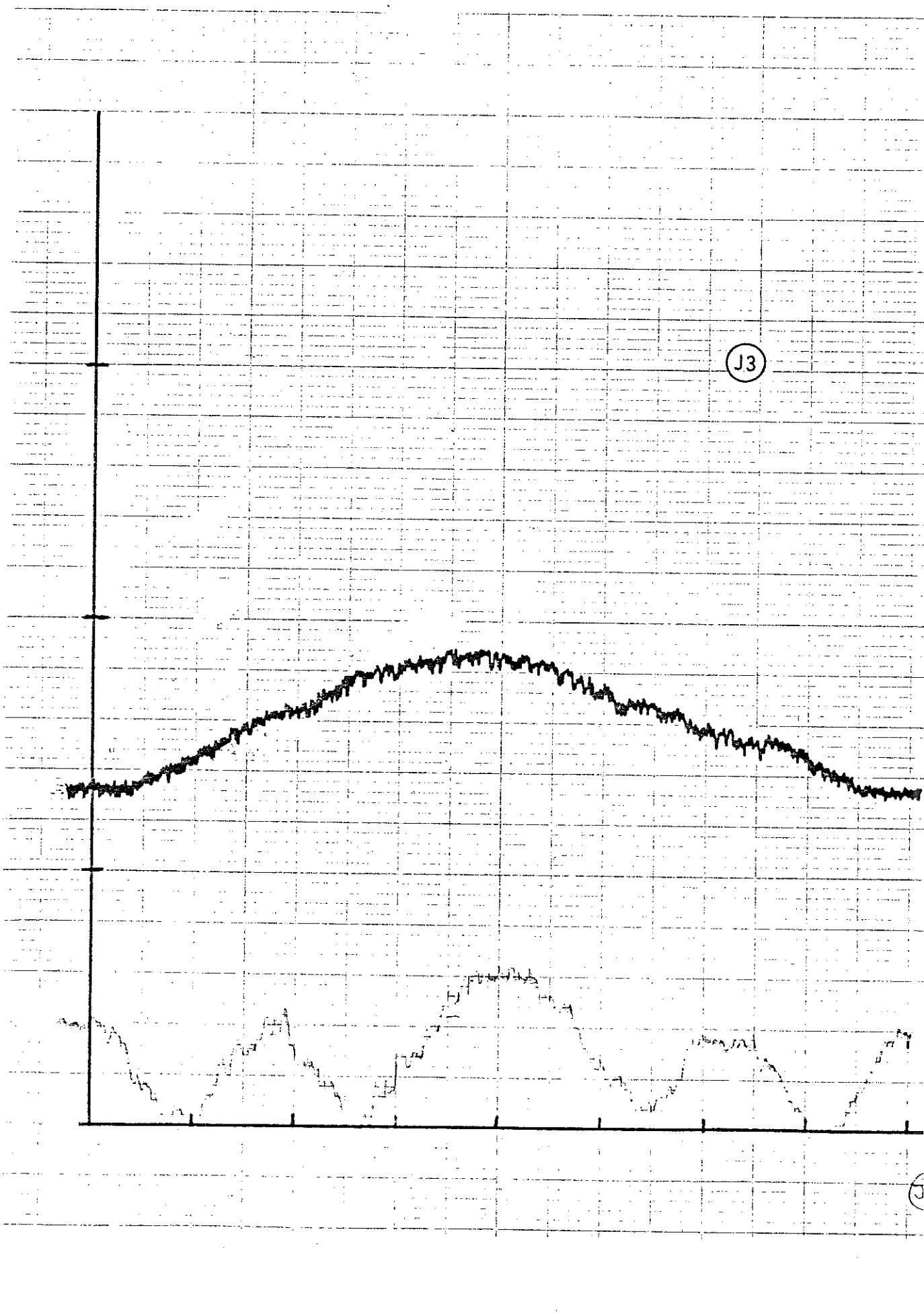
J3

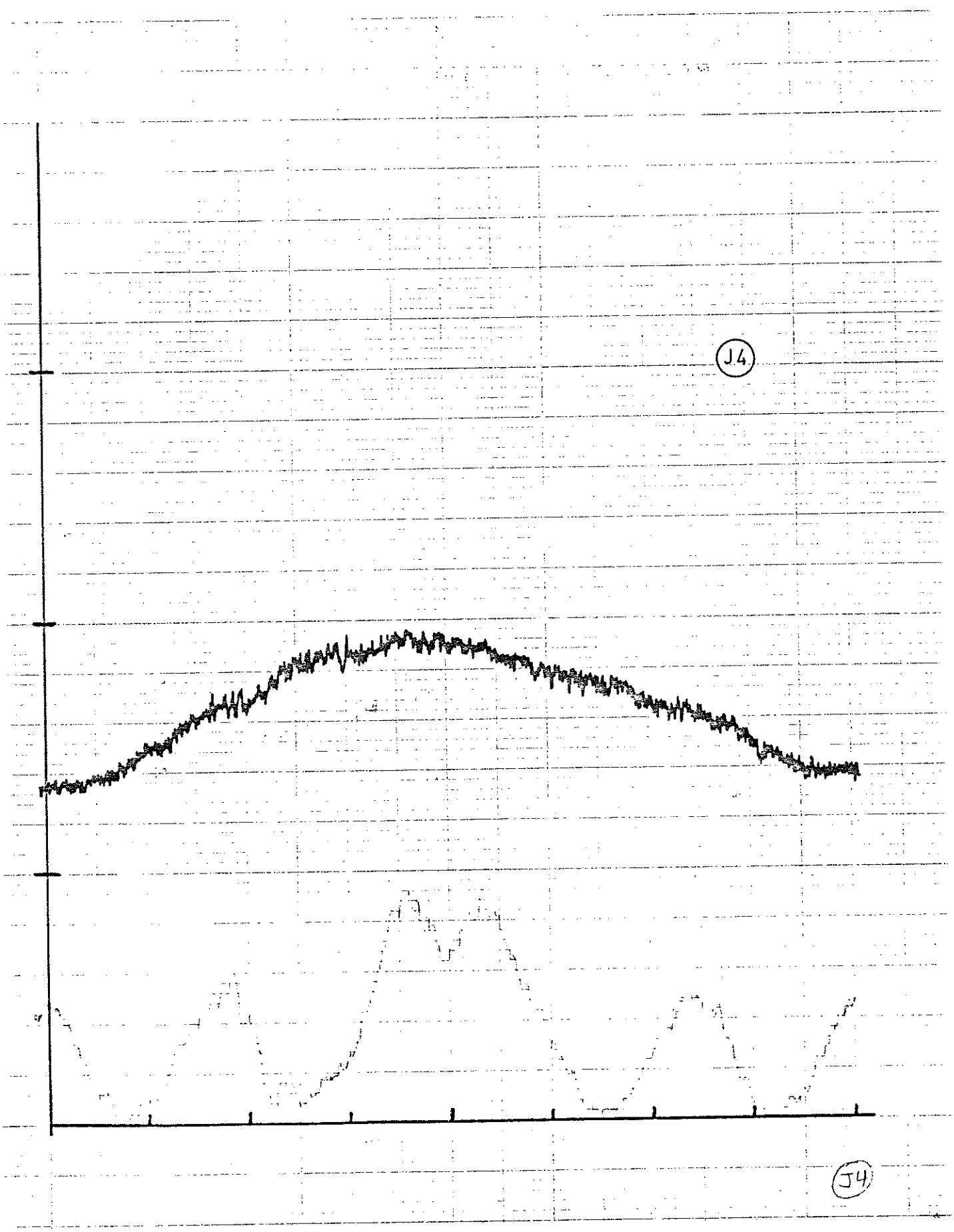
J4
J4

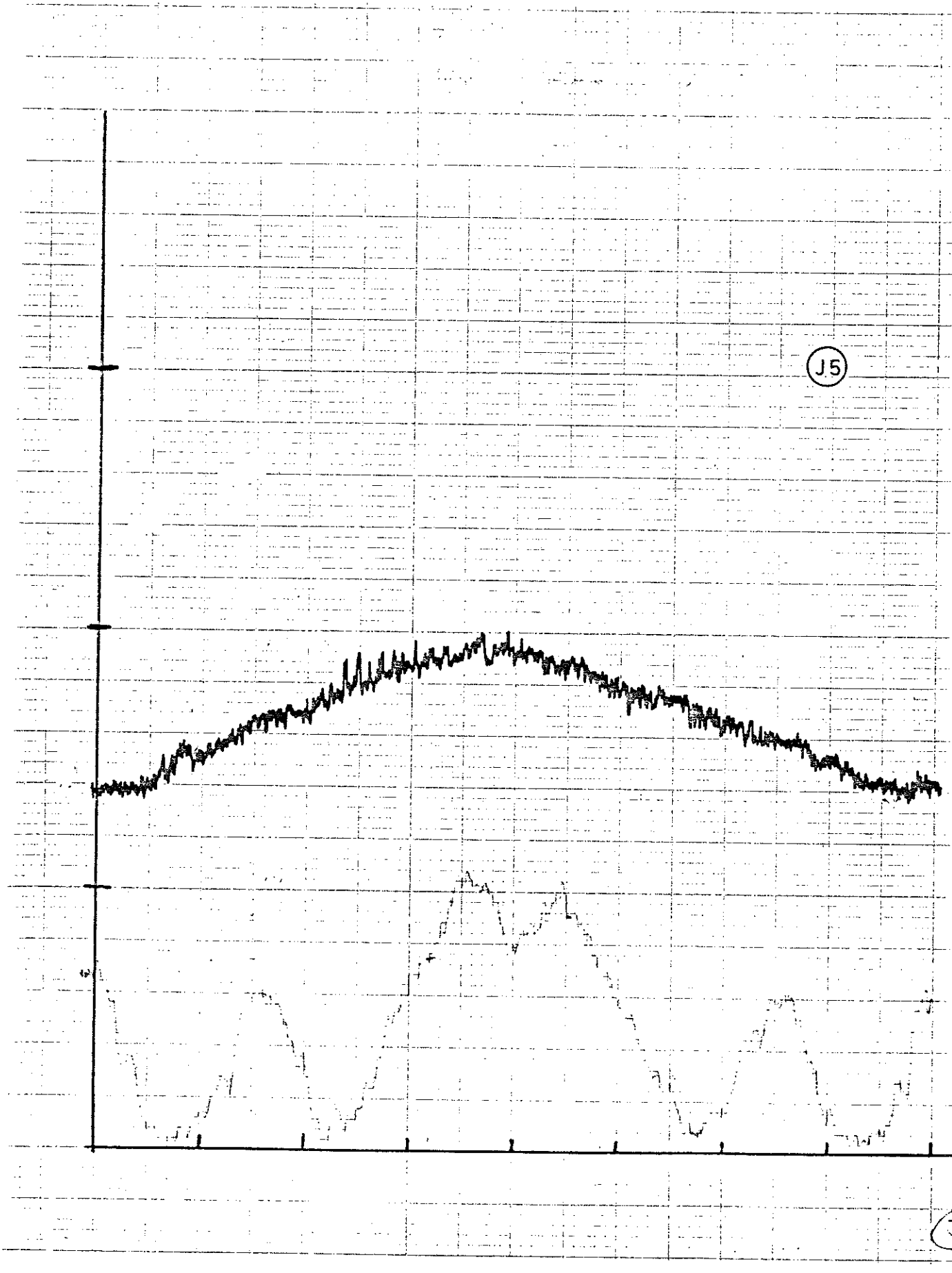
J5

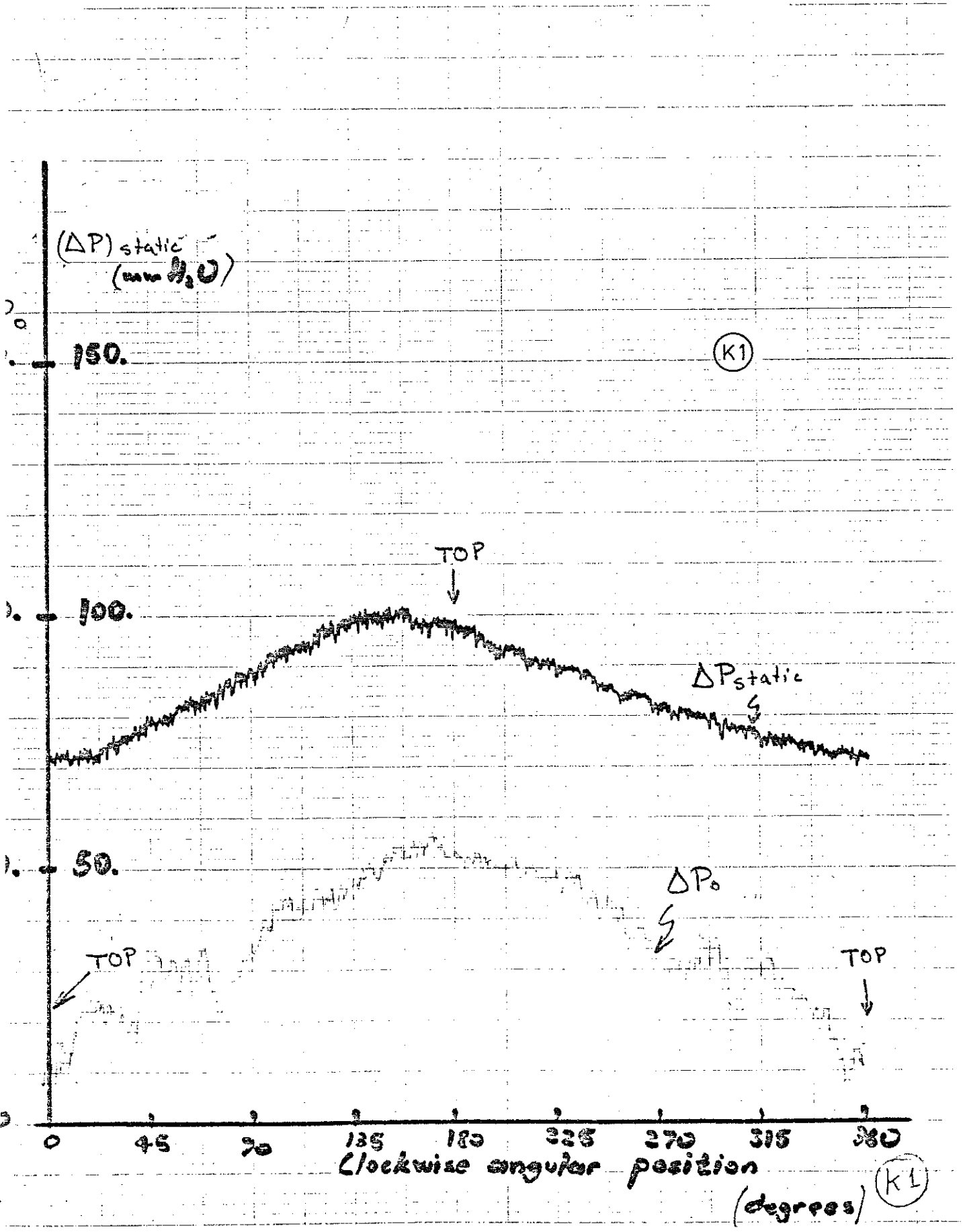
(ΔP) static
(mm H2O)
150.
100.
50.
K1
TOP
ΔPstatic
ΔPo
TOP
TOP
0
45
90
135
180
225
270
315
360
Clockwise angular position
(degrees)
K1

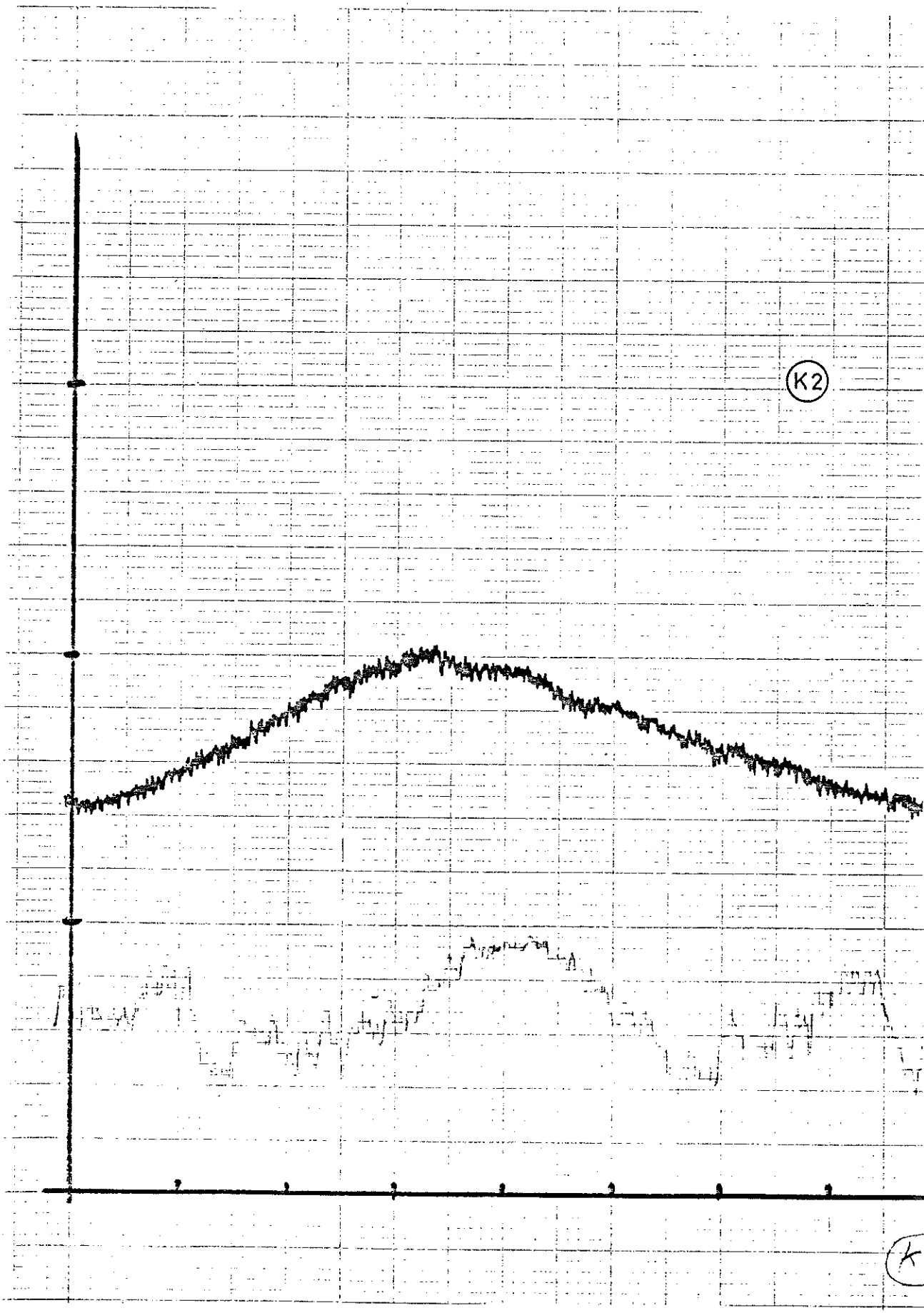
K2

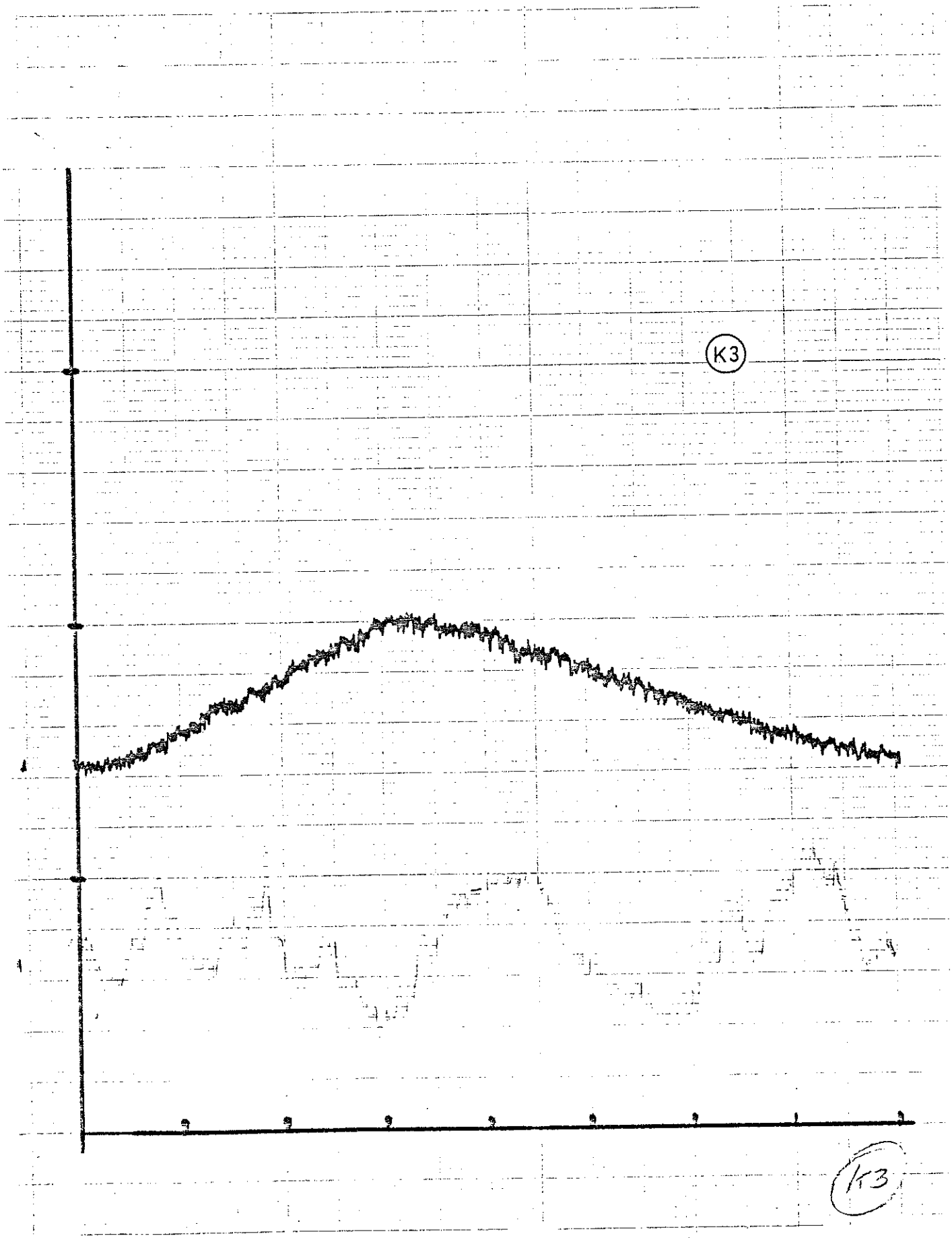
K3
KT3

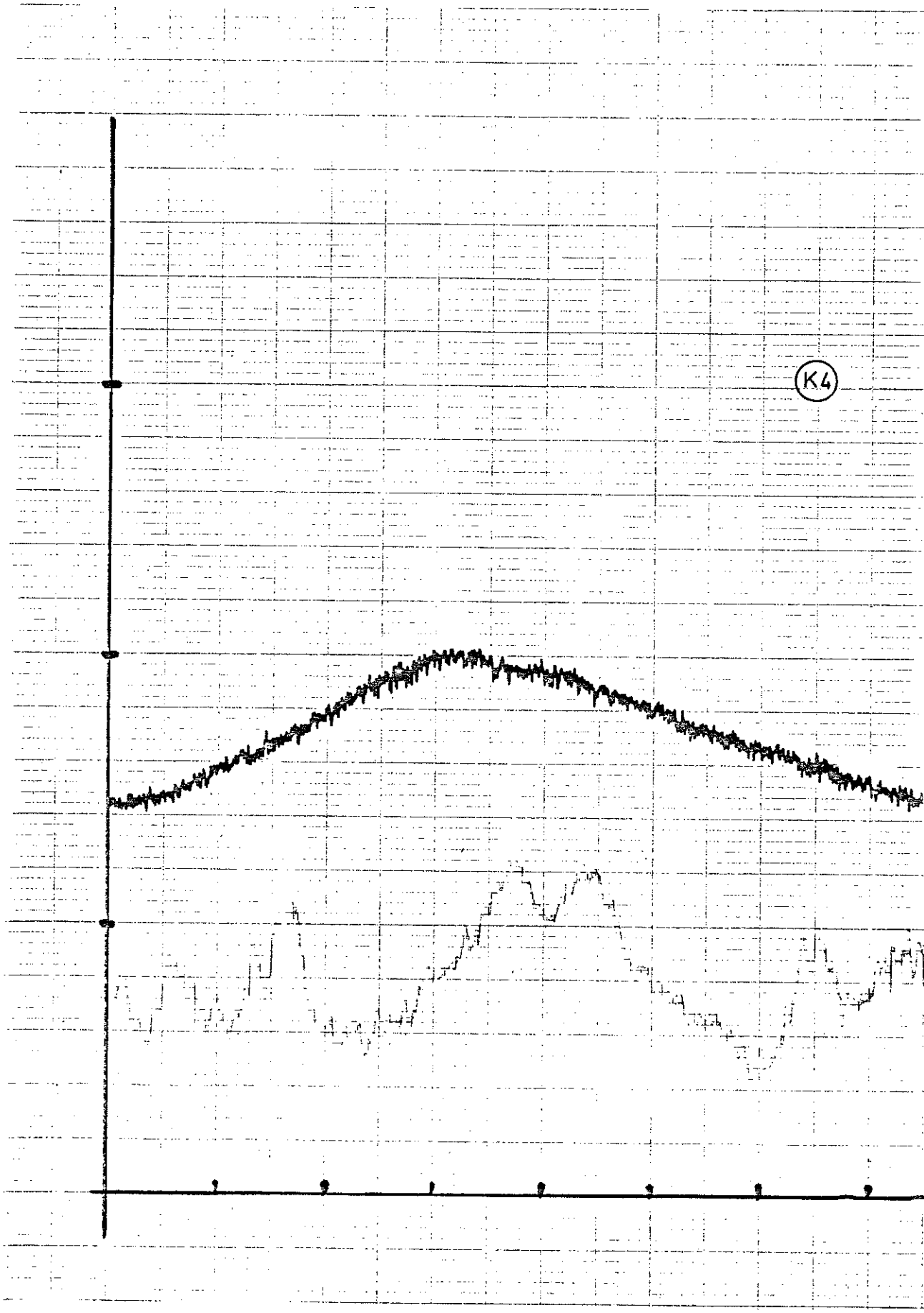
K4

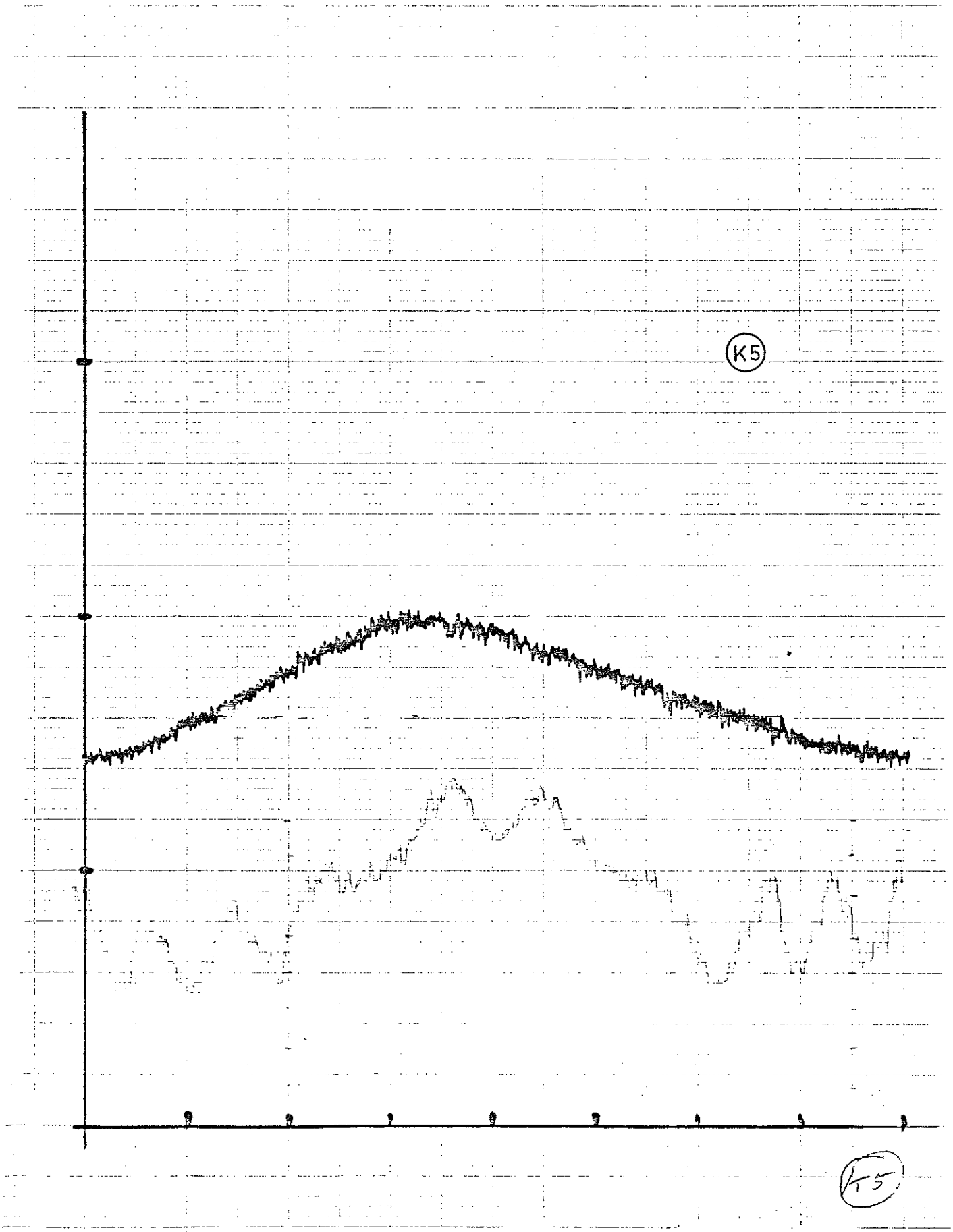
K5
K5

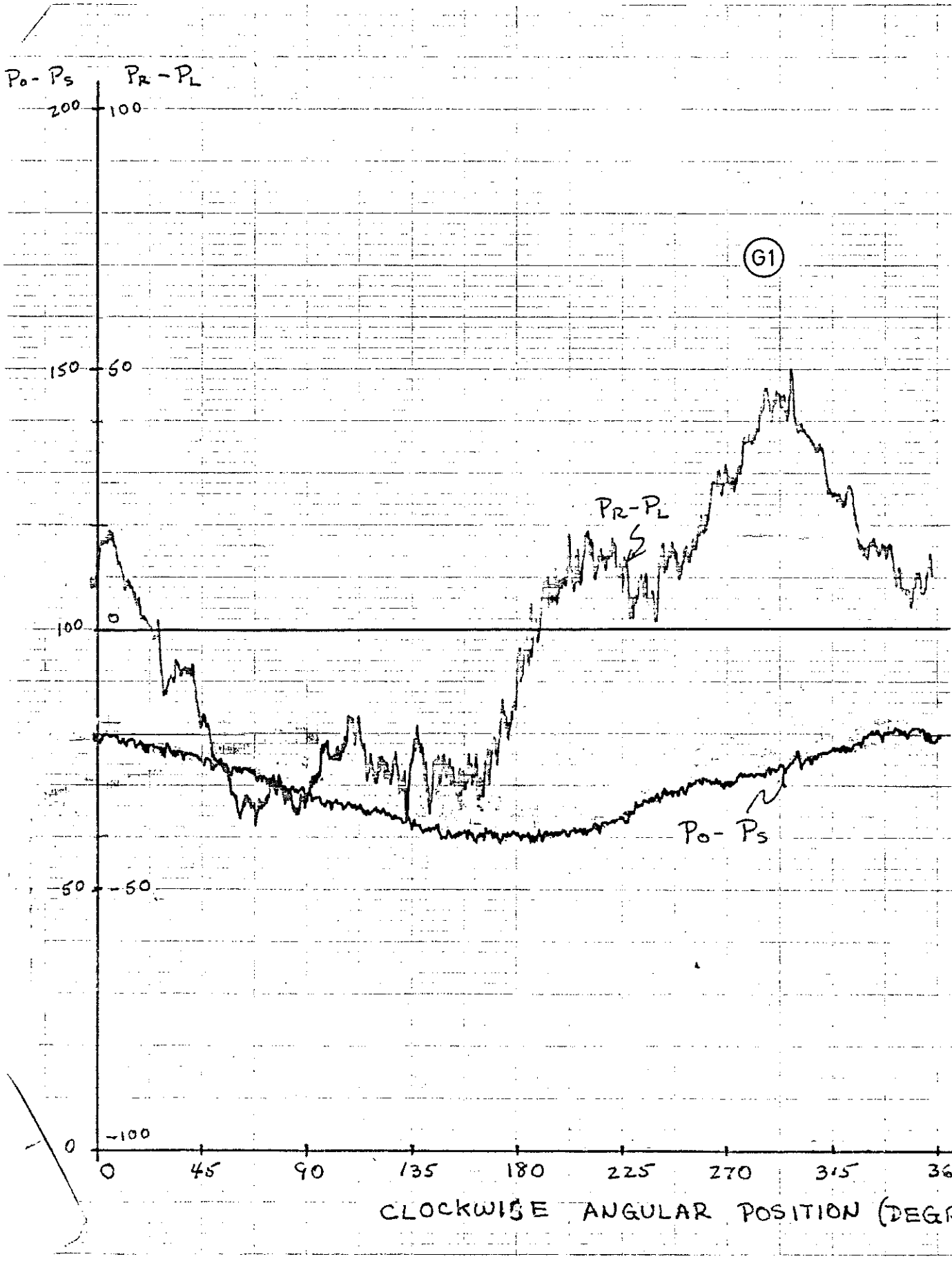
$P_o - P_s$
$P_R - P_L$
200
100
150
50
100
0
-50
-50
0
-100
G1
$P_R - P_L$
$P_o - P_s$
0
45
90
135
180
225
270
315
CLOCKWISE ANGULAR POSITION (DEGR

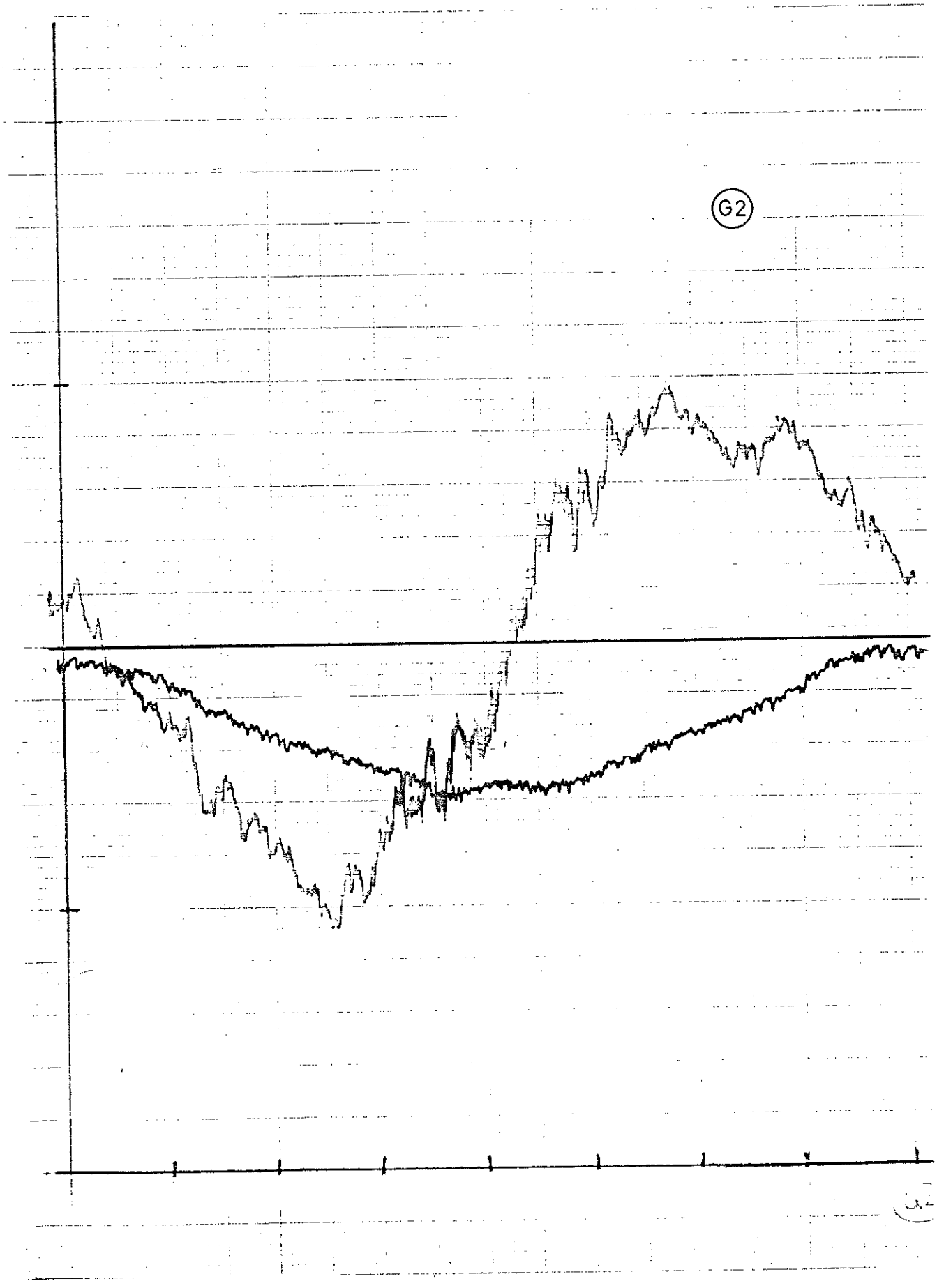
G2

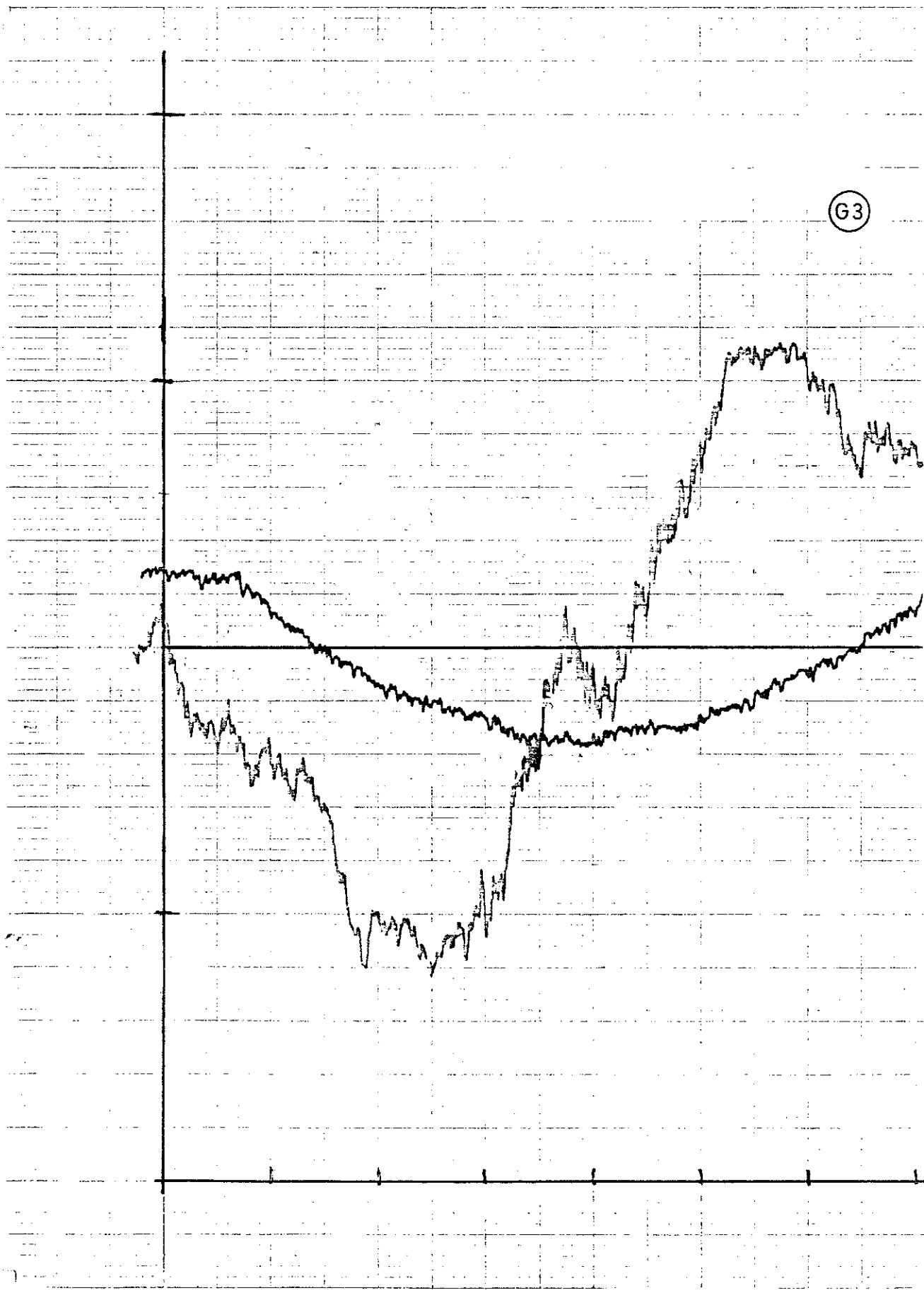
G3

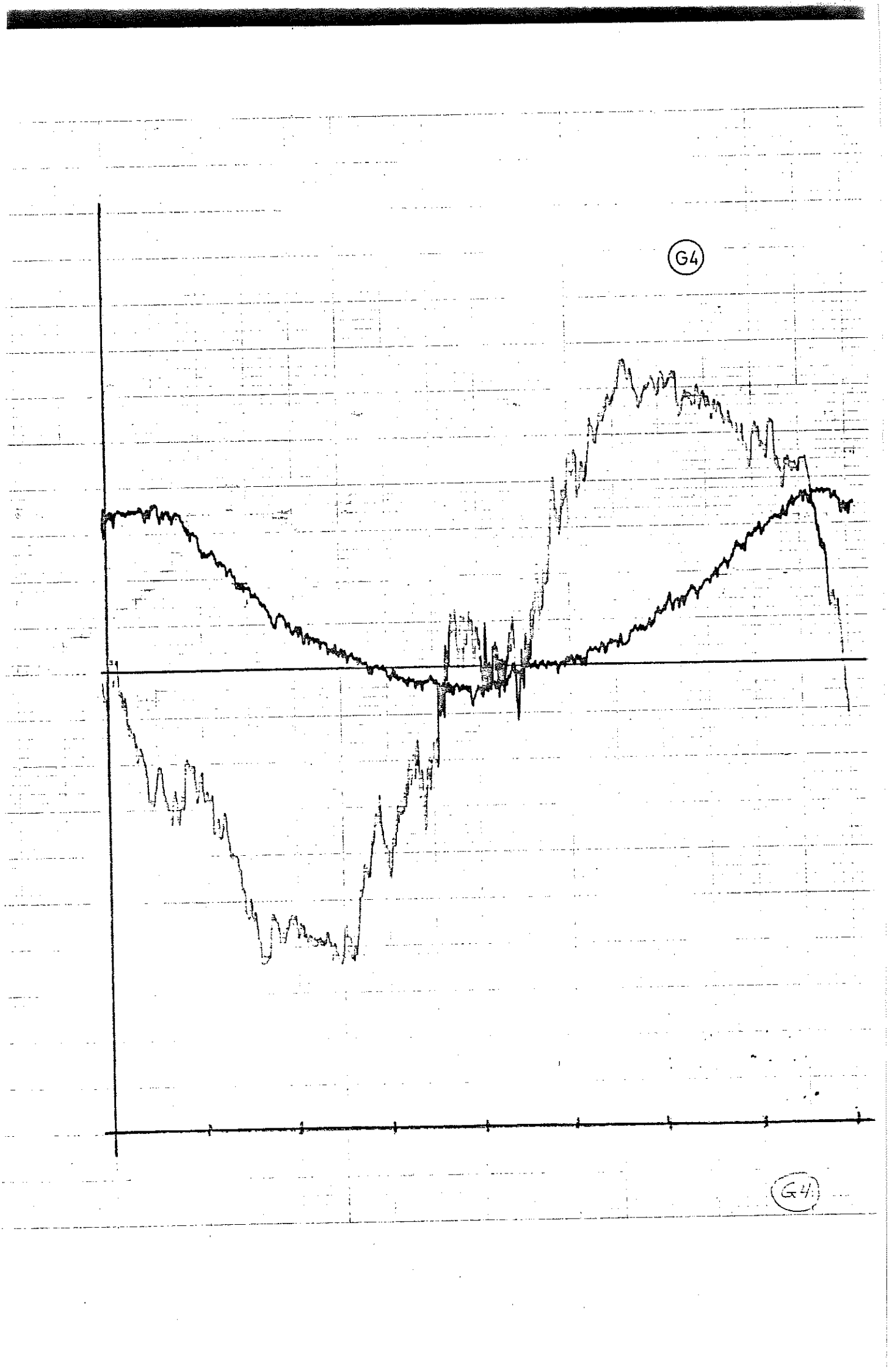
G4
G4

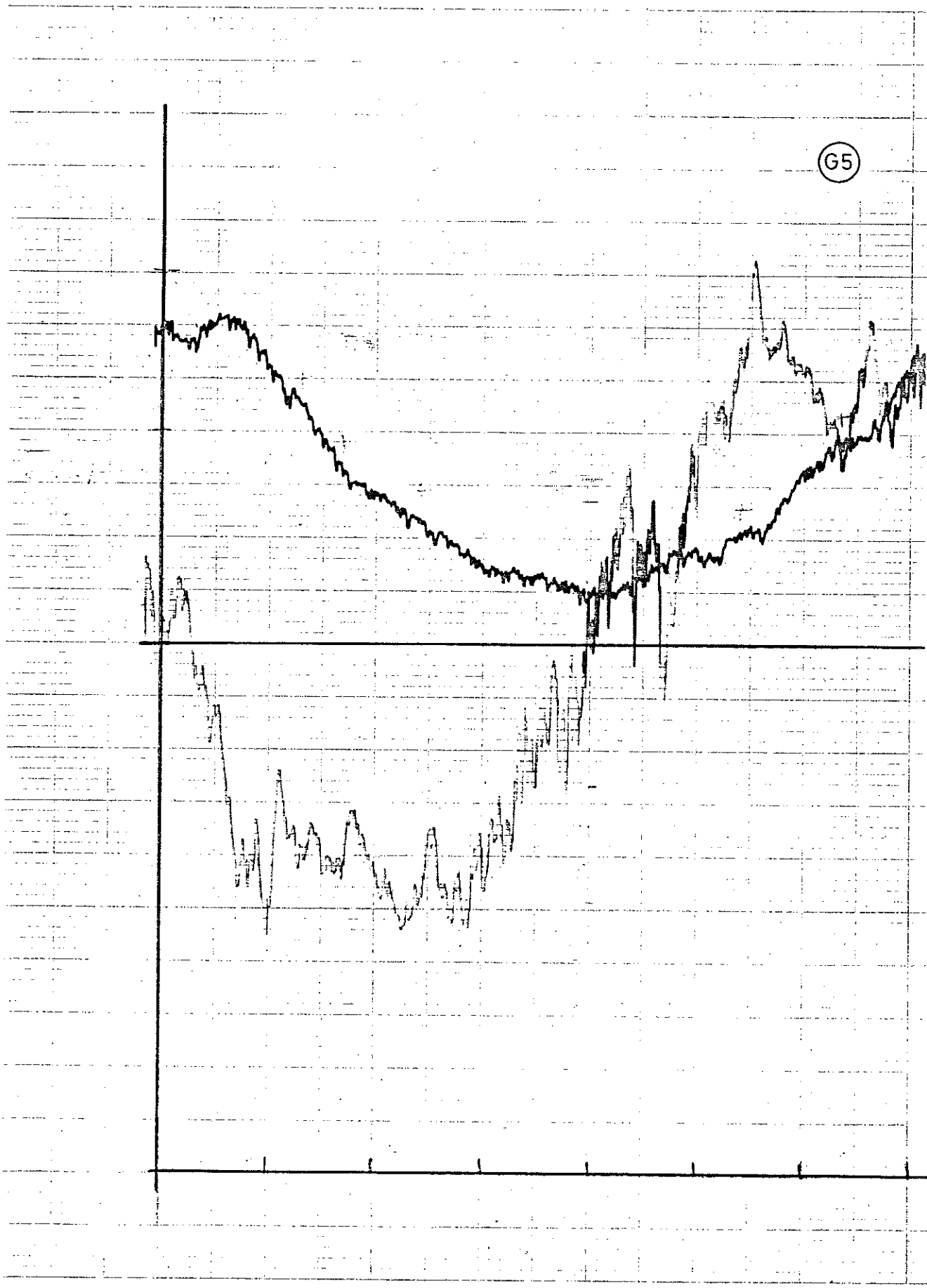
G5

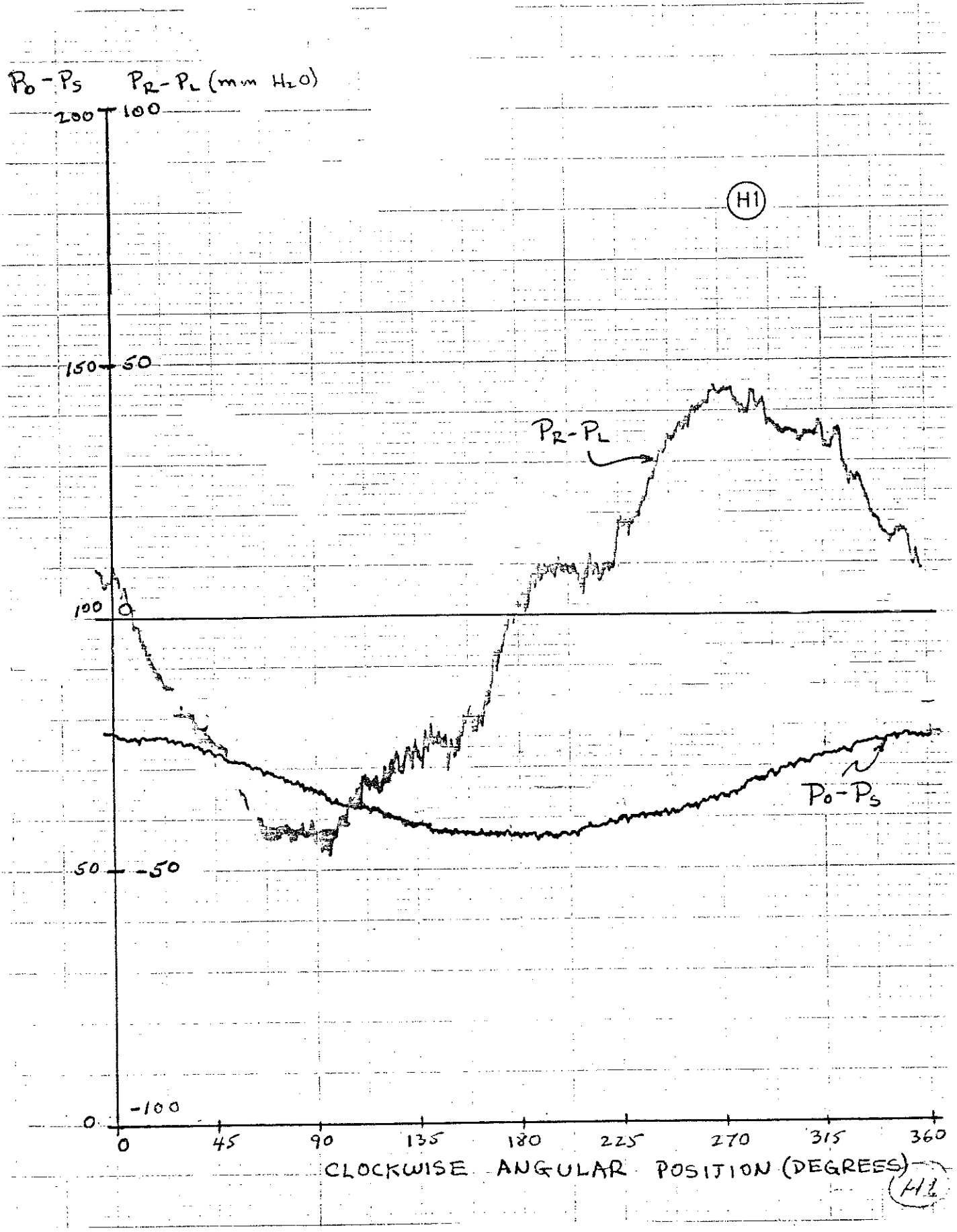
$P_o - P_s$
$P_R - P_L$ (mm H_2O)
200
100
150
50
100
0
50
-50
0
-100
H1
$P_R - P_L$
$P_o - P_s$
0
45
90
135
180
225
270
315
360
CLOCKWISE ANGULAR POSITION (DEGREES)
H1

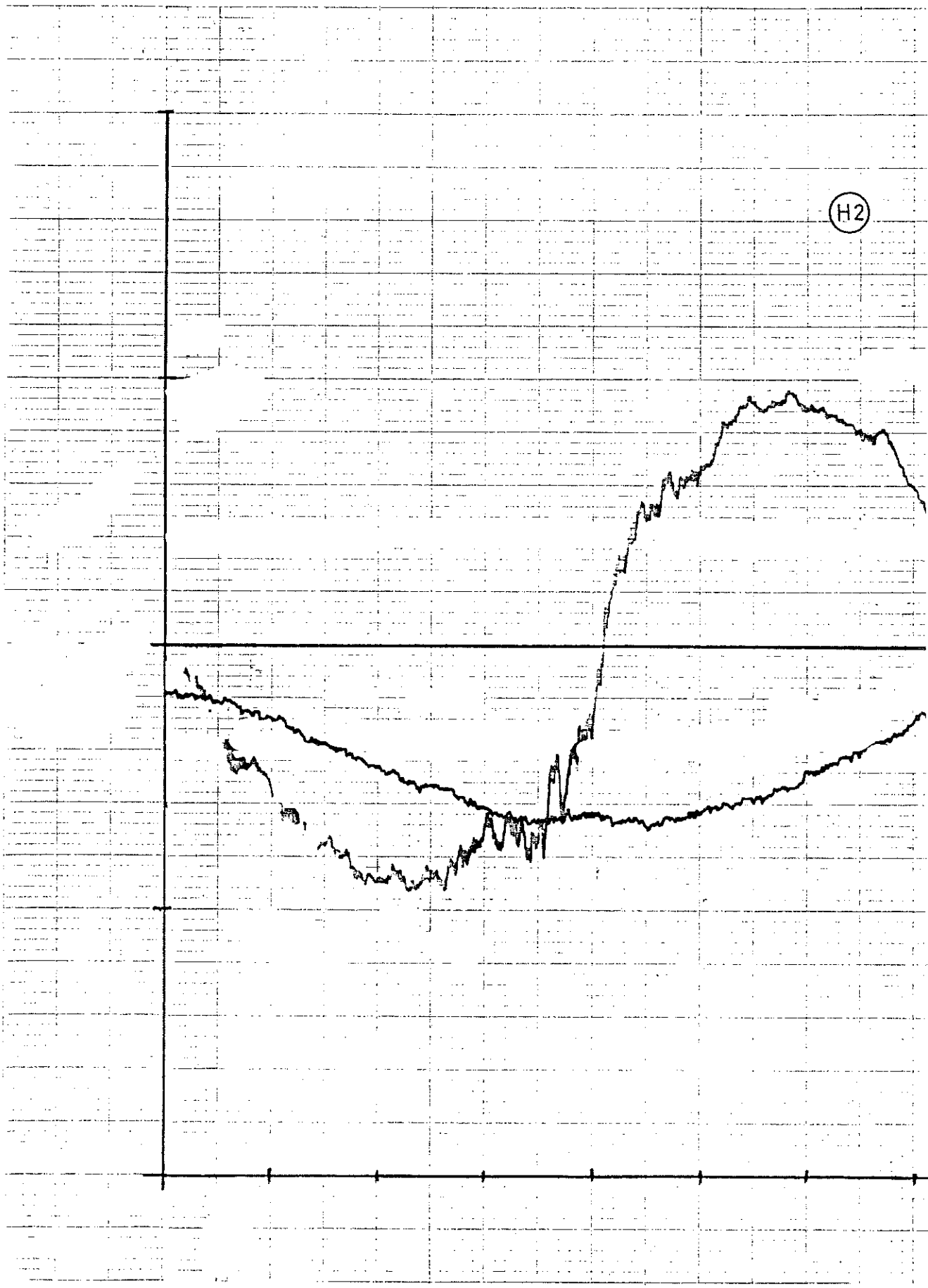
H2

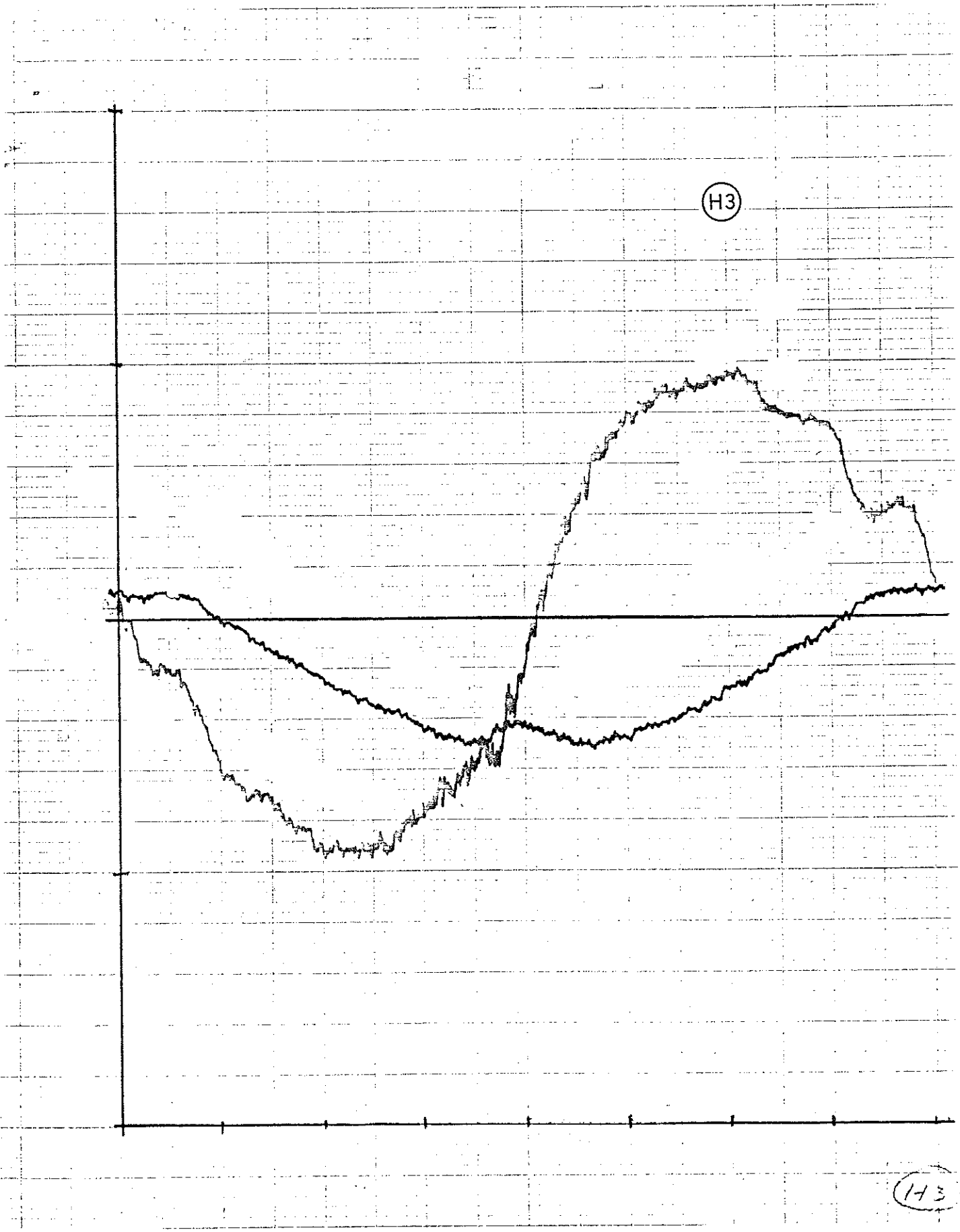
H3
1H3

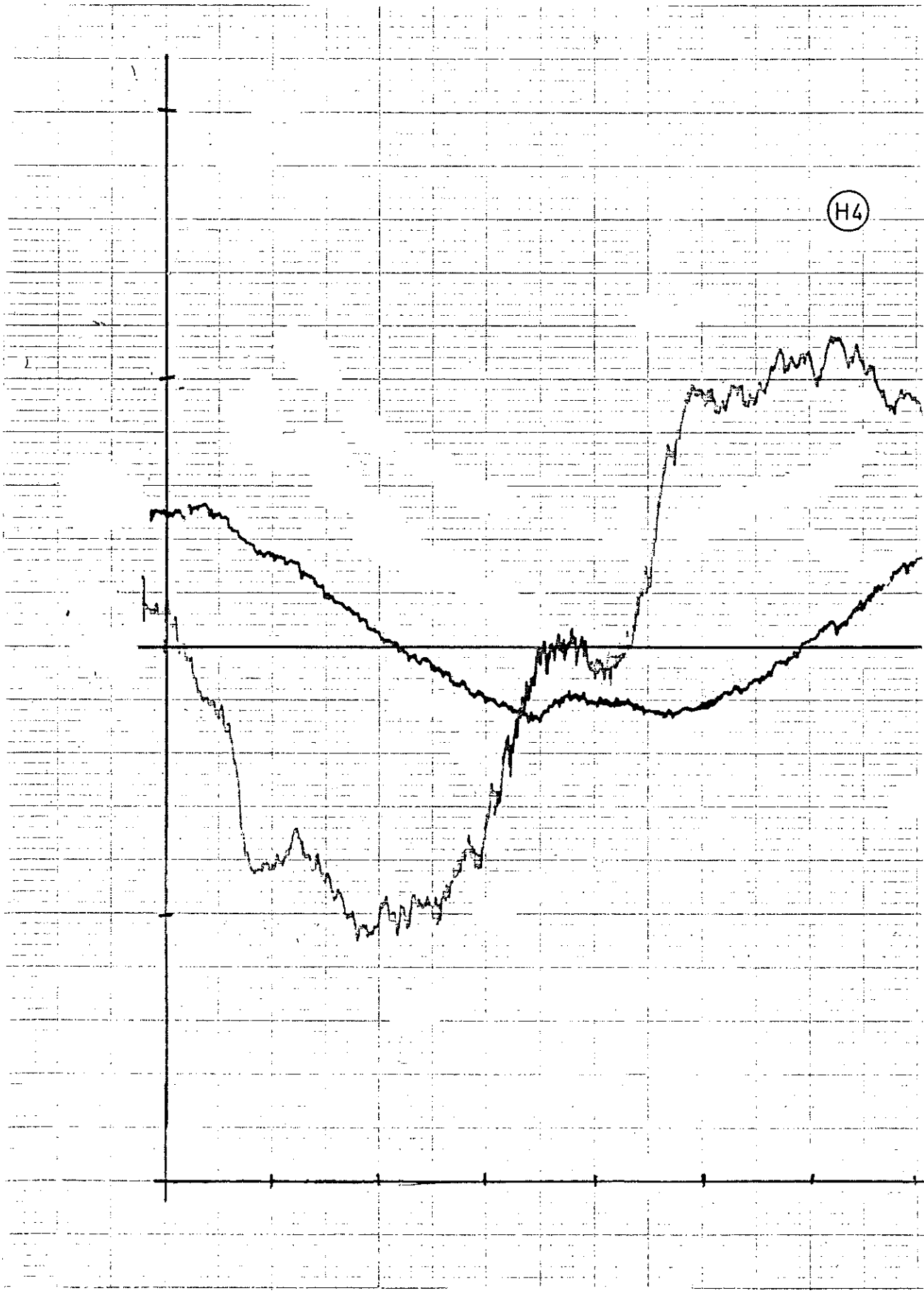
H4

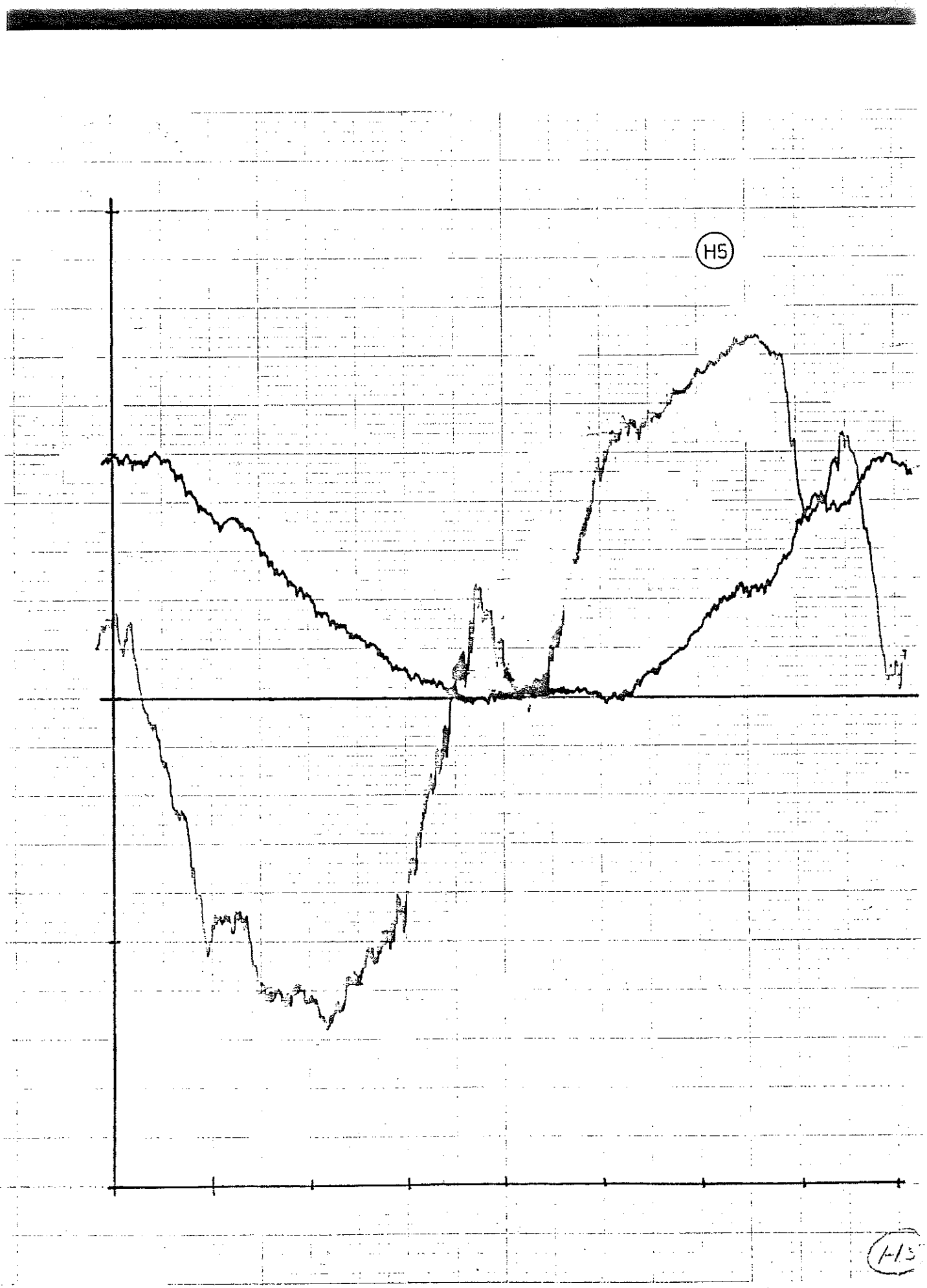
H5

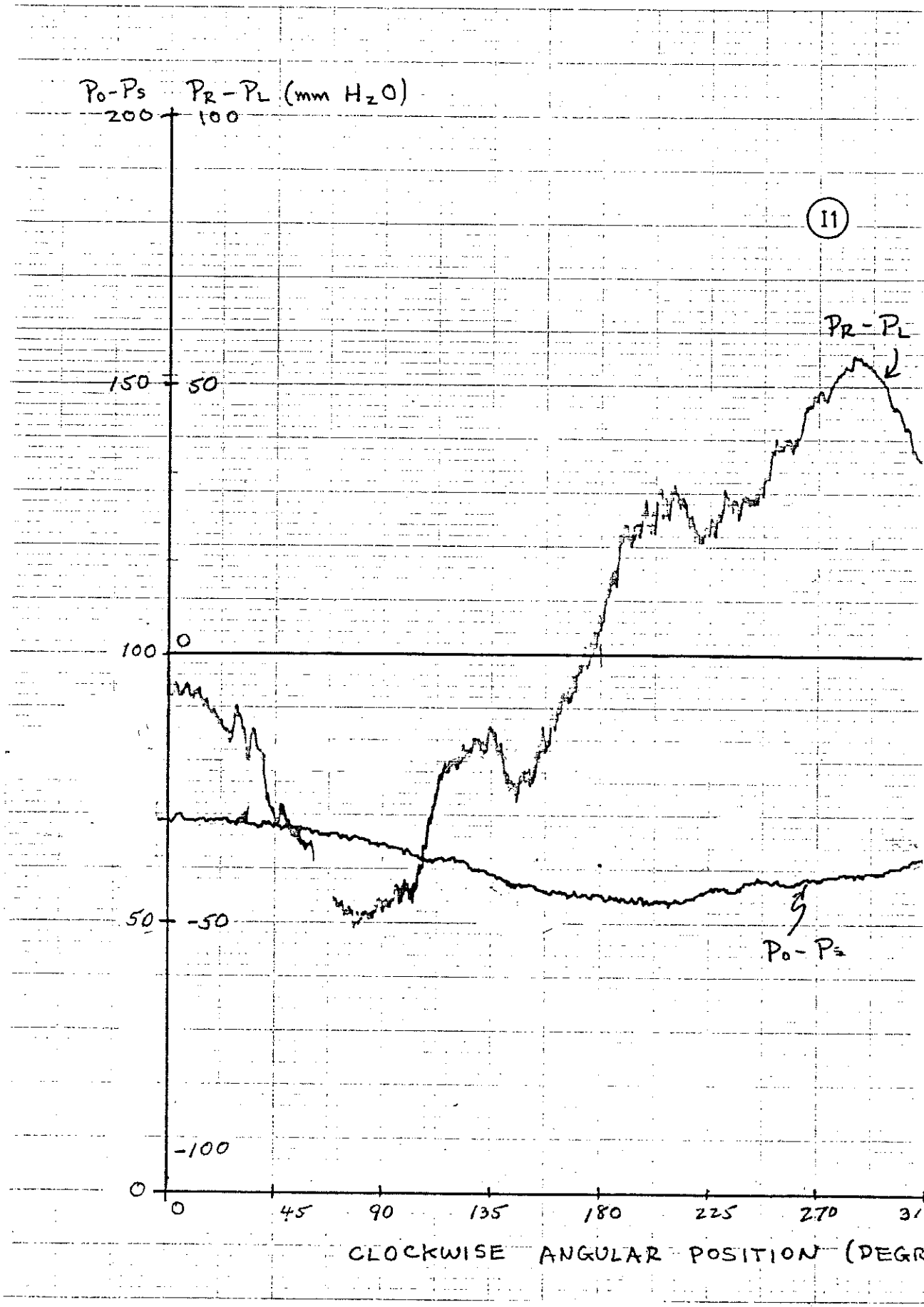
$P_o - P_s$
$P_R - P_L$ (mm H_2O)
200
100
150
50
100
0
50
-50
-100
0
0
45
90
135
180
225
270
11
$P_R - P_L$
$P_o - P_s$
CLOCKWISE ANGULAR POSITION (DEGR

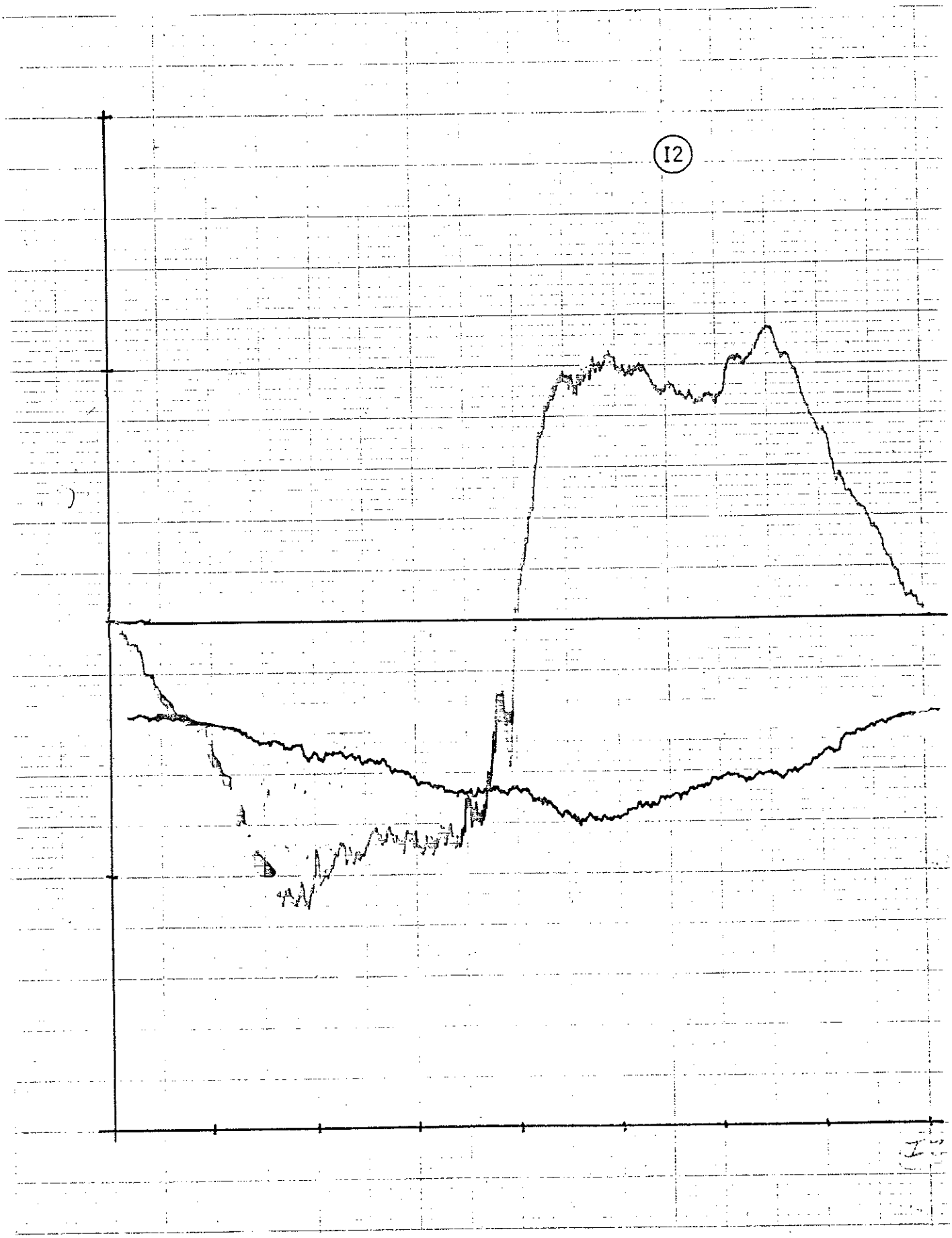
12


13

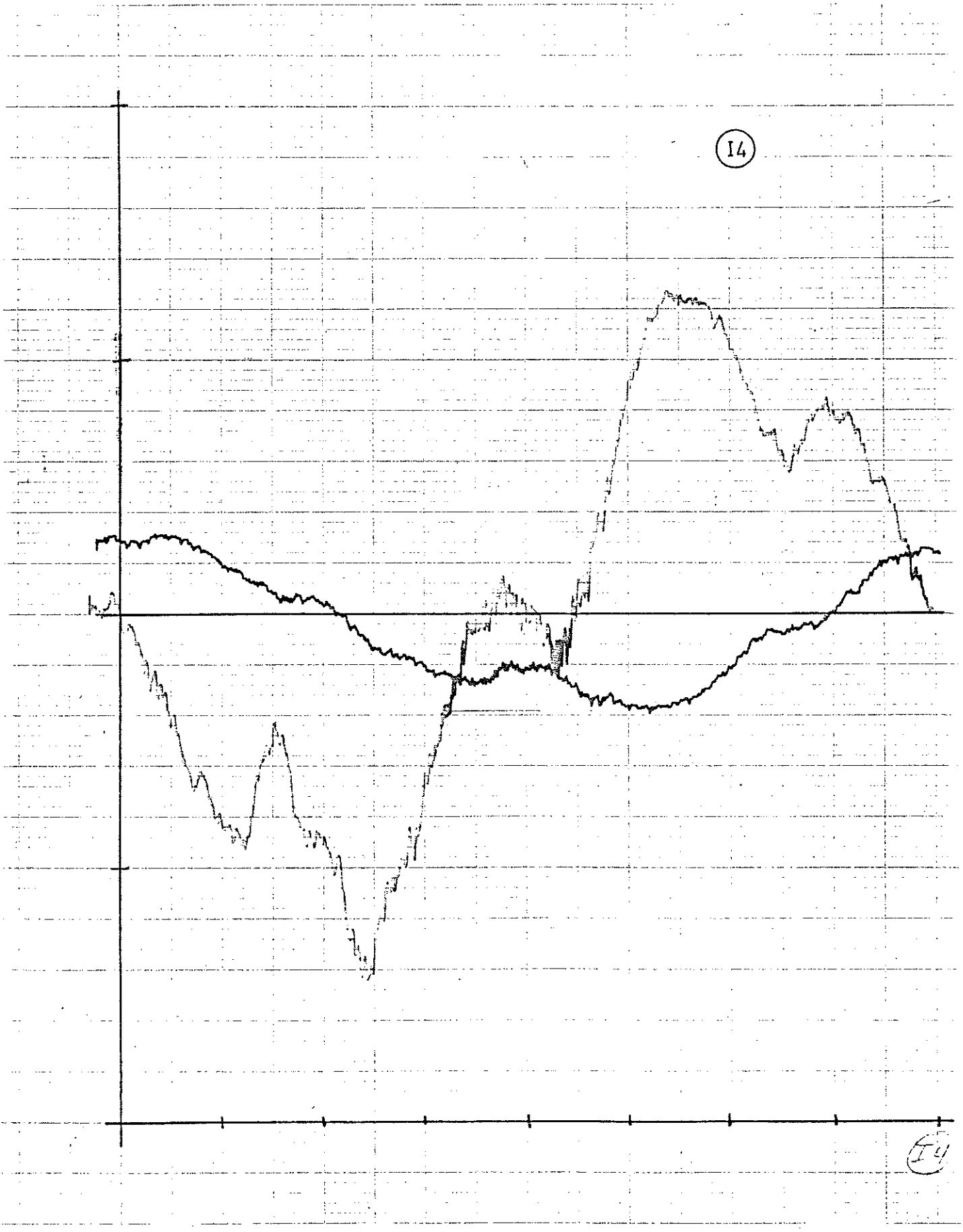
14
14

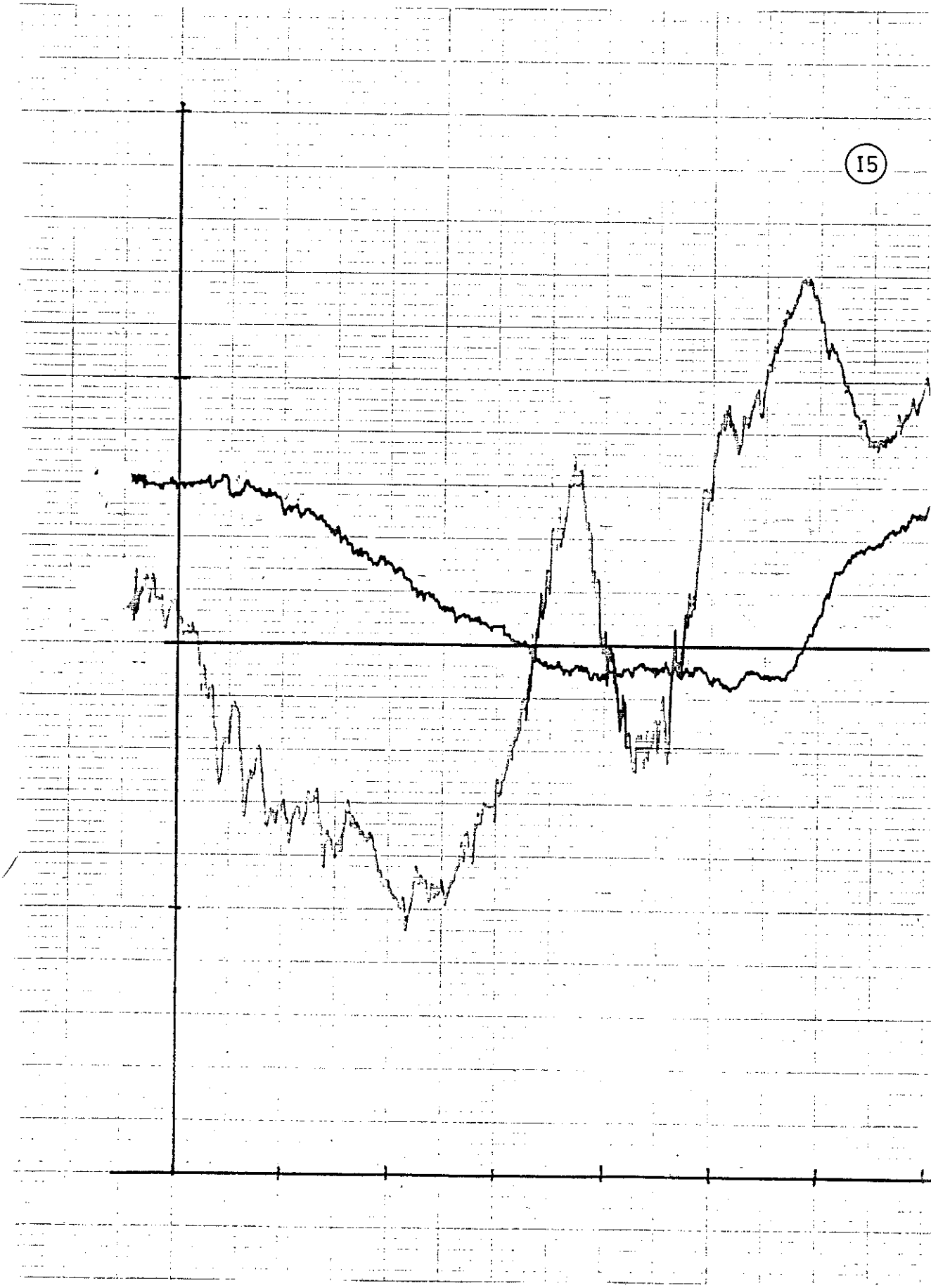
I5

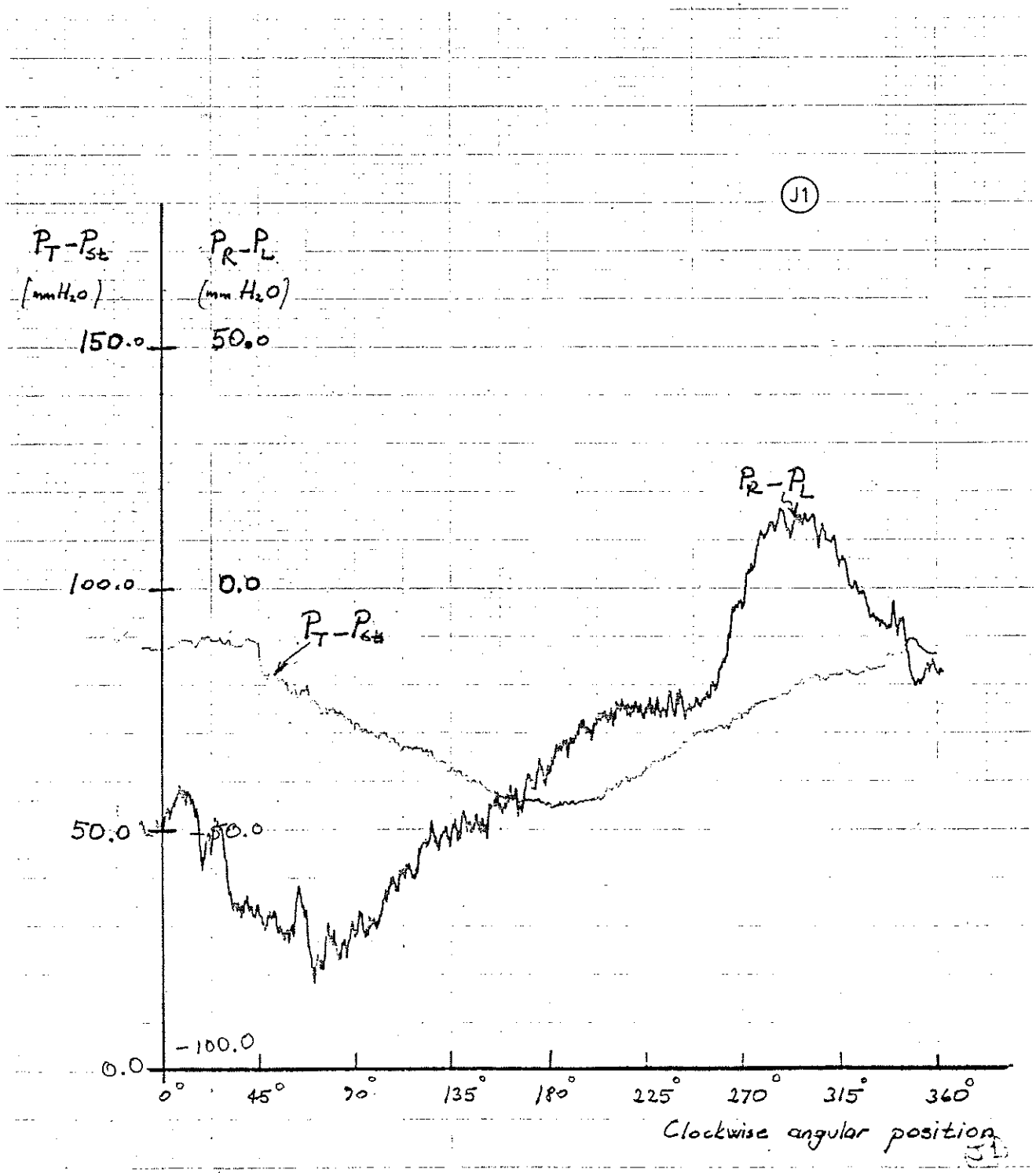
J1
$P_T - P_{st}$
[mm H_2O]
$P_R - P_L$
(mm H_2O)
150.0
50.0
100.0
0.0
50.0
0.0
-100.0
$P_R - P_L$
$P_T - P_{st}$
0°
45°
90°
135°
180°
225°
270°
315°
360°
Clockwise angular position
J1

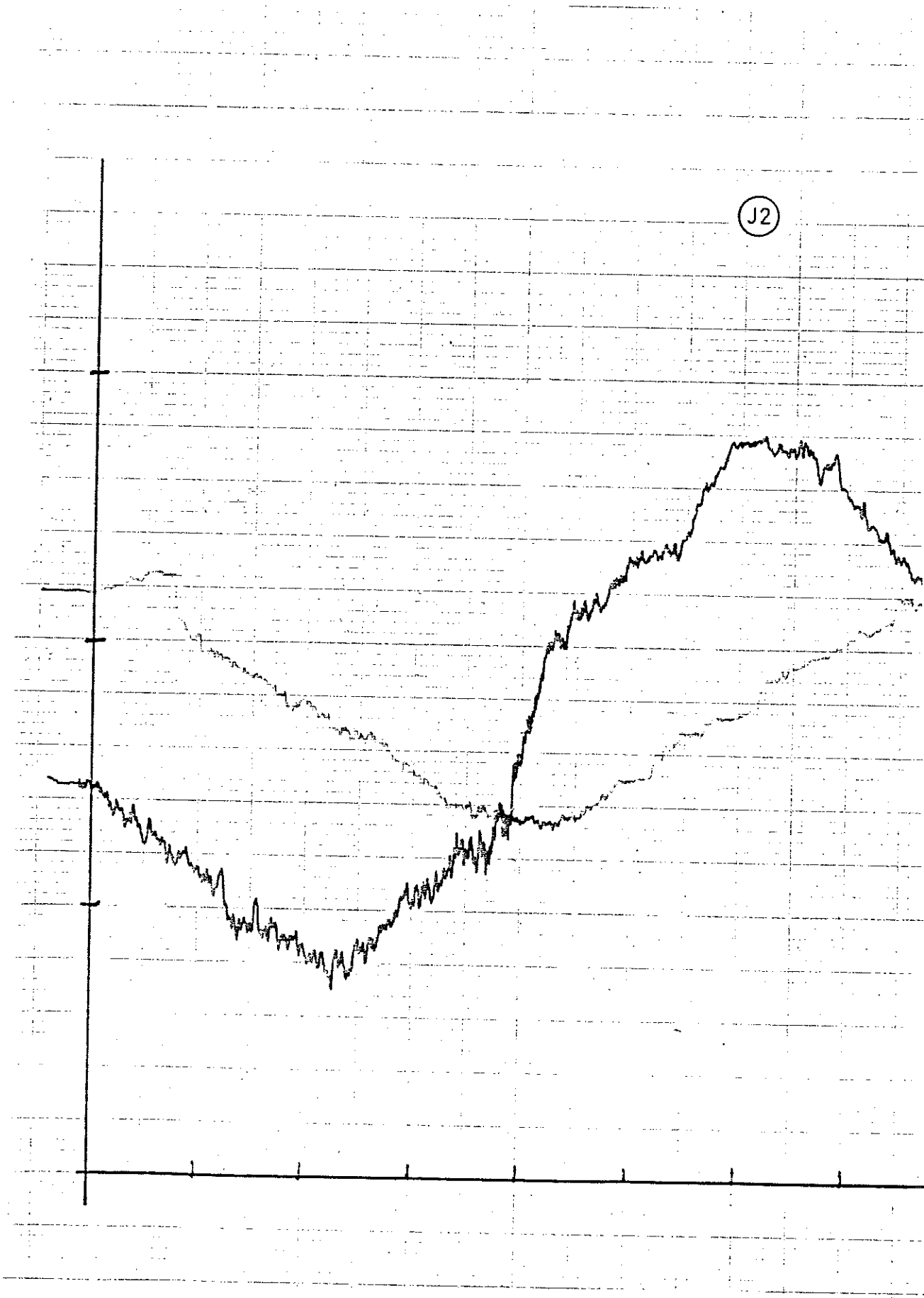
J2

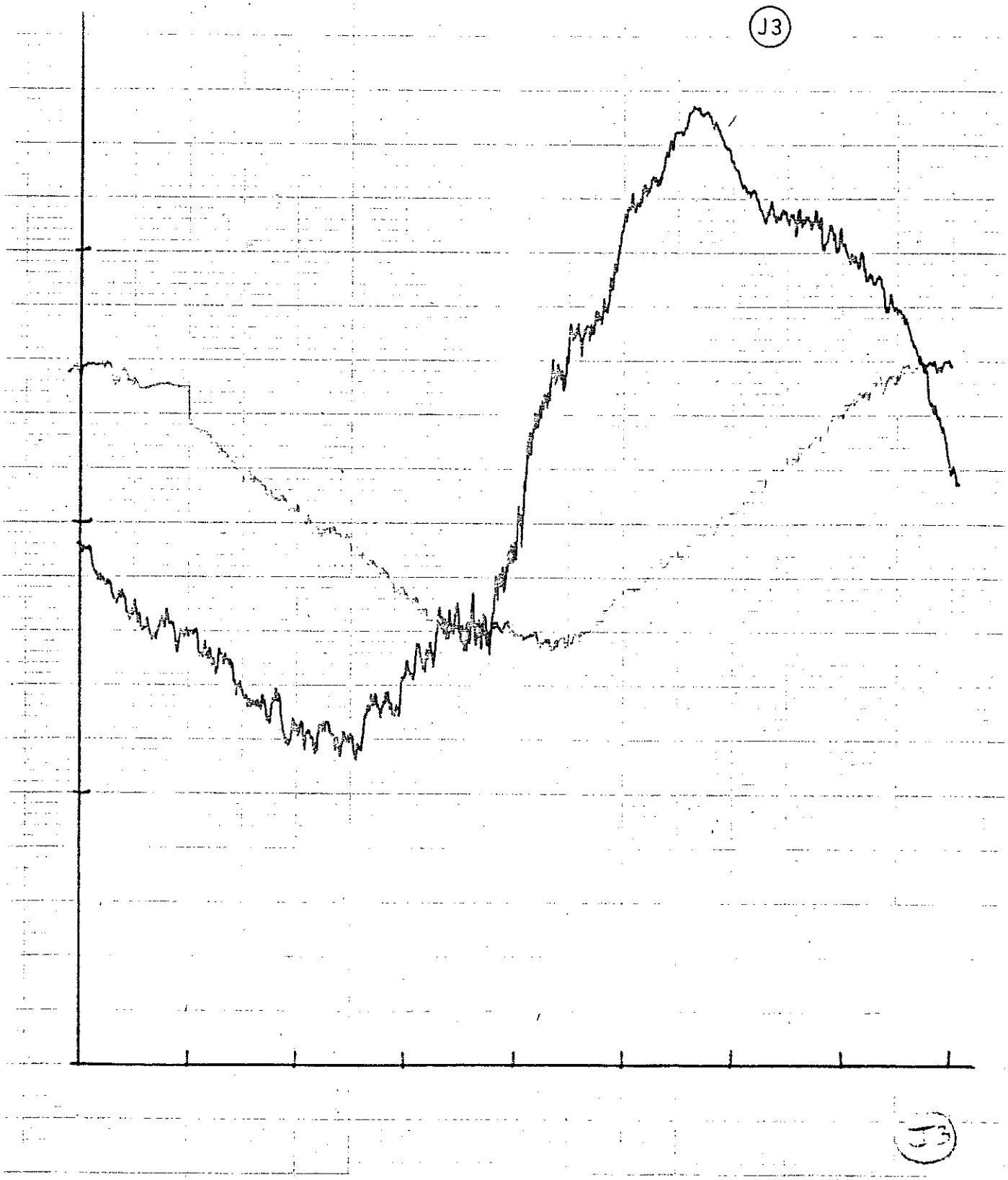
J3
J3

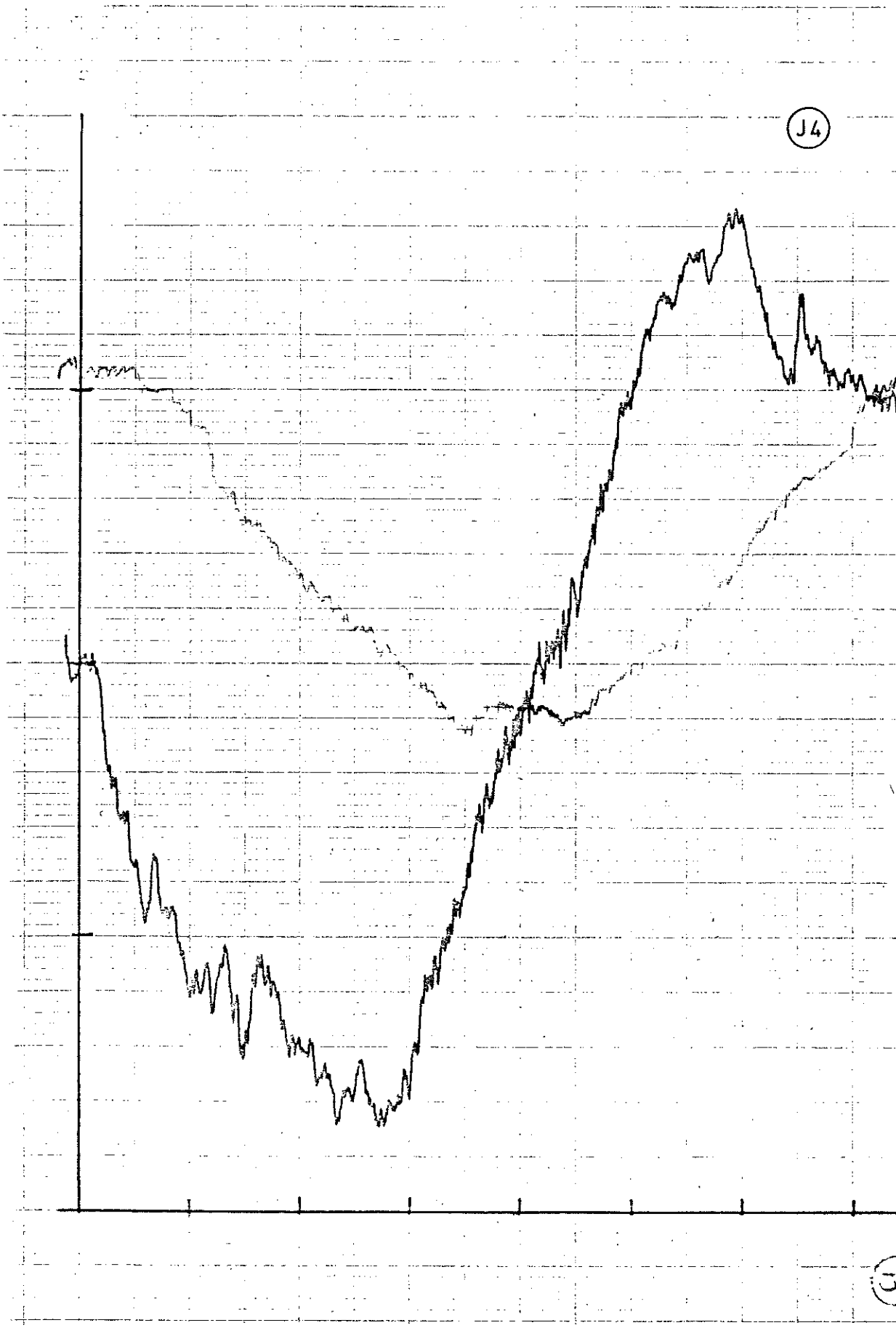
J4

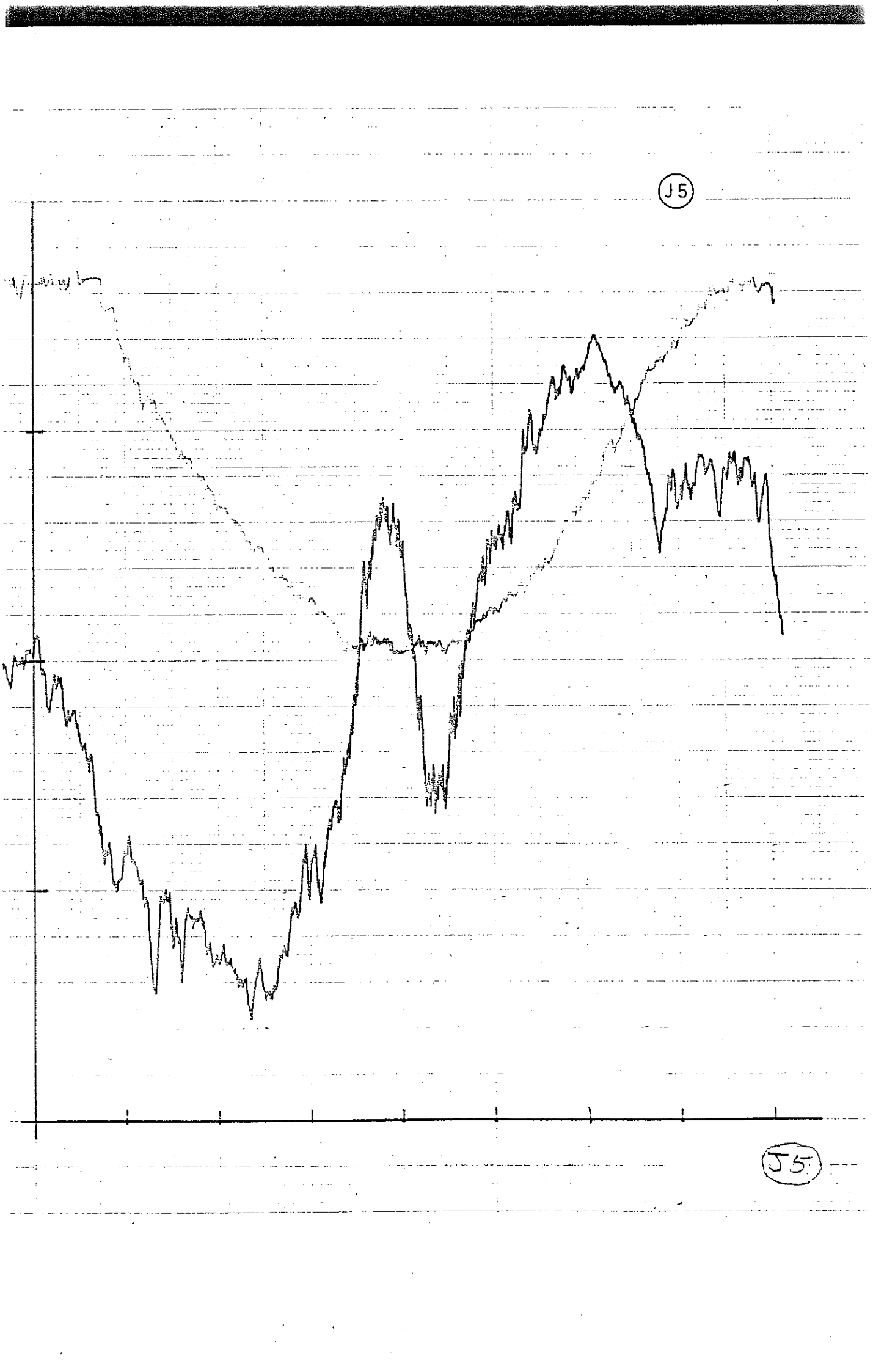
J5
J5

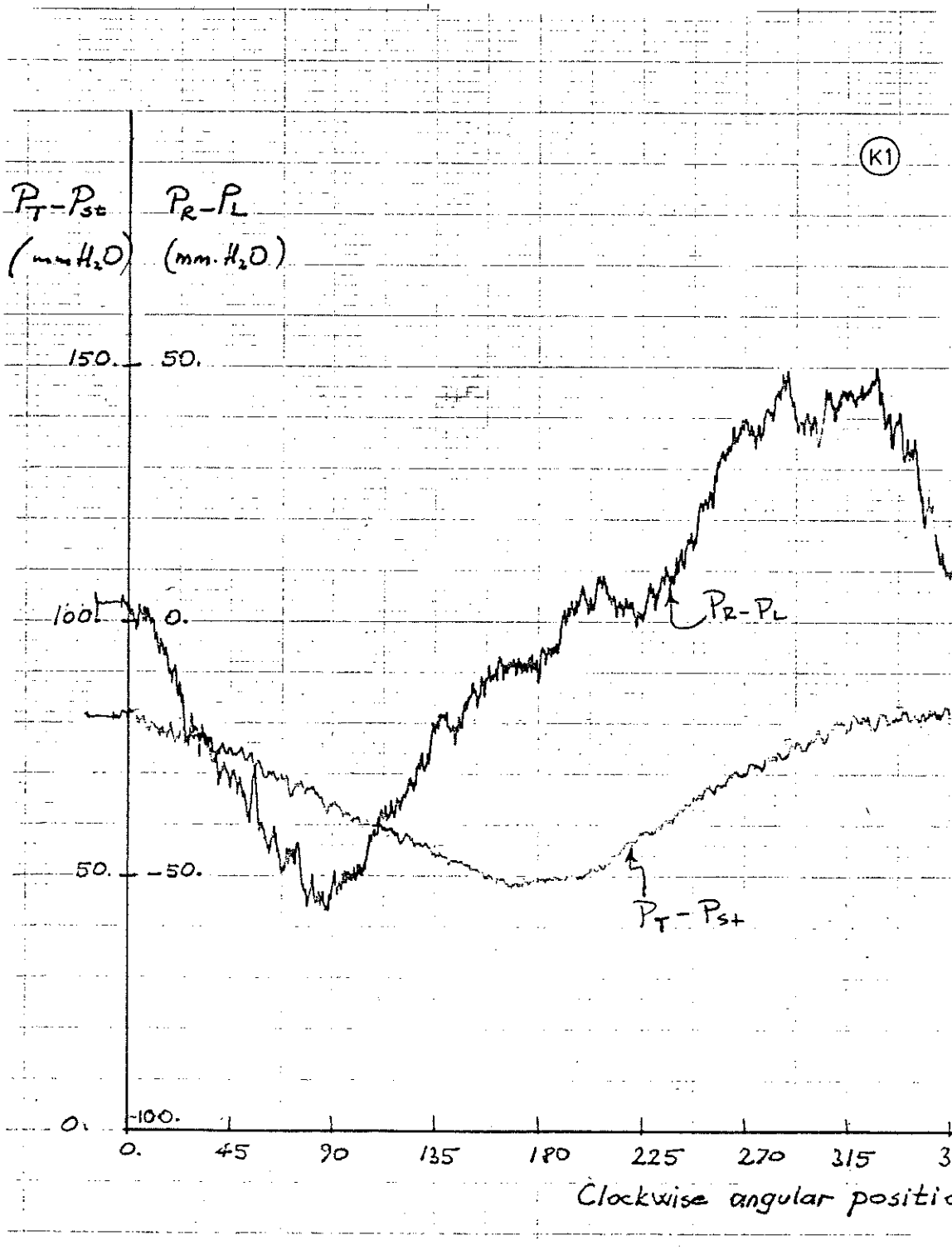
K1
$P_T - P_{st}$ (mm. H_2O)
$P_R - P_L$ (mm. H_2O)
150.
50.
100.
0.
50.
-50.
0.
-100.
$P_R - P_L$
$P_T - P_{st}$
0.
45
90
135
180
225
270
315
Clockwise angular positi

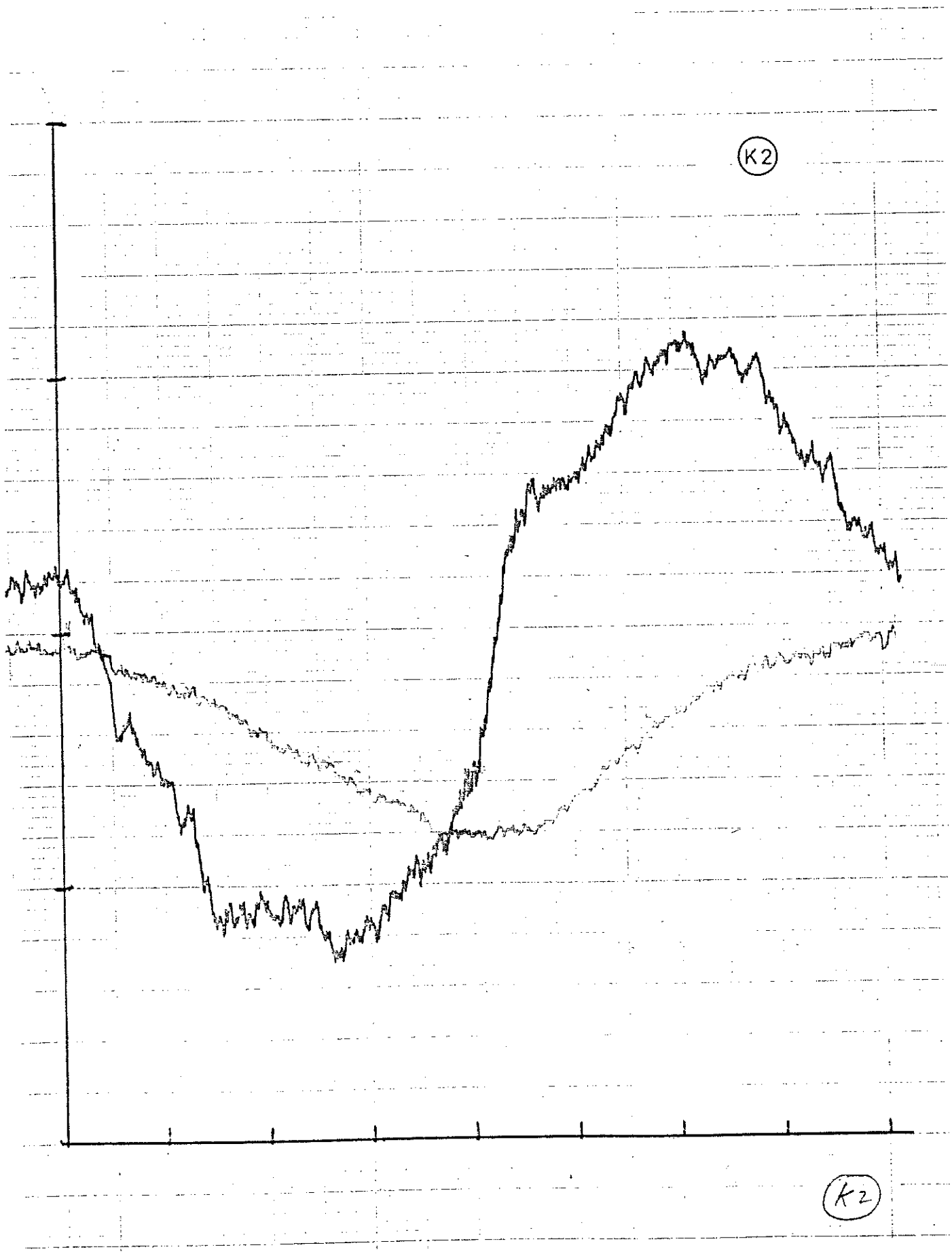
K2
K2

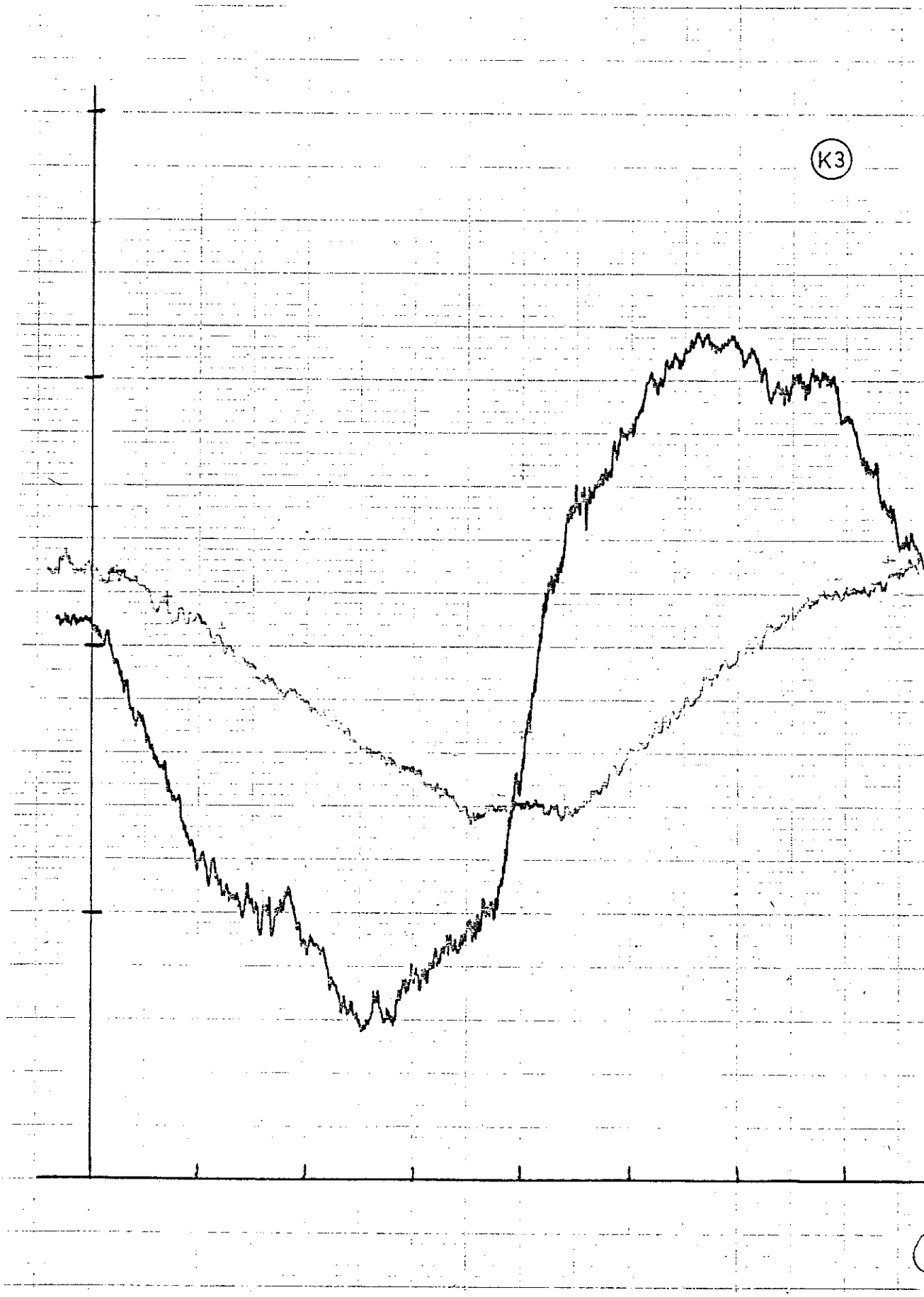
K3

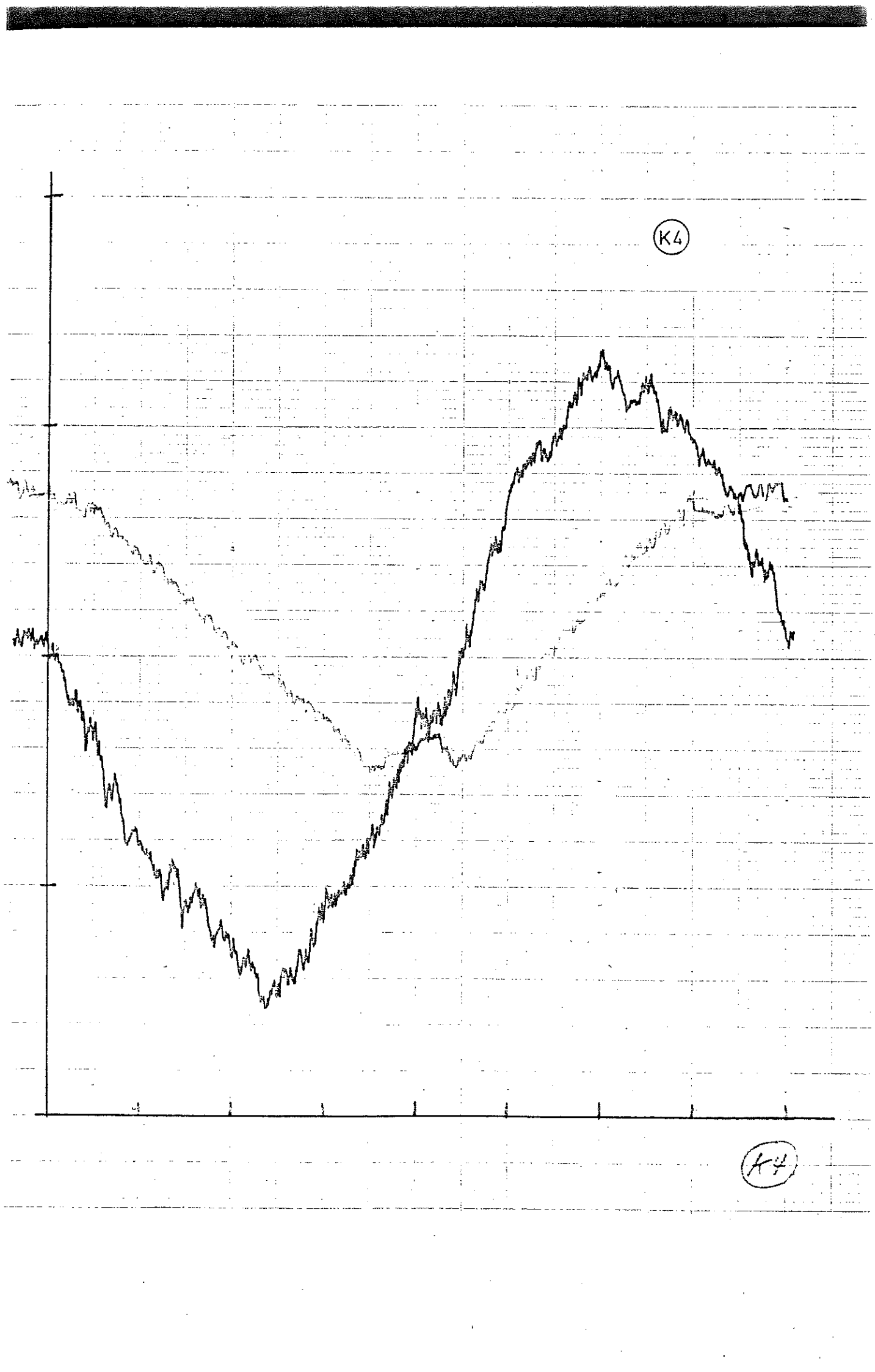
K4
A4

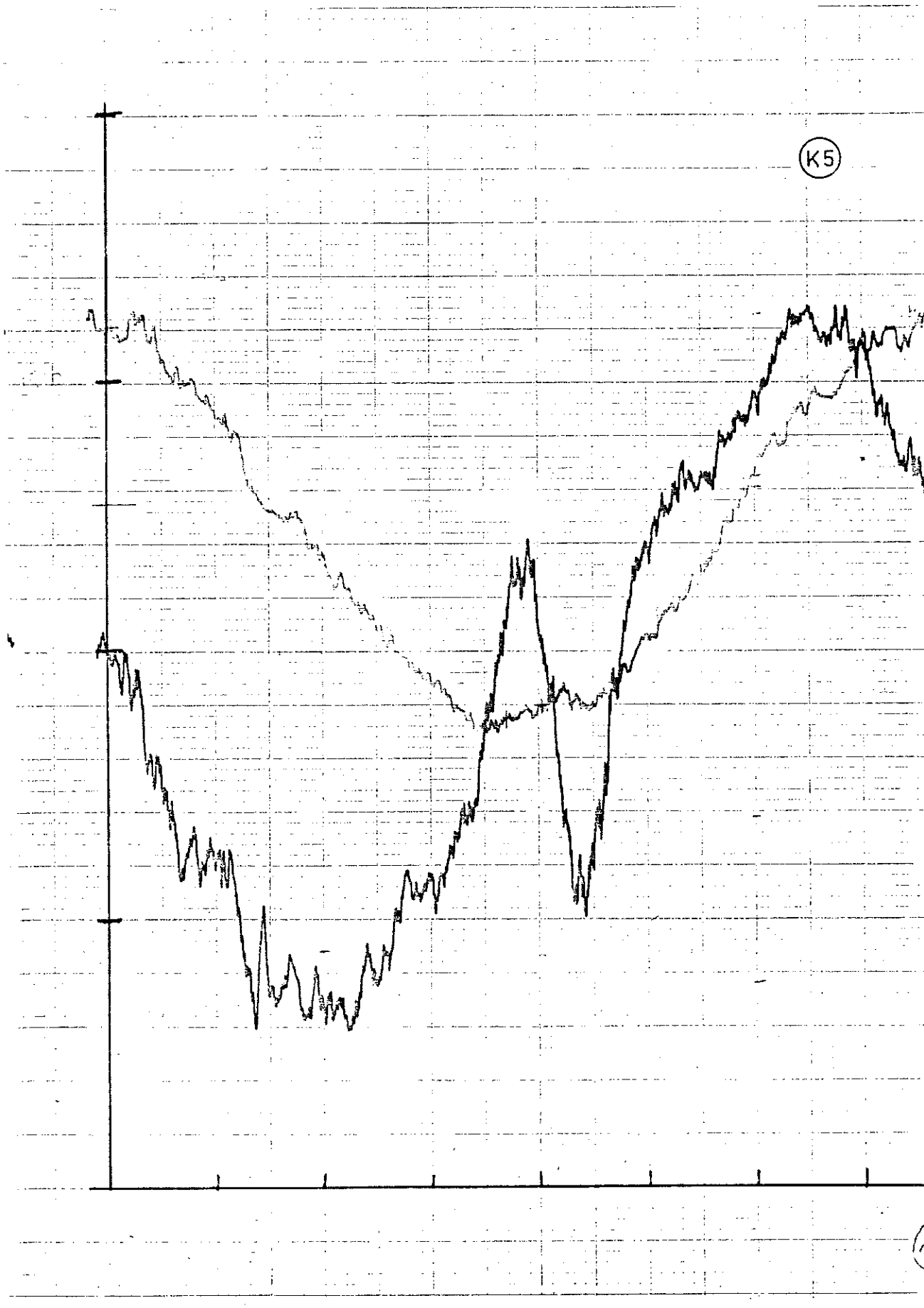
K5